A Review of Aeronautical Fatigue and Structural Integrity Research and Application in China

June 2017-May 2019

Presented at the 36th conference of the International Committee of Aeronautical Fatigue and Structural Integrity (ICAF)

Compiled by: China ICAF Office
Chinese Aeronautics Establishment(CAE)

Table of Contents

1. INTRODUCTION

This review summarizes the studies on the research on aeronautical fatigue and structural integrity investigations in China during the period June 2017 to May 2019 and is presented at the 36th conference of the International Committee Aeronautical Fatigue and Structural Integrity (ICAF) in Krakow Poland.

This report includes the research on the fatigue and structural integrity analysis of advanced material, advanced methods, widespread fatigue damage, corrosion fatigue and resistances, structural health monitoring, load acquisition and spectrum compilation, and full-scale structural test etc.

China Delegation ICAF office organizes relevant professional institutions and academics to carry out the research inside China and cooperate with ICAF partners. The China National Review is integrated and compiled by China ICAF Office based on the recent researches progress contributed by the following organizations.

1 AVIC Aircraft Strength Research Institute

2 AVIC Shenyang Aircraft Design and Research Institute

3 AVIC Chengdu Aircraft Design and Research Institute

4 AVIC Beijing Aeronautical Manufacturing Technology Research Institute

5 AVIC Harbin Aircraft Industry Group Co, LTD

6 AVIC Xi'an Civil Aircraft Industry Company LTD

7 AVIC The First Aircraft Institute

8 AVIC China Aviation Industry General Aircraft Co., Ltd

9 AVIC Chinese flight test establishment

10 AVIC China Helicopter Research and Development Institute

11 Shanghai Aircraft Design and Research Institute of COMAC

12 AECC Beijing Institute of Aeronautical Materials

13 Beihang University

14 Naval Aeronautical Engineering Institute

15 Civil Aviation University of China

16 Air Force Engineering University

17 Nanjing University of Aeronautics and Astronautics

18 Xi'an Jiaotong University

Each item of the report lists the corresponding contributors. The generous contributions provided by these research institutes, aerospace industries and universities are sincerely acknowledged.

2. FUNDAMENTAL RESEARCHES ON AERONAUTICAL FATIGUE AND STRUCTURAL INTEGRITY

2.1 Effects of Heat Treatment Process on the Microstructure and Mechanical Properties of TA15 Titanium Alloy Linear Friction Welding Joint[1]

The effect of heat treatment process on the microstructure and mechanical properties of TA15 titanium alloy Linear Friction Welding (LFW) joint was investigated in this part. The results show that the microstructure of metastability needle-like transforms to the lamellar α phase and β phase during the heat treatment process. As the temperature of heat treatment process increased, the lamella of the microstructure increased. The fracture positions of the tensile samples are all presented on the base metal. The mechanical properties, named the tensile strength, yield strength, are better than the base metal after heat treatment process. And the fatigue strength and impact properties increased after this process. In order to obtain a synthetically performance of the weld joint, the temperature of the heat treatment process should not exceed 750℃. Figure 2-1~Figure 2-3 are the results of microstructure and mechanical properties of TA15 titanium alloy.

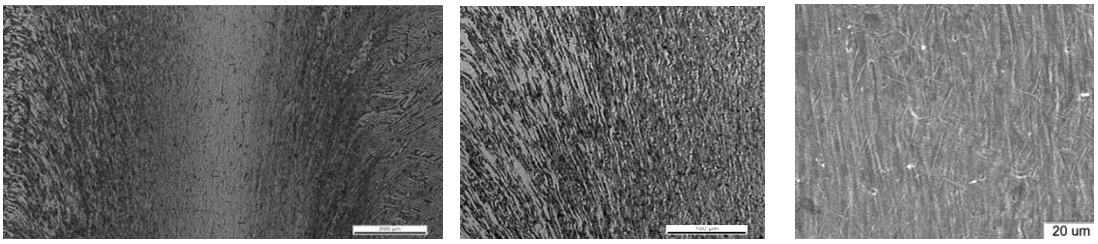

a) Morphology of the welding zone b) Thermal-mechanically affected zone c) Weld nugget zone

Figure 2-1 Micrographs of linear friction welded TA15 alloy

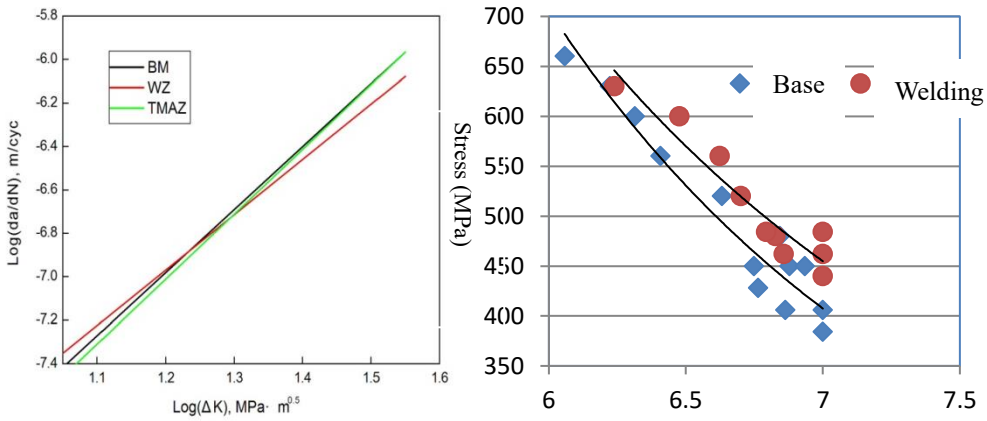

(a) Crack propagation rate curve (b) S-N curve

Figure 2-2 Fatigue properties of Linear Friction Welded for TA15 alloy and base metal

说明 TMAZ 是什么？

[1] AVIC Beijing Aeronautical Manufacturing Technology Research Institute. LIU Ying: Liuying_lsh@163.com.

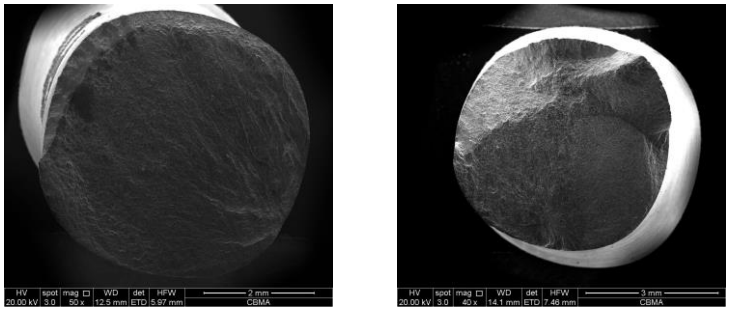

a）BM　　b）LFW

Figure 2-3 Fracture morphologies of linear friction welded TA15 alloy (LFW) and base metal (BM) in high-cycle fatigue tests

2.2 Mechanical Properties and Residual Stress Characteristics in Titanium Alloy Fabricated by Laser Additive Manufacturing[2]

Additive manufactured process can fabricate a complicated structure, which is impossible to be produced by traditional processes, efficiently reducing the weight of aircraft structures, yet the scattered property data limits its application in aerospace industry. This work presents the static and fatigue mechanical properties of titanium alloy built by Selective Laser Manufacturing (SLM) in three status: as-built, annealed and Hot Isostatic Pressing (HIP). Residual stress induced by the characters of process was measured by neutron diffraction (Figure 2-4) and X-Ray diffraction methods. In addition, the static strength, detailed fatigue rating and crack growth rate (Figure 2-5 and Figure 2-6) were discussed with respect to process parameters; the static and fatigue properties of short beam fabricated by laser forming repair were also investigated (Figure 2-7) by four-point bending test. Key conclusions are received: a) HIP and machining processes can produce the compressive residual stress, which improve the static and fatigue properties of SLM titanium material, and lower its crack growth speed; the specimens with laser forming repair process will have the similar properties to the forged ones.

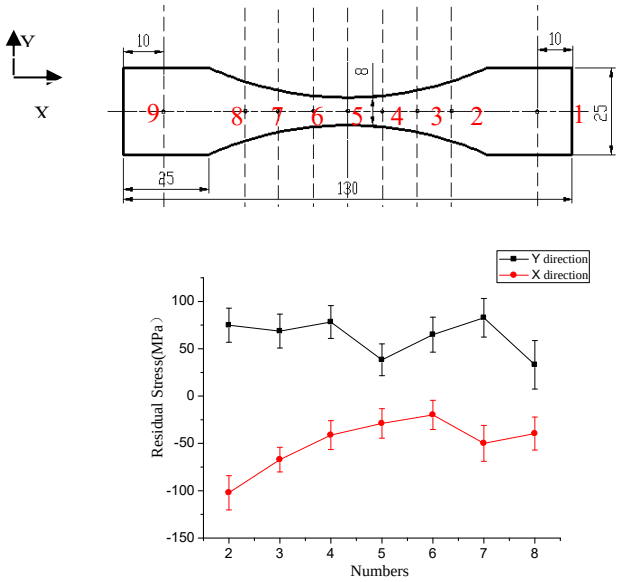

Figure 2-4 Distribution of residual stress in specimen by Neutron Diffraction Method

[2] AVIC Aircraft Strength Research Institute.　DONG Dengke: dengke623@sina.com.

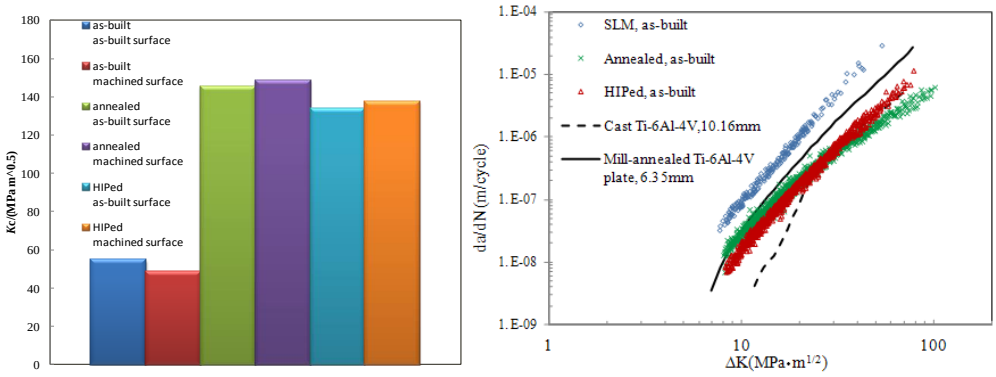

Figure 2-5 Comparisons of fracture toughness and FCGR for SLM TC4 with different conditions

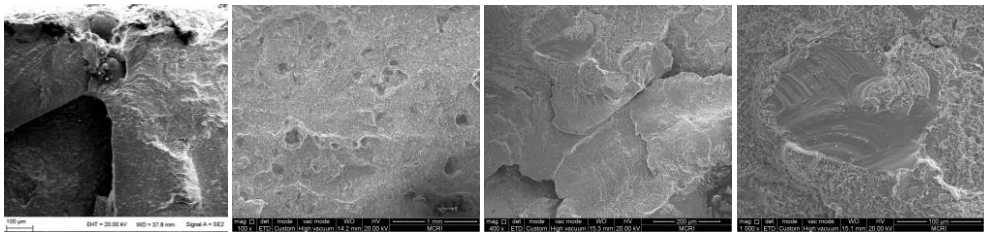

Figure 2-6 Typical defects in SLM TC4

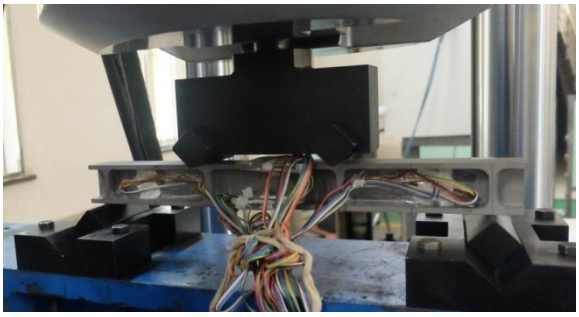

Figure 2-7 Schematic diagram of test jig for short beam fabricated by laser forming repair

2.3 Fatigue Behavior and Life Distribution of DED Ti-6.5Al-2Zr-Mo-V Titanium Alloy[1]

Directed energy deposition, or DED, is a metal additive manufacturing (AM) technology, which has great advantages in the formation of large-scale titanium alloy structures in aviation industry. For reusable aircraft structures, fatigue performance is the most critical mechanical property. In this case, metallographic features were observed and fatigue test under three stress levels (720, 760 and 800MPa) was conducted. The mixed failure behaviors and relationship between defects and fatigue life were discussed in detail. The double-peak characteristics of the fatigue life distribution have been observed, and a bimodal lognormal distribution (BLG) with five variables can be used to describe the fatigue life variation.

Fatigue test

The fatigue test was performed on an Instron 8801-100kN electrohydraulic servo fatigue system in an

[1] Beihang University. HE Xiaofan: xfhe@buaa.edu.cn.

atmospheric environment at room temperature under a sine-wave constant-amplitude (CA) stress with a stress ratio of 0.06 and frequency of 10Hz. Three sets of fatigue tests with peak stresses of 720, 760 and 800MPa were carried out.

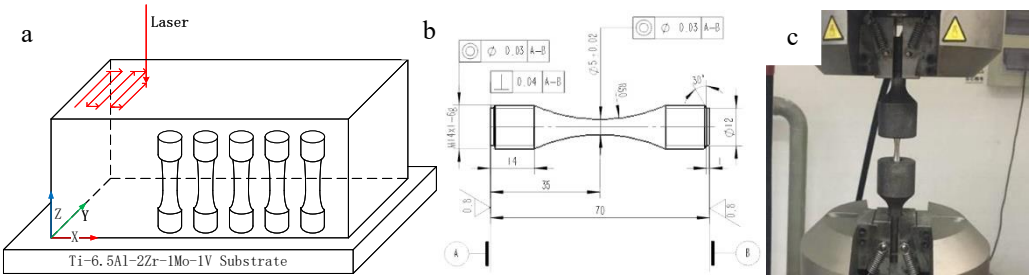

Figure 2-8 (a) Direct energy deposited (b) Specimen (c) Fatigue test

Metallographic

Two typical sections (X-O-Z and X-O-Y, Z is the deposition direction) were selected and observed by metallographic microscope. The results are shown in Figure 2-9. For the X-O-Z section, columnar grain grown along the deposition direction and disordered acicular α phase inside the columnar grains can be observed. For the X-O-Y section, the cross section of multiple columnar grains can be clearly seen. At higher magnification, the columnar grain boundary and internal acicular α are similar to the X-O-Z section.

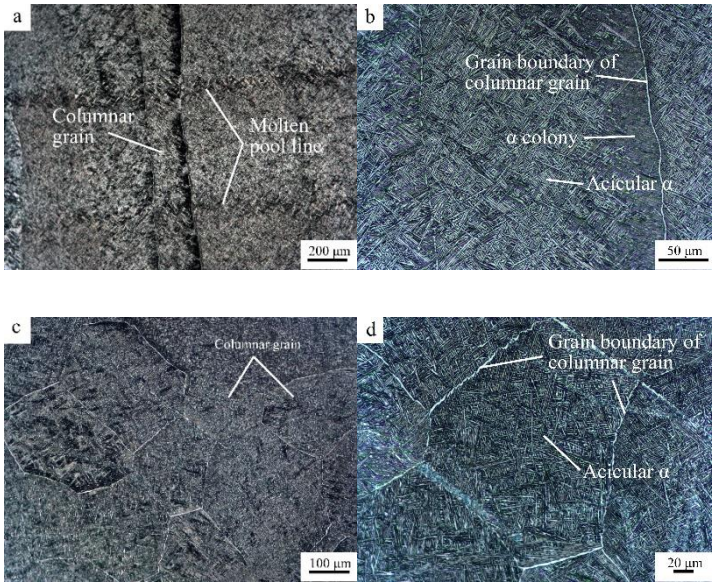

Figure 2-9 X-O-Z section: (a) macroscopic (b) microscopic, X-O-Y section: (c) macroscopic (d) microscopic

Mixed failure behaviors

The fractography, in Figure 2-10, shows that mixed failure behaviors appeared. The fracture surfaces can be divided into three regions: (i) crack initiation site (CIS); (ii) crack propagation region (CPR); (iii) fast fracture region (FFR).

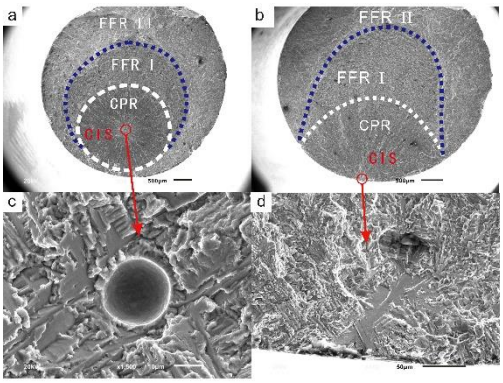

Figure 2-10 Fractography of two typical failure behaviors

Relationship between pore defects and fatigue life

Differences in the size of the pores led to different modes of crack initiation. According to the diameter of pore, the crack initiation modes of all specimens can be divided into four categories:(i) Crack initiates at small pores: d_{pore} is less than 20μm; (ii) Crack initiates at medium pores: d_{pore} is larger than 20μm and smaller than 60μm; (iii) Crack initiates at large pores: d_{pore} is greater than 60μm. The relationship between the fatigue life and pore diameter was discussed. When using Murakami's formula, a general trend was obtained, but the accuracy of the results was not high. It can be found that under the classification discussion, a good linear relationship at high stress levels (760 and 800MPa) can be presented.

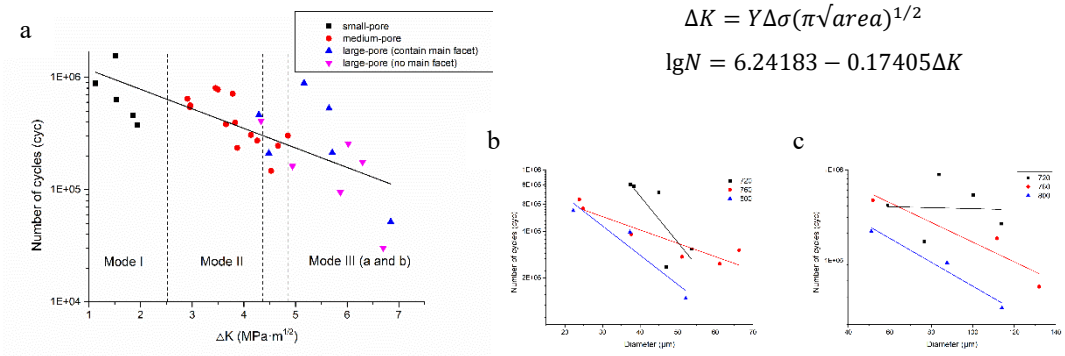

Figure 2-11 (a) △K-N (b) Diameter-N of medium pore (c) Diameter-N of large pore

2.4 Fatigue Crack Growth in Additive Manufactured Titanium Alloys[1]

Breakthrough in Additive Manufacturing (AM) technologies of large-scale-high-performance metallic integral structures is a significant milestone and a leading direction in the 3-D printing field; the application to the aerospace industry will revolute the methods to achieve further structural weight reduction and manufacturing cost saving. However, the difference in material microstructure between the AM alloys and conventional wrought or casting alloys sets new challenges to the damage tolerance evaluation, consequently, restricts the wide application of AM components in the primary load-bearing aircraft structures. In this project, experimental investigations and numerical simulations will be carried out to study the crack growth behavior and the corresponding mechanical parameters under the fatigue

[1] Beihang University. BAO Rui: rbao@buaa.edu.cn.

loading for samples manufactured by the Laser Metal Deposition (LMD) process.

There are three key techniques in the present research, which are as follows: experimental investigation on crack path change due to material micro structure; crack tip measurements on crack tip strain field, crack closure, etc. to understand the loading effect and material factors on crack growth dominating parameters; peridynamic simulations considering the material micro structure and fatigue degradation.

The key finds in the present research are as follows: the LMD Ti-alloy microstructures has respective impacts on fatigue crack growth behavior; and in specific, the impacts of α_p laths on the crack path is particularly significant; the variations of crack-tip strain fields can be used to predict retardation effects and fatigue lifetime more accurately; the proposed peridynamic fatigue model can reflects the effects of both microstructure and loading sequence on fatigue crack growth properly.

Fatigue crack growth path - Microstructure effect

The material textures in AM Ti-alloy made by LMD process are different from those in conventional wrought or casting alloys. The columnar grains and equiaxed grains are alternately arrayed due to the LMD technology, while their mechanical properties of different zones and with respected to different orientations are different as shown in Figure 2-12.

The crack path deflection is observed in the CT specimens with different orientations. When the angle between columnar grains and crack growth direction decreases, the straight crack path may deflect as shown in Figure 2-13. The scanning electron microscope (SEM) results in Figure 2-14 show that the deflection is affected by the angle γ between the expected crack growth direction and α_p laths orientations. The fatigue crack tends to propagate along α_p laths when is small; as γ increases, the effect of α_p laths is no longer strong enough to completely deflect the crack path along α_p laths, but the path still deflects locally; When γ is sufficiently large, the crack will pass through the α_p laths directly. This indicates that the crack path might be "guided" by controlling α_p laths orientations to extend fatigue lifetime. As shown in Figure 2-15, the possible crack paths with different α_p laths orientation distributions are predicted by peridynamics (PD).

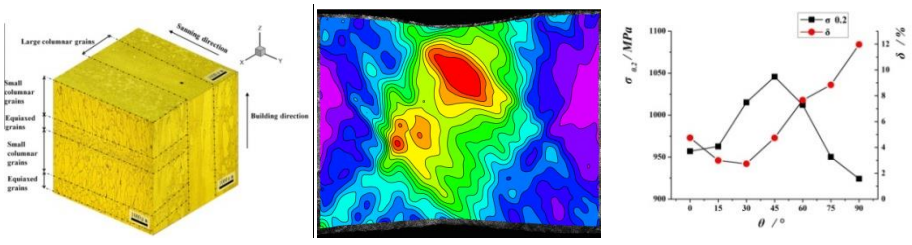

(a) (b) (c)

Figure 2-12 Material-structure characteristics and its effect on static properties: (a) alternately arrayed columnar grains and equiaxed grains, (b) strain field in different zones, (c) yield stress and critical elongation rate with respected to different orientations.

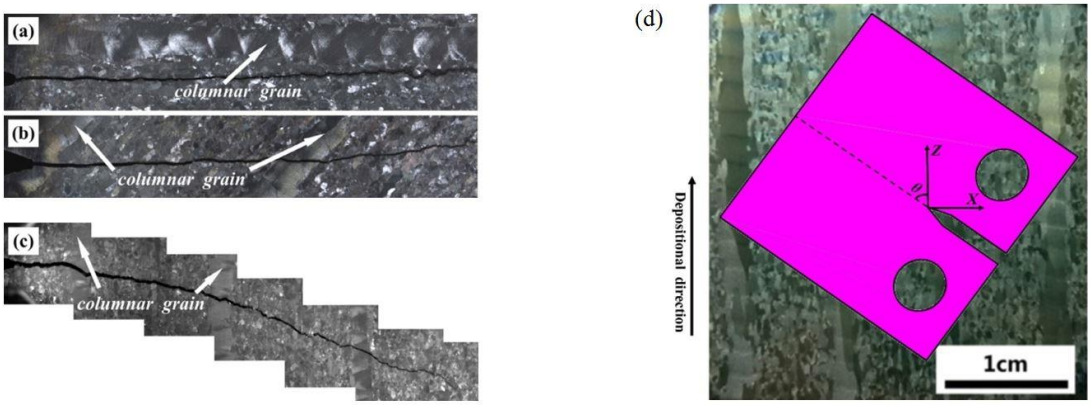

Figure 2-13 Crack growth paths in different oriented CT specimens, (a)θ=0°, (b)θ =45°, (c)θ =90°and (d) specimen orientation.

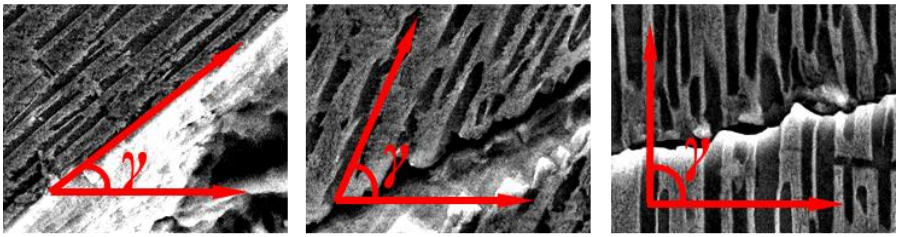

Figure 2-14 The crack deflection is affected by the angle between crack growth direction and α_p laths orientations.

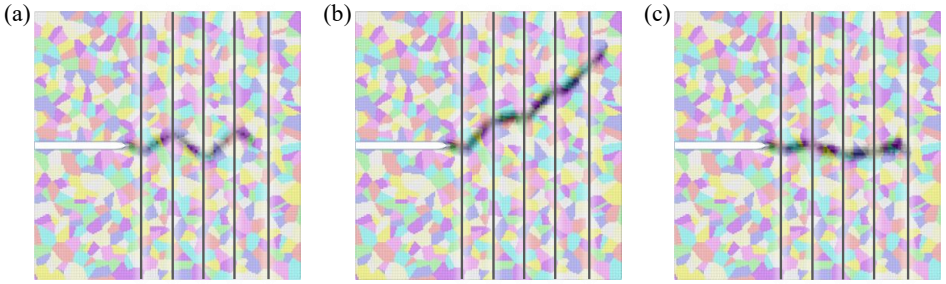

Figure 2-15 The crack path might be "designed" by controlling α_p laths orientations (Peridynamic simulations: (a) 45/-45/45/-45; (b) 45/0/45/0; (c) 75/-75/75/-75).

Crack growth rate – Spectrum loading effects

Aimed at studying the mechanical parameters of crack propagation in different microstructures, the digital image correlation (DIC) method is adopted to measure the crack-tip strain fields before and after overload (OL). Due to the differences in plastic properties, the overload effects on crack closure are different in columnar grains and equiaxed grains, as shown in Figure 2-16. It is observed that the OL retardation distances are consistent with the intersection points of strains corresponding to the maximum load between the before and after OL, which is shown in Figure 2-17; that is, the retardation of crack growth rate can be characterized by the variations of crack-tip strain fields before and after OL. The above discoveries can be used to modify retardation models and thus improve the accuracy for lifetime prediction under spectrum loading.

A peridynamic degradation model is proposed based on S-N curve and Goodman equation, which can be used not only to simulate the crack initiation life but also the crack growth rate and life in case of no crack growth data. As shown in Figure 2-18, the peridynamic model give satisfying predictions under

simple variable amplitude loading blocks compared with NASGRO results.

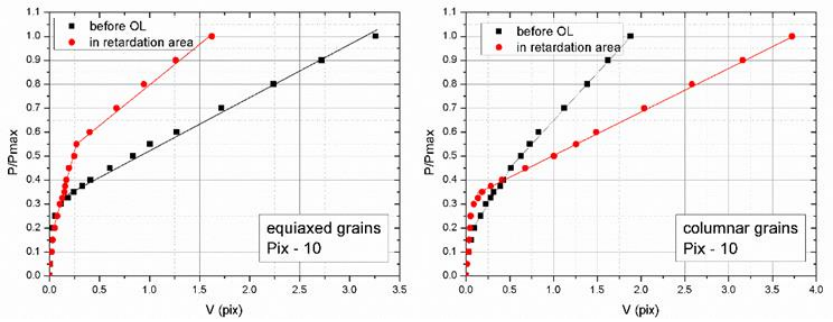

Figure 2-16 The overload effects are different in columnar grains and equiaxed grains.

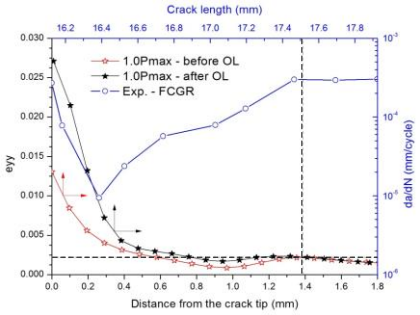

Figure 2-17 The retardation of fatigue crack growth rate can be characterized by the variations of crack-tip strain fields before and after OL.

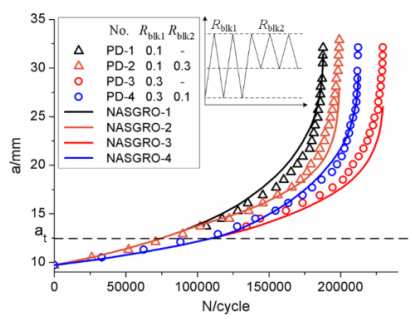

Figure 2-18 FCGR predictions under simple variable amplitude loading blocks: peridynamics and NASGRO

2.5 Determination of Internal Stresses Using the Weight Function Method[1]

The purpose of most crack-problem analyses is to determine fracture mechanics parameters, e.g. stress intensity factors and crack opening displacements, for fracture and fatigue crack growth assessment. In such analyses, the crack-line stress must be known beforehand. However, there are problems in engineering practice for which the crack-line stress distribution is unknown and needs to be determined. A typical example of such problem is related to residual stresses induced by various manufacturing processes such as welding, forging, rolling, shot-peening and cold working.

Key Techniques

A method for the determination of crack-line stress from known crack mouth opening displacements (CMOD) is developed in the present study. The approach is based on an inverse utilization of the weight function method, in which a crack-like slit is cut in the component and the CMOD is used as input. The crack-line stress is assumed to be either a polynomial type or a large number of constant stress segments. By a least-squares routine for solving the integral equation of crack opening displacements, the unknown crack-line stress can be calculated. To verify the inverse weigh function approach, three types of crack geometry/loading combinations are investigated, including periodic array of collinear cracks subjected to sinusoidal crack-line stress, radial cracks at a circular hole in an infinite plate subjected to remote uniform tension and a single edge crack in a finite rectangular plate under pure bending. By taking the

[1] AECC Beijing Institute of Aeronautical Materials. TONG Dihua: tongdi133@163.com.

analytical CMOD-expressions from the well-known Tada-Paris-Irwin Handbook, the calculated crack-line stresses are all in good agreement with the corresponding load cases. It is demonstrated that the inverse weight function approach provides a very efficient and reliable tool for the determination of crack-line stress from the predetermined CMODs, and will be useful for the evaluation of unknown residual stress and bridging stress.

Results

$$\frac{\sigma}{E'}\begin{pmatrix} \int_0^{0.01a_{max}}\int_0^s m(s,x)\mathrm{d}x\cdot m(s,x=0)\mathrm{d}s, & 0, & 0,\cdots\cdots\cdots\cdots\cdots\cdots\ 0 \\ \int_0^{0.01a_{max}}\int_0^s m(s,x)\mathrm{d}x\cdot m(s,x=0)\mathrm{d}s, & \int_{0.01a_{max}}^{0.02a_{max}}\int_0^s m(s,x)\mathrm{d}x\cdot m(s,x=0)\mathrm{d}s, & 0,\cdots\cdots\cdots\cdots\cdots\cdots\ 0 \\ \int_0^{0.01a_{max}}\int_0^s m(s,x)\mathrm{d}x\cdot m(s,x=0)\mathrm{d}s, & \int_{0.01a_{max}}^{0.02a_{max}}\int_0^s m(s,x)\mathrm{d}x\cdot m(s,x=0)\mathrm{d}s, & \cdots, \int_{0.99a_{max}}^{1.0a_{max}}\int_0^s m(s,x)\mathrm{d}x\cdot m(s,x=0)\mathrm{d}s \end{pmatrix} \cdot \begin{pmatrix} \sigma_1 \\ \sigma_2 \\ \sigma_3 \\ \vdots \\ \sigma_n \end{pmatrix} = \begin{pmatrix} u(\frac{a}{a_{max}}=0.01, x=0) \\ u(\frac{a}{a_{max}}=0.02, x=0) \\ u(\frac{a}{a_{max}}=0.03, x=0) \\ \vdots \\ u(\frac{a}{a_{max}}=1.0, x=0) \end{pmatrix}$$

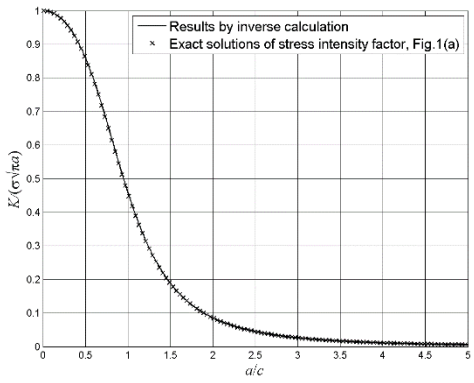

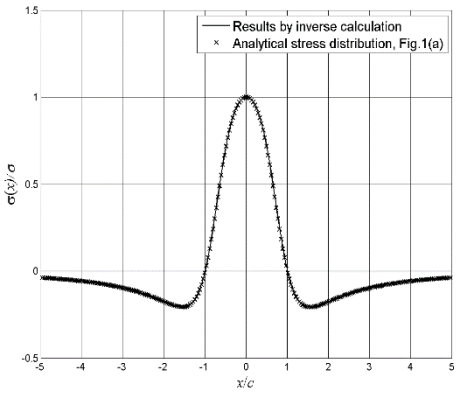

$$K = \sigma_0\sqrt{\pi a}\cdot\left\{\frac{\sqrt{1+(\frac{a}{c})^4}-(\frac{a}{c})^2}{1+(\frac{a}{c})^4}\right\}^{\frac{1}{2}} \qquad \frac{\sigma(x)}{\sigma} = \frac{1-(\frac{x}{c})^2}{1+(\frac{x}{c})^4}$$

Figure 2-19 Comparison of SIF and s(x) from inverse WF and known exact CMOD , a center crack in an infinite plate, under welding residual stress.

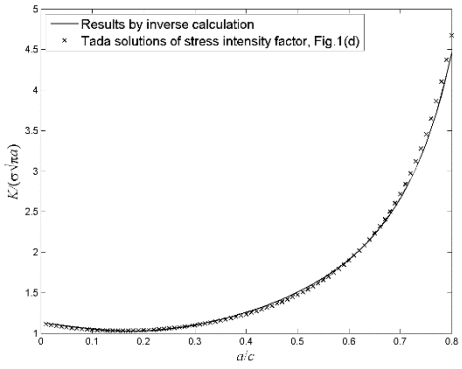

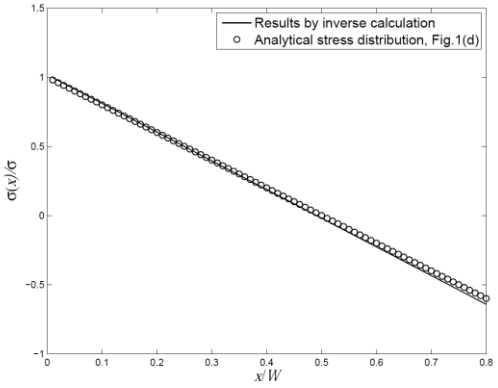

$$K=\sigma_0\sqrt{\pi aW}\cdot\sqrt{\frac{2}{\pi a}\tan\frac{\pi a}{2}}\frac{0.923+0.199(1-\sin\frac{\pi a}{2})^4}{\cos\frac{\pi a}{2}} \qquad \frac{\sigma(x)}{\sigma}=1-2x$$

Figure 2-20 An edge crack in a finite plate subjected to pure bending

2.6 Research on Crack Measurement Technique in Solid Material with Digital Image Correlation[2]

An algorithm of locating the crack tip based on displacement filed around crack tip is proposed in this paper. The problem of locating the crack tip is turned to a minimum solution of optical problem by building the objective function including crack tip location firstly. And then the location of crack tips is assumed in a format of mesh, nonlinear optimal problem can be analyzed through a linear least squares approach after an assuming crack tip is chosen. The exact crack tip is gotten by iterative analysis. This research can provide theoretic basis for crack measurement technique. Figure 2-21 shows the analytical flowchart of locating crack tip algorithm. Figure 2-22 shows that the distribution of objective function value in mix-mode crack case. The point which objective function value is least is exactly the crack tip position.

[2] AVIC Aircraft Strength Research Institute. ZHANG Wendong: dongzi.666@163.com.

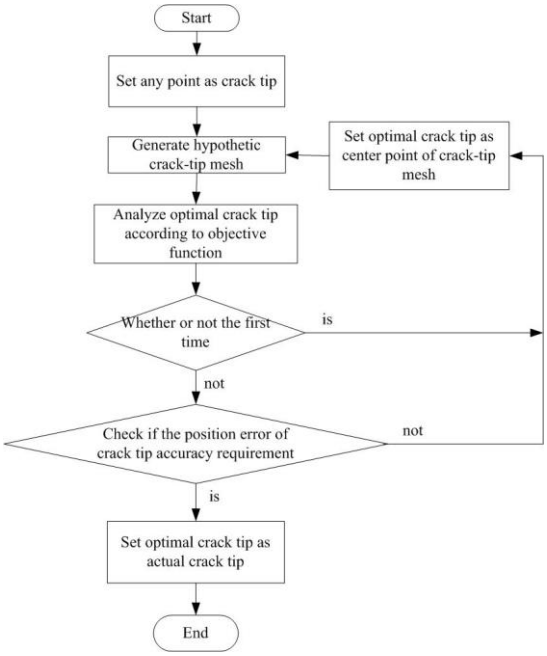

Figure 2-21 Analytical flowchart of locating crack tip algorithm

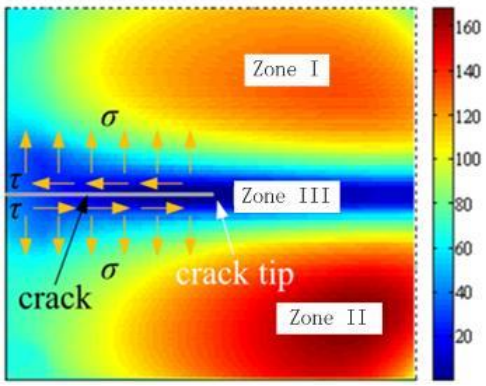

Figure 2-22 Distribution of objective function value in mix-mode crack case

Table 2-1 Two types of displacement fields and corresponding Williams expression coefficients

Type	Stress intensity factor		Coefficient value			
	K_{I} / MPa$\sqrt{\mathrm{mm}}$	K_{II} / MPa$\sqrt{\mathrm{mm}}$	a_1 / $MPa\sqrt{mm}$	a_2 /MPa	b_1 / $MPa\sqrt{mm}$	b_2 /MPa
Pure I mode	10	0	3.9894	0	0	0
I-II mixed mode	10	10	3.9894	0	3.9894	0

Hereby two types of displacement fields are present for verifying crack measurement technique. Table 2-1 Two types of displacement fields and corresponding Williams expression coefficients is two different types of displacement field and corresponding Williams expression coefficients. In addition, certain values are used as crack tip position. Figure 2-23 and Figure 2-24 show the displacement fields of I-mode crack and mix-mode crack respectively. The coordinator of I-mode crack tip is (4.53mm, 4.47mm), and the coordinator of mix-mode crack tip is (4.17mm, 5.23mm). Through crack measurement method, crack

tip positions are figured out in Table 2-2. From the results in Table 2-2 Analysis results of the current method for the displacement fields of different crack types, it can be concluded that this crack measurement technique has much less computation expense with high accuracy and a rapid convergence in both I mode crack case and I-II mode crack case.

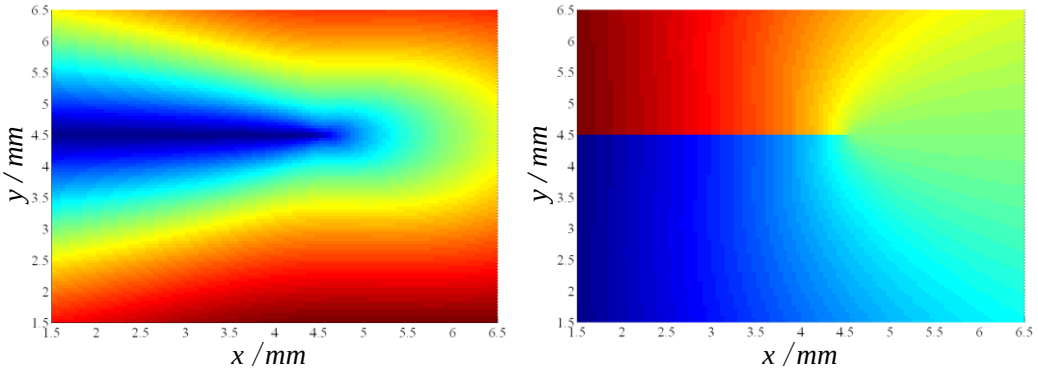

a) Horizontal displacement field b) Vertical displacement field

Figure 2-23 Artificial displacement around the I-mode crack tip

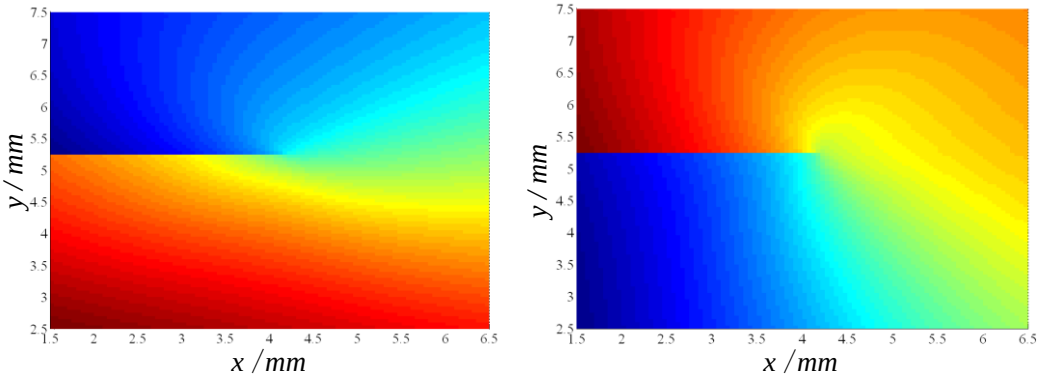

a) Horizontal displacement field b) Vertical displacement field

Figure 2-24 Artificial displacement around the mix-mode crack tip

Table 2-2 Analysis results of the current method for the displacement fields of different crack types

Type	Iteration	Crack-tip location before iteration		Crack-tip location after iteration		Exact crack-tip Final location		error		time/s
		x/*mm*	*y*/*mm*	*x*/*mm*	*y*/*mm*	*x*/*mm*	*y*/*mm*	*x*	*y*	
Pure I mode	1	2.00	2.00	4.50	4.50	4.53	4.47	0%	0%	0.219
	2	4.5	4.5	4.55	4.45					1.000
	3	4.55	4.45	4.53	4.47					1.844
	4	4.53	4.47	4.53	4.47					2.610
I-II mixed mode	1	2.00	2.00	4.00	5.50	4.17	5.23	0%	0%	0.219
	2	4.00	5.5	4.15	5.25					1.015
	3	4.15	5.25	4.17	5.23					1.812

4	4.17	5.23	4.17	5.23	2.594

2.7 Studies on the Fatigue Damage Behavior of Active Jet Engine Chevron[3]

The combination of theoretical research, experimental test and finite element simulation is used to study the fatigue damage behavior of active jet engine chevron. The main research contents are as follows: Firstly, as an actuator of the jet engine chevron, the experimental researches for shape memory alloys are uniaxial tensile test and DSC test to obtain the various thermodynamics and physical properties parameters. Fatigue tests are performed on smooth shape memory alloys specimens with different maximum stress and different stress ratios to obtain the stress-strain curve under different cycles and the fatigue life.

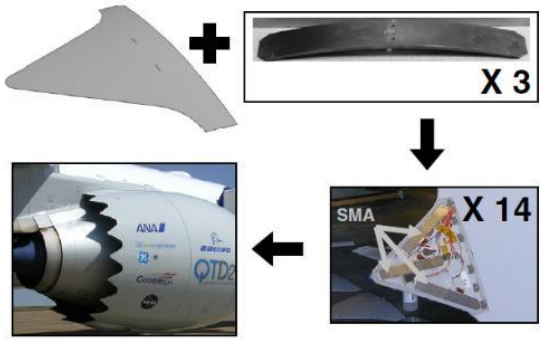

Figure 2-25 Structure layout of aero engine with VGC device (Hartl et al.,2010a)

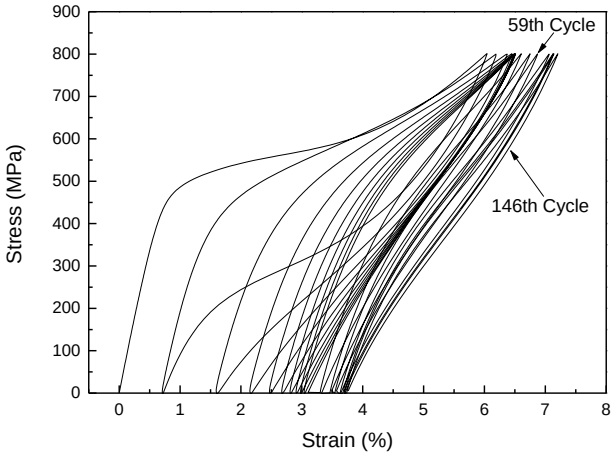

Figure 2-26 Cyclic deformation behavior of SMA materials

[3] Civil Aviation University of China. LIU Bingfei: Bingfeiliu2@126.com.

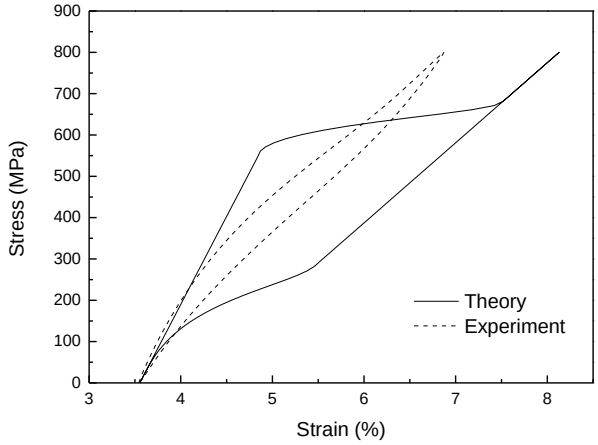

Figure 2-27 The stress-strain curve in 59th cycle

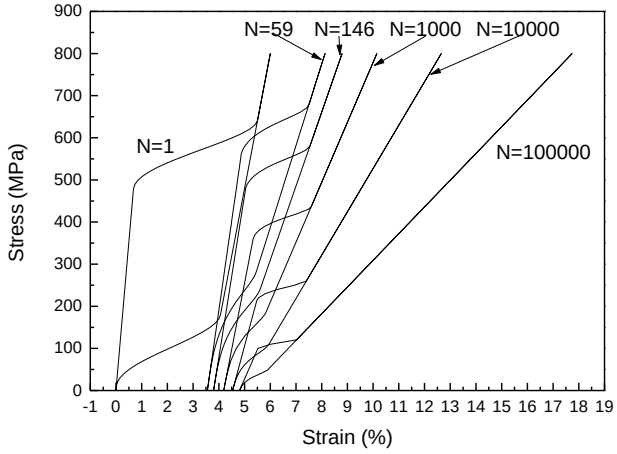

Figure 2-28 Simulation results when N=1, 59, 146, 1000, 10000 and 100000

Secondly, the thermo-mechanical constitutive model is then developed to describe the behavior of shape memory alloys considering the damage. Based on the continuum damage mechanics theory, assumed that when the damage happens, the mass density, the elastic compliance tensor, the thermal expansion coefficient tensor, the specific heat, the specific entropy and the maximum phase change strain are all caused damage. The model is started from the second law of thermodynamics, a detailed procedure for the estimation of the stress-strain relationship is presented while the plastic strain caused by phase change is ignored. The relationship between the evolution law of the damage extent and the number of load cycles is then established according to the theory of damage mechanics. Numerical results of the stress strain relationship for the shape memory alloys under different damage extent are finally discussed, and comparing with the experimental results to verify the correctness of the model. When the damage disappears, the model can be degenerated to the no damage condition.

Finally, a finite element model of the jet engine chevron is established combined with the finite element software, and the fatigue damage behavior of active jet engine chevron is then studied by cycle loadings, and the mechanical behaviors such as stress distribution, strain distribution and tip deflection for the jet engine chevron under different degree of fatigue damage are discussed, respectively.

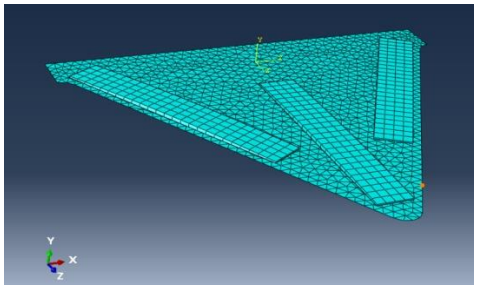

Figure 2-29 Finite element modeling of the jet engine chevron

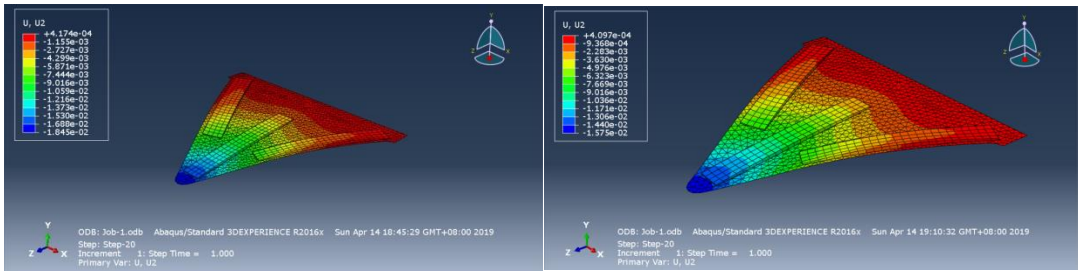

(a) no damage degrees (b) damage degree is 0.1

Figure 2-30 The max tip deflection of the jet engine chevron

2.8 Material Configurational Forces Applied to Mixed Mode Crack Propagation[4]

New fracture criterion (termed as *C*-force criterion) based on the material configurational forces is proposed. The basic assumption is that the onset of crack growth occurs when the resultant of configurational forces reaches a critical value and the crack growth takes place in the direction of resultant configurational forces. The experimental procedure on evaluation the configurational forces is proposed by using the digital image correlation. It is demonstrated that the C-force criterion provides a more convenient and accurate procedure to predict the mixed mode crack propagation.

Key Techniques

The main concept is to present a failure criterion based on the concept of configurational forces which are regarded as the crack driving forces. The implementations of the configurational forces into the finite element are presented. The newly proposed *C*-force criterion is further validated through a series of examples. We can conclude that the predictions of mixed-mode crack propagation by *C*-force criterion are in good agreement with experimental data in the open literatures. Then, the configurational force based fracture criterion is validated to successfully describing the crack propagation under mixed-mode loading conditions. In addition, the digital image correlation technology ensures the further applications of present theory to the aviation industry.

The *C*-force Fracture Criterion

The mixed mode crack propagation will be deflected from its original path due to the non-symmetric material structure or mixed-mode loading with respect to the crack plane. Herein, an intriguing theory to predict the mixed-mode crack propagation can be proposed according to the physical interpretation of

[4] State Key Laboratory for Strength and Vibration of Mechanical Structures, School of Aerospace, Xi'an Jiaotong University. LI Qun: qunli@mail.xjtu.edu.cn.

the crack tip configurational forces. The C_1-force is identical to the crack extension forces and it has been given as the rate of total potential energy release per unit crack-tip advance along its original direction. Analogously, the C_2-force has been given a precise and clear physical significance as the rate of total energy release by postulating that the crack will skew the tip advances perpendicular to its original direction, as described in Figure 2-31.

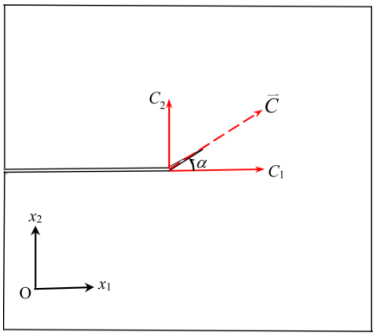

Figure 2-31 *C*-force criterion in the mixed mode crack problems.

Under these considerations, a new fracture criterion (termed as *C*-force criterion) is proposed where two basic stipulations on crack propagation will now be made in plane problems:

i) The initial crack growth takes place in the direction ahead of the crack tip along the configurational resultant forces $\vec{C}$. The initiation angle of crack can be determined by

$$\alpha = \arctan\frac{C_2}{C_1}$$

where α is the crack-kinking angle.

ii) The onset of crack growth occurs when the magnitude of configurational resultant forces |C| overcomes the material resistance. i.e.,

$$|C| = \sqrt{C_1^2 + C_2^2} \geq C_R$$

where C_R is the material fracture resistance which is a material constant regardless of the crack configuration and loading conditions. The value of C_R provides a knowledge of mixed mode crack extension in that it specifies the fracture toughness of the material.

Finite Element Simulations

The special treatment of *C*-force criterion to predicting the crack growth path and the critical load will be clarified and addressed by a series of representative crack examples. The crack propagation is simulated by using the finite element method for each propagation step, then the mesh near the crack tip is modified to take into account the new crack advance. Figure 2-32 shows the numerical results presented by *C*-force criterion are compared with experiment results.

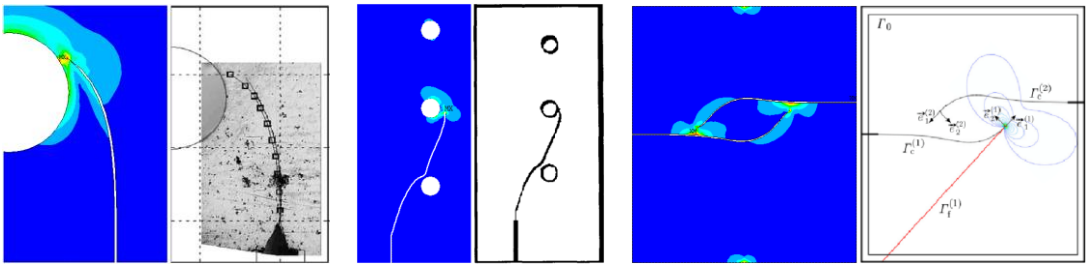

Figure 2-32 Comparison of crack growth trajectory for different crack configurations between numerical results by *C*-force criterion and those by experiments.

Experimental Evaluation of Material Configurational Forces by Digital Image Correlation

The optical measuring method using digital image correlation (DIC) provides the feasibility to determine the whole strain-displacement fields for the damaged material (Figure 2-33).

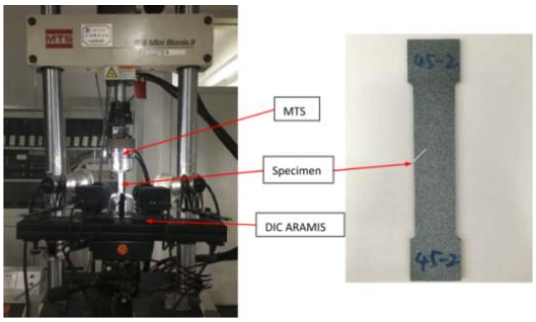

Figure 2-33 Experimental evaluation of configurational forces using digital image correlation.

2.9 Numerical Investigations on the Three-Dimensional I/II Mixed-mode Elasto-plastic Fracture for Through-thickness Cracked Bodies [5]

Based on three-dimensional (3-D) I/II mixed-mode fracture experiments on an LC4CS aluminium alloy, 3-D I/II mixed-mode elasto-plastic finite element models were established using the commercial software package ANSYS. The coupled effects of the varied degrees of mode-mixing Φ and thickness B on the stress field around the crack tip were analyzed, and then the coupled effects of mode-mixing Φ, thickness B, and relative length a/W on the load-crack opening displacement curve were investigated. The results showed that the angle of the maximum tangential stress and the minimum out-of-plane stress constraint factor (T_z) appeared at the same angle with each increment of Φ, and the effects of thickness became weaker with changes to the direction angle of $\sigma_{\theta\theta max}$ and T_{zmin} with each increment of thickness. The load-crack opening displacement curve was affected by loading angle, relative length a/W, and thickness: the thickness effect was stronger when mode I loading predominated. The load-crack growth length curve can be plotted with reference to the experimental load-crack opening displacement curve, which can be used to predict initiation load in static fracture experiments.

[5] Nanjing University of Aeronautics &Astronautics. WANG Fangli: wangfangli2010@163.com.

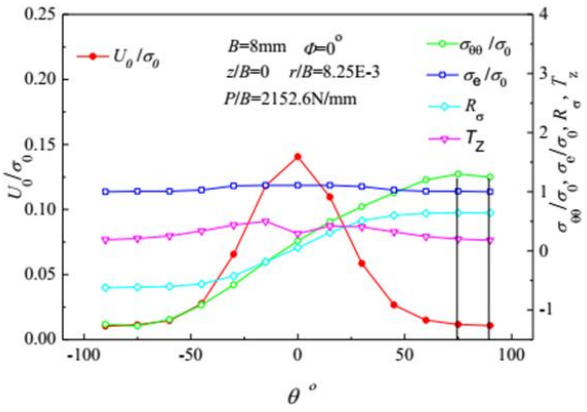

Figure 2-34 Angular distributions of parameters near crack tips for 8 mm thickness under various loading angle conditions.

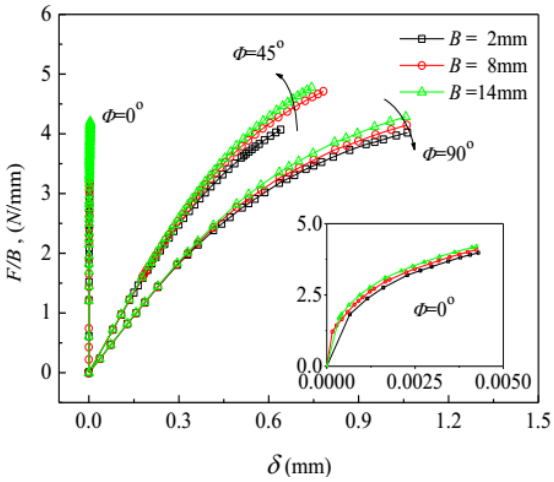

Figure 2-35 Load-crack opening displacement curves for different thicknesses under various loading conditions.

2.10 The Optimization and Design of Complicated-Surface Panel Based on Automate Fiber Placement [6]

Due to the developments of high-performance composite materials, multi-constraint optimization designing methodologies and automate fiber placement (AFP) technologies, various advantages of applying AFP to fabricate composite panels are obtained. However, in terms of the composite panels subjected to the out-of-plane pressures, there are still many problems to be solved. For the purpose of minimizing the panel' weight and optimizing the best manufacturing technology, this paper investigates the optimal designing of the composite panel considering the panel layout, stiffeners' details and the routine of AFP.

According to the requirements of structure's stiffness, strength, stability, durability, damage tolerance, maintenance capability, the structure is not allowed to buckle under the limit load, while local buckling can occur before the ultimate load (Figure 2-36). Besides, when the overpressure is applied, some local damages of the materials are permitted in such a structure which is designed based on constraints of the loads, temperature, sealant condition, corrosion resistance and so on. To gain the lightest structure, four options including the thick-skin panel, the sandwich panel without stiffeners, the panel with hoop

[6] AVIC Shenyang Aircraft Design and Research Institute. LIU Liyang: llyjsls@sohu.com.

stiffeners and the rigid stiffened panel are optimized and compared.

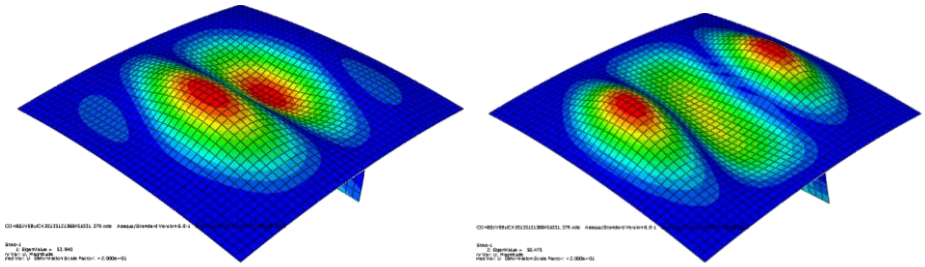

Figure 2-36 The First-order and Second-order Buckling Mode of a Double-curvature Stiffened panel

For the special characters, such as the irregularly double curvature and largely negative curvature, the panel under the complicated loading conditions, the analysis method and failure criteria are proposed. The iso-parametric shell element (Figure 2-37) is utilized to simulate the skin and stiffeners, and the interface between the above two components is simplified as a specially defined element. Accordingly, the process of buckling, post-buckling and the damaging can be analyzed, which means the interlaminar damage of both skin and stiffeners is detailed through the corrected Hashin criteria. Furthermore, the interlaminar damages at the normal and tangential directions are controlled by the tension and shear criteria respectively. With the combination of all the validation experiments at every level of the pyramid procedures, the availability and veracity are validated and corrected. All the designing allowables of the composite panel are confirmed. Finally, the analysis methodologies of the stiffness, strength and load-carrying capability of the rigid stiffened panel with negative curvature are established.

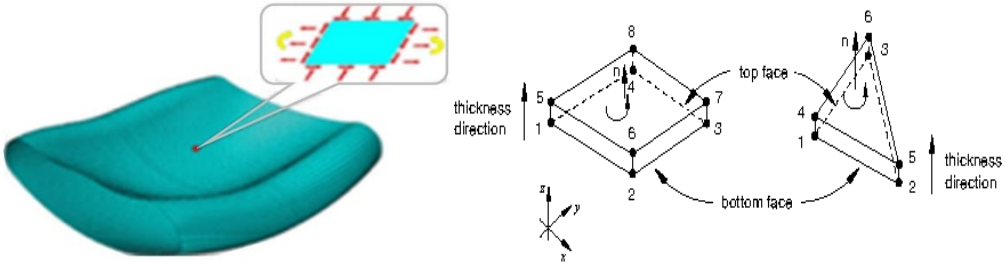

Figure 2-37 The Iso-parameter Shell Element

It is known that the sophisticated surface of the composite panel generates quite different curvatures at different positions. The fibers tracks of AFP on the regular surface cannot cause obvious errors, while it is inversed for the irregular surface whose fibers tracks could offset the expected seriously. This could cause some fibers overlapped or separated. Consequently, it is very of difficulty to ensure the practical fibers' angles in line with finite element models. This phenomenon, especially the serious areas, can rise the problem of fibers' torsion and warping deformation, resulting in the reduce of panel's stiffness, strength and load-carrying capability. In order to minimize this effect, all the requirements about the structural strength, manufacture-process realize and quality control are taken into account, when the composite panel is designed. The effects of direction's offset, overlaps, and gaps of the fibers on the structural strength, surface smoothness and structural weight are investigated and validated. The designing criteria as well as the manufacturing standards are defined. In addition, the fiber tracks are optimized through numerous iterations, which generate the accurate definition of designing parameters of the complex composite panel.

2.11 Fatigue Properties of Composite Laminates with VID Damage[7]

Fatigue behavior of composite laminates with VID impact damage is an important part of durability and damage tolerance research of Aeronautical composite structures. In this paper, two kinds of woven composite laminates with the same thickness and different proportions of layers are selected. VID impact damage introduction test, compression-compression fatigue test with VID damage and post-fatigue residual strength test are carried out. At the same time, damage propagation, dent rebound and stiffness change of the composite laminates with VID damage are monitored during fatigue process, and the characteristics of damage propagation, dent rebound and stiffness change are obtained. The results show that dent depth will rebound rapidly at the initial stage of fatigue, and the rebound rate will decrease dramatically thereafter, and the rebound rate is very slow. Under typical fatigue load, the damage propagation of composite materials is not obvious during fatigue, and the stiffness of laminates remains constant.

Table 2-3 Test specimen information

No. of Ply	[(±45)/(0/90)]	Ply	Pro Company	Thickness t /mm
1	50%/50%	$[(\pm45)/(0,90)]_{5S}$	A	4.6
			B	4.6
2	60%/40%	$[(\pm45)_3/(0,90)_2/(\pm45)_2/(0,90)_2/(\pm45)]_S$	A	4.6
			B	4.6

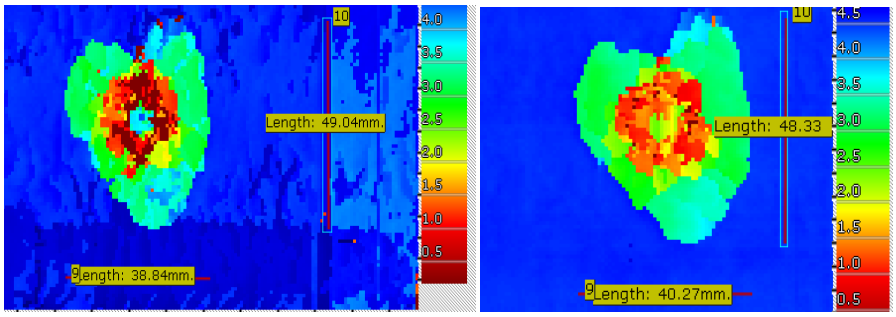

a) Before and after fatigue test of 1# Ply

[7] AVIC Aircraft Strength Research Institute. CHENG Pengfei: yydsdy2008@126.com.

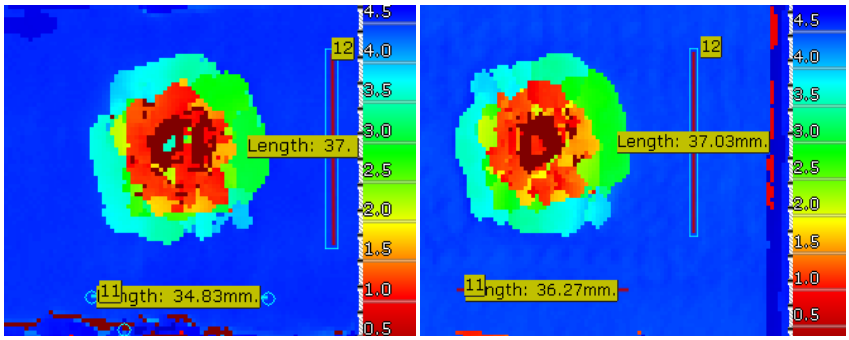

b) Before and after fatigue test of 2# Ply

Figure 2-38 Damage image comparison before and after fatigue of Two kinds of Plies

2.12 A New Prediction Model for Corrosion Fatigue Analysis[1]

The fatigue behavior of pre-corroded LD2CS and LD10CS aeronautic aluminum alloys were tested. A practical parabolic model of corrosion pits was presented and novel formulations were deduced to calculate stress intensity. It is showed that the new model and algorithm can predict more accurate than the traditional half elliptical and semicircle models, and the stress intensity were more realistic. Afterwards, an algorithm was developed to predict fatigue life of pre-corroded aeronautic aluminum alloy subjected to cyclic loading. The life predicted for pre-corroded aluminum alloys are shown in Figure 2-40.

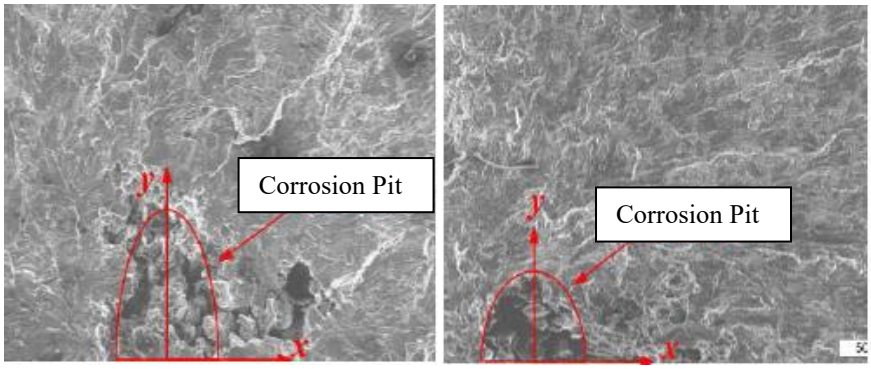

(a) LD2CS, pre-corroded 1540h (b) LD10CS, pre-corroded 1540h

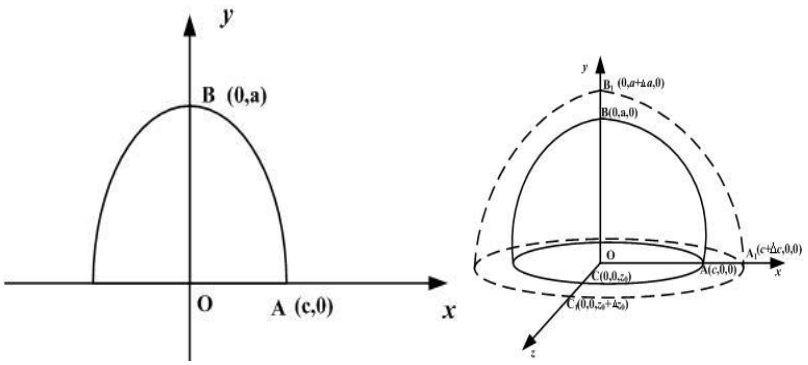

(c) theoretical corrosion pits boundary (d) theoretical corrosion pits geometry

Figure 2-39 Corrosion pit topography of Aluminum alloy

[1] AVIC China Helicopter Research and Development Institute. CHEN Yaping: cyp28503059@avic.com.

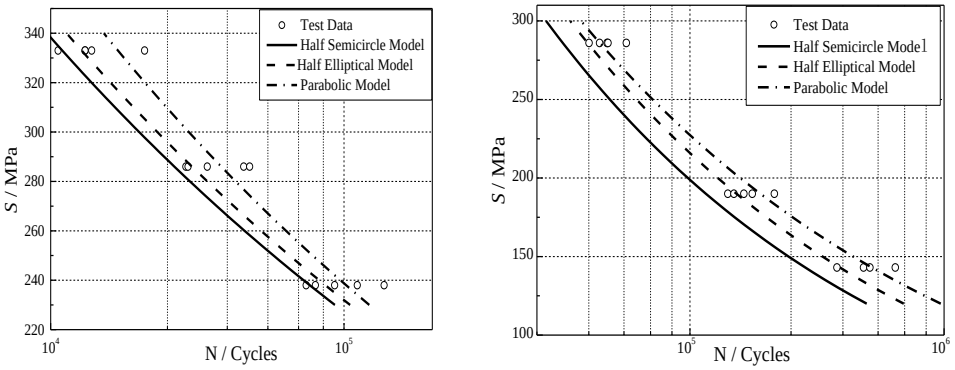

(a) LD2CS, pre-corroded 1540h (b) LD10CS, pre-corroded 1540h

Figure 2-40 Fatigue test results and predictions of two pre-corroded aluminum alloys

2.13 Technique for Predicting the Corrosion of Multi-material Coupling System on Aircrafts [1]

Corrosion as a major phenomenon triggering multi-site damage poses a great threat to the safety of aircraft. Corrosion damage also can act synergistically with fatigue damage to destroy the aircraft structure and reduce aircraft life. Corrosion protection in today's air fleet plays a very important role and it is an ongoing, dynamic process that starts with design and manufacturing and continues with inspection and maintenance to assure structural integrity and airworthiness for continued flight safety under economical operational costs, regardless of airplane age. In order to meet the strength requirements and minimize the weight of the aircraft, the material system on aircrafts often contains many kinds of materials, such as aluminum alloy, titanium alloy, high strength steel and so on. The increased application of this "mixed materials" enhances the risk of galvanic corrosion when they are coupled in the presence of a corrosive electrolyte.

Technique Targets

As everyone knows, corrosion testing is extremely time-consuming, and it often fails to meet the time requirements for aircraft design. Corrosion prediction models based on finite element models (FEM) will save aircraft development and implementation cost via minimization of testing. It also can be combined with expert systems and databases to allow a more efficient and reliable materials selection. Corrosion under common marine atmospheric environment and solution immersion conditions of aircraft was considered. The realization of corrosion simulation will be helpful to the quantitative design of aircraft corrosion and the life evaluation and extension.

Test Device

[1] Naval Aeronautical Engineering Institute. CHEN Yueliang: CYL0532@sina.com.

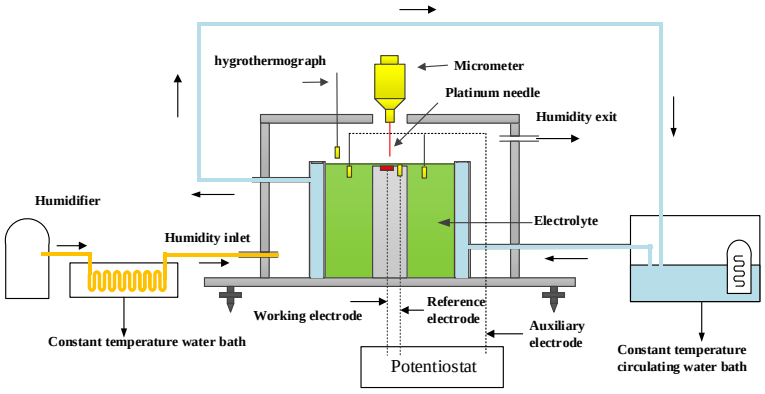

Figure 2-41 Atmospheric corrosion polarization measuring device

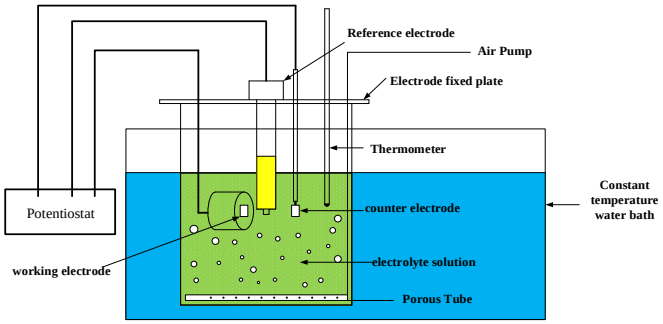

Figure 2-42 Polarization measurement device under solution soaking conditions

Key Techniques and Some achievements

A complete simulation prediction system, test pieces→simulation specimen→structural parts→overall unit, for the atmospheric and immersion corrosion of aircraft is proposed to provide guidance for aircraft anticorrosion design and outfield maintenance. Some achievements are shown in Figure 2-43 and Figure 2-44.

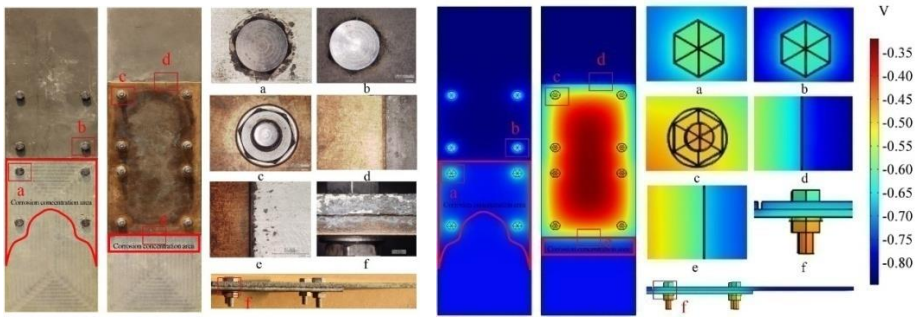

Figure 2-43 Comparison of simulation and test results of simulation specimen

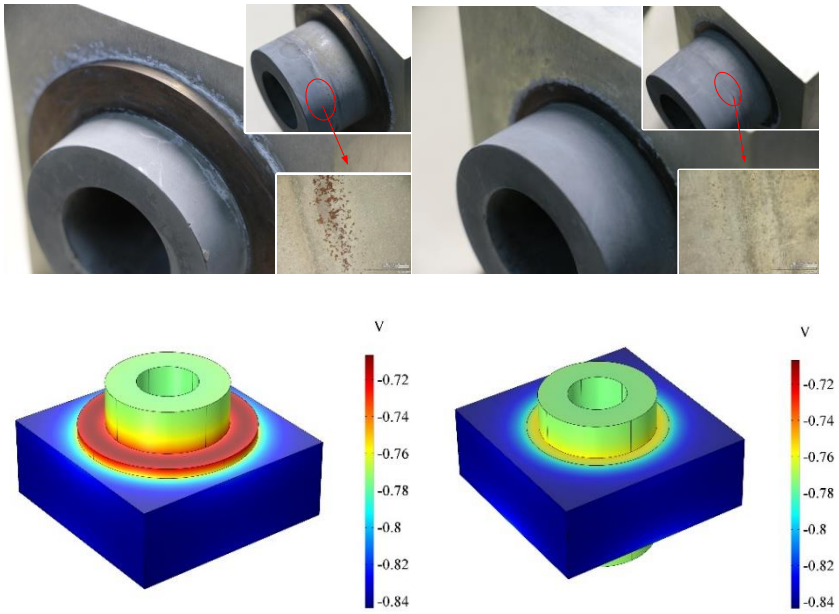

Figure 2-44 Comparisons between simulation and test results of structural parts

2.14 ASE Flight Test Motivation Response Simulation Technology [1]

Before the aero-servo-elasticity (ASE) test flight, configuration state of ASE flight test aircraft, all test points according to ASE flight test outline, simulation and ASE flight test excitation response under control surface excitation. It has the following advantages: (a) it can quantify the acceleration and displacement of the aircraft vibration response at each test point, and can be used for flight test monitoring at each test point of ASE flight test; (b) the dynamic stability of aircraft can be judged according to the Dynamic characteristics of time domain signals; (c) the amplitude of excitation signal and resonance can be given, which can provide reference for ASE flight test excitation signal.

Using excitation response analysis in ASE test flight can not only increase the safety guarantee of ASE test flight, but also accelerate the test progress of ASE and improve the test flight monitoring level of test of ASE.

The simulation scheme of excitation response in ASE test flight is shown in Figure 2-45, including the following steps: (a) confirm the ASE flight test status points; (b) building structural dynamics model of ASE flight test aircraft (mass, stiffness and damping, steering surface rotation frequency); (c) according to ASE flight test points, time-domain excitation response simulation and prediction dynamic models (including structure and control law) for ailerons, rudders and elevators were established respectively; (d) according to ASE flight test points, the time domain excitation response simulation analysis of aileron, rudder and elevator excitation states was carried out; (e) according to the analysis results, after data processing, the peak curve and attenuation coefficient trend curve of time-domain response were classified and drawn, and the key monitoring points and vibration response acceleration, displacement, damping and other parameters of ASE flight test point were given.

The simulation response of the wing tip acceleration of the aileron frequency exciter is shown in Figure

[1] AVIC Chinese flight test establishment. LEI Ming: leiming061012@163.com.

2-46, the simulation response of the wing tip acceleration of the aileron pulse exciter is shown in Figure 2-47.

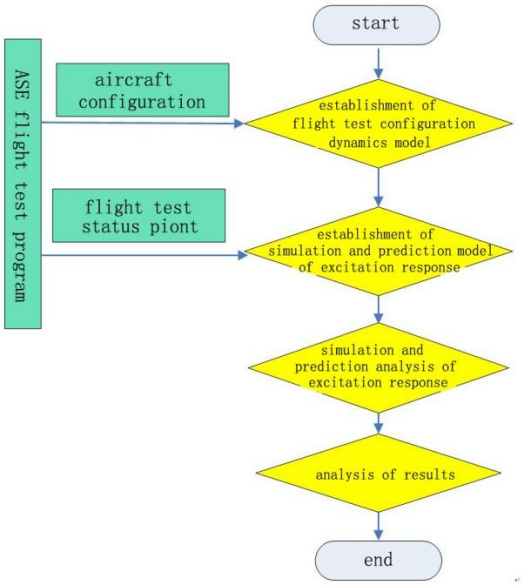

Figure 2-45 ASE flight different excitation aeroelastic response simulation scheme

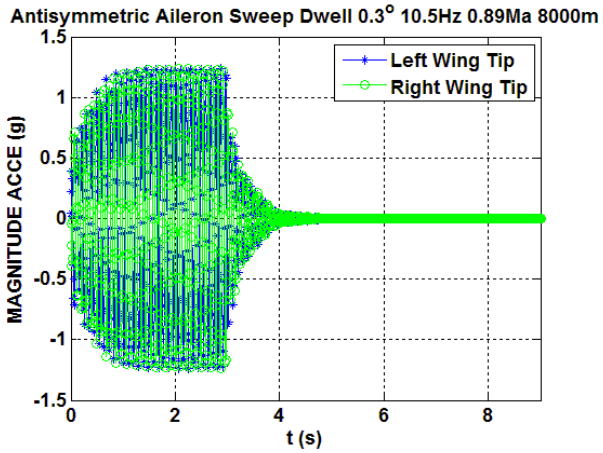

Figure 2-46 The relation between the tip acceleration and time of aileron constant frequency airfoil

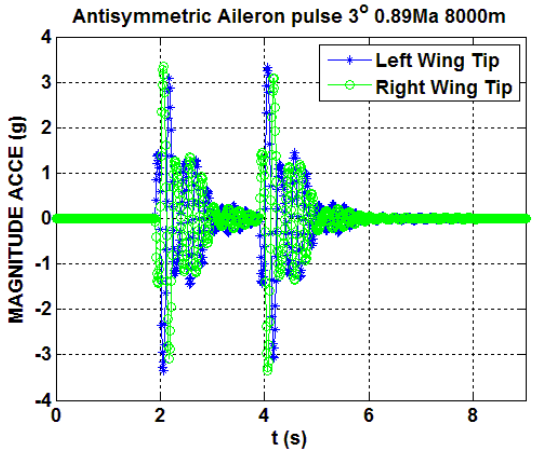

Figure 2-47 The relation between the acceleration of the tip of the wing and time

2.15 The Flight Test Technology of the Helicopter Rotor Strains Based on the Fiber Optical Sensor[1]

The blade strain reflects blade local characteristics, real-time dynamic measurement of blade strain can predict the local load state, and this method can provide reliable evidence which can evaluate and improve blade structure and improve blade quality. The working environment of helicopter blade is very special, there are some problems in the application of traditional electrical strain gauge to the measurement of helicopter blade strain, such as large additional mass and large influence of blade profile. The fiber grating sensing technology concentrates a large number of strain sensors in a signal fiber, forming a quasi-distribution, quasi-fixed point sensor array and having the advantages of simple structure and strong anti-interference capability, especially suitable for distributed strain measurement of helicopter blade. The developed FBG strain airborne test system is applied to helicopter flight test, the feasibility of applying distributed FBG network to helicopter blade strain test flight is verified.

Comparative test analysis

The comparison test between light grating technology and resistance strain technology was carried out, the result showed that both measures maintained a good linear relationship, and the deviation of strain data measured by the former is 1.22%, while that of the latter is 1.36%, therefore, the reproducibility of the former is better than that of the latter.

On the physical simulation platform of blade flight attitude, Fig1 shows the strain change of a certain section when the light grating measurement is used to simulate the flapping motion of the blade. The result shows that the fiber grating can monitor the strain condition of blade surface very well, at the same time, the symmetry of the curve reflects that the method has good repeatability。In conclusion, the fiber grating can monitor the strain condition of the blade surface in real time, and the data obtained is reliable comparing with the data from the traditional strain tests.

[1] Chinese flight test establishment. CHENG Weizhen: avicavic@eyou.com.

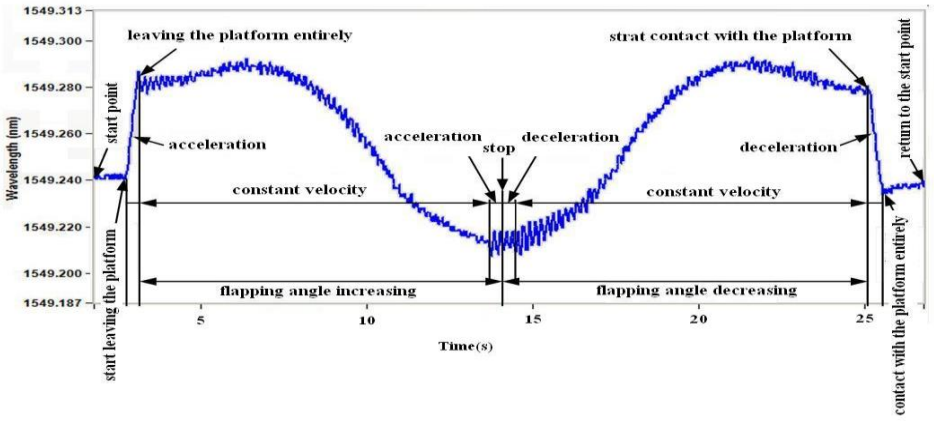

Figure 2-48 Blade surface FBG strain detection curve

Fiber grating strain airborne test system

The FBG strain airborne system is composed of customized FBG string, GPS timing module, power module and so on, as shown in Figure 2-49. The system can simultaneously measure the distributed flap-wise strain and the azimuth signal of the blades. The FBG strain airborne system is mounted on top of the rotor hub and rotates synchronously with the rotor. The azimuth of the blades is measured by a reflective photoelectric switch.

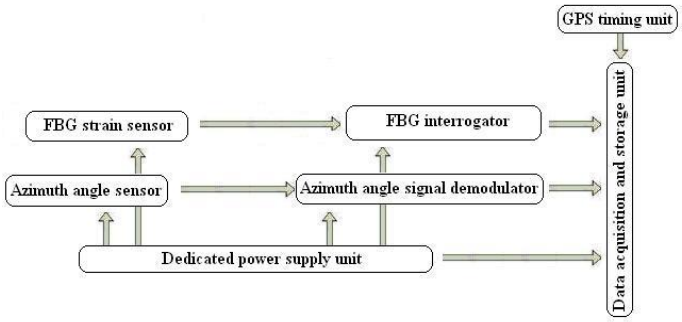

Figure 2-49 Fiber grating strain airborne test system

Flight test results

According to the test flight outline, the test machine was equipped with the required sensors and airborne test equipment and completed all the test flight subjects. Figure 2-50 and Figure 2-51 show the measured blade profile strain time history and spectrum analysis under hovering and flying conditions. The result show that the periodicity and regularity of the measurement are obvious and accord with the theoretical analysis

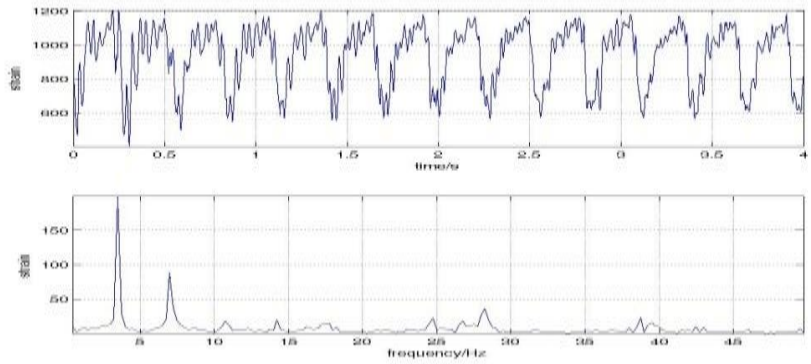

Figure 2-50 Measured blade profile strain time history and spectrum analysis in hovering

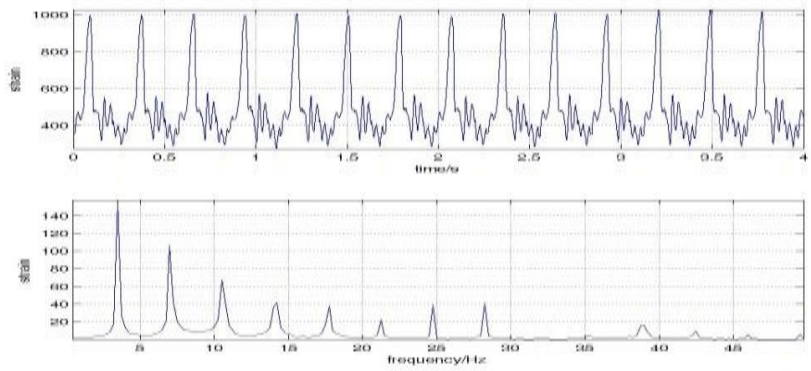

Figure 2-51 Measured blade profile strain time history and spectrum analysis in flat flight.

Figure 2-52 and Figure 2-53 show that the measured strain history curves of the 4 profile optical of the blade under flying conditions; the mean values of the four sections of the blade measured by FBG and strain bridge are shown in Figure 2-54. The result shows that the periodicity, regularity and order of magnitude of the FBG measurement results and the wheat stone bridge measurement results can be mutually verified. The measured value of strain gauge in profile is greater than that of FGB, because the weight and speed of the helicopter by the strain gauge measure are greater than those by the FBG measure. Therefore, it is feasible to measure the strain using FBG on the rotor blade of helicopter.

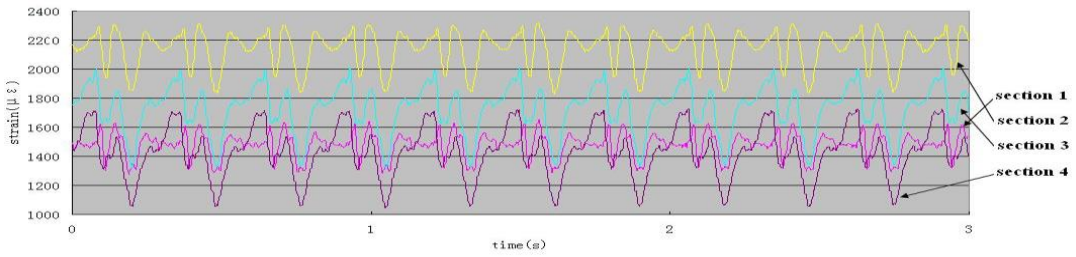

Figure 2-52 Measured FBG strain history curves

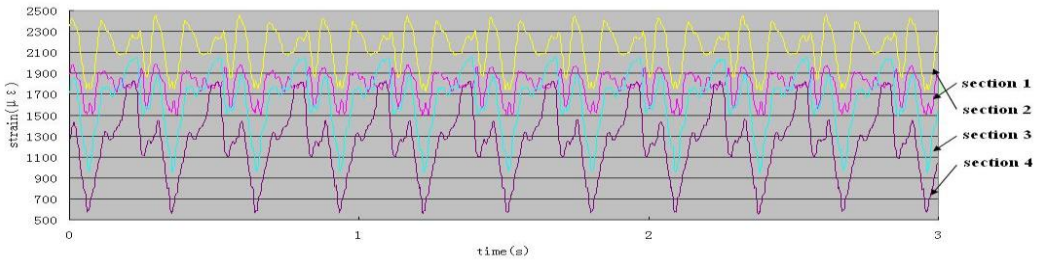

Figure 2-53 Measured history curves by traditional strain bridge

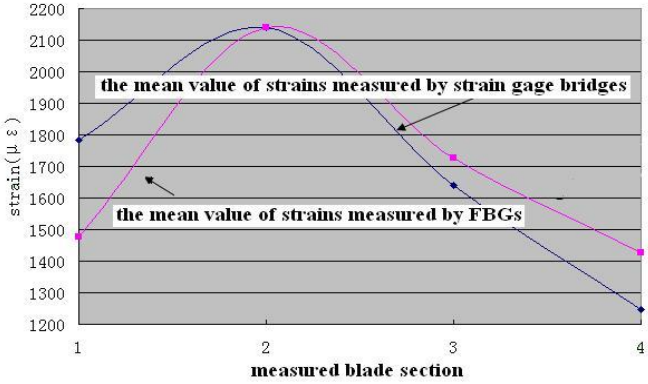

Figure 2-54 Mean values of the four sections of the blade measured by FBG and strain bridge

3. APPLIED RESEARCHES ON FATIGUE AERONAUTICAL AND STRUCTURAL INTEGRITY

3.1 Assessment of Aircraft Structural Service Life using Generalized Correction Methodology[1]

Aircraft structural service life assessment with high accuracy is one of the key techniques of Individual Aircraft Tracking (IAT) Program and Structural Prognosis and Health Management (SPHM). In the state-of-the-art IAT programs, fatigue life analysis and crack growth analysis used by different countries and different aircrafts vary from each other based on different methodologies and philosophies.

Concept

This research proposes a generalized correction methodology by determining the scaling of fatigue life or damage and crack growth rates (CGR) between test results and predictions, which is divided into life correction rule and CGR correction rule, the former is the linear scaling of crack initiation life or damage (as Eq. 3.1 and Figure 3-1) used for crack initiation modeling, the latter is the linear scaling of CGR (as Eq. 3.2 and Figure 3-2) used for effective block approach (EBA) model.

$$Life_{2,e} / Life_{1,e} = Life_{2,p} / Life_{1,p} \text{ or } Damage_{1,p} / Damage_{2,p} \quad (3.1)$$

[1] AVIC Chengdu Aircraft Design and Research Institute. DUI Hongna: duihn060379@126.com.

$$CGR_{2,e} / CGR_{1,e} = CGR_{2,p} / CGR_{1,p} \quad (3.2)$$

where the subscripts 1 and 2 represent the tested and untested spectra, respectively; the subscripts *p* and *e* indicate "predicted" and "experimental", respectively.

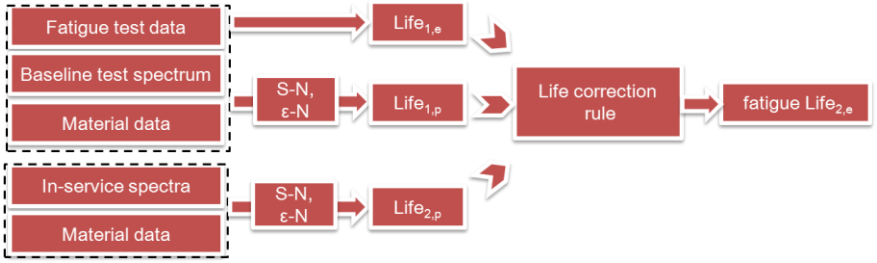

Figure 3-1 Flowchart of application of life correction rule

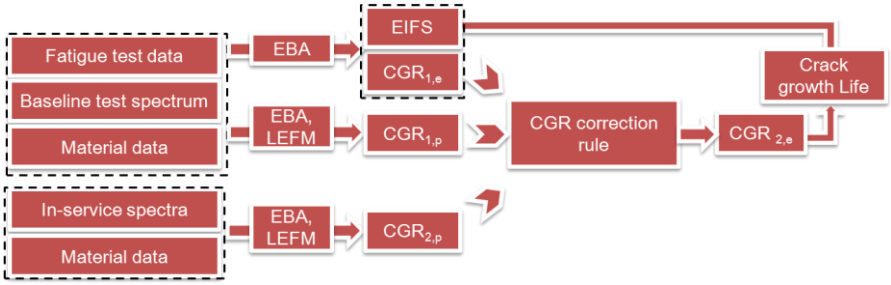

Figure 3-2 Flowchart of application of CGR correction rule

Application

According to different management philosophies, structural service life can be categorized as durability life referring to crack initiation life or maintenance life and damage tolerance life referring to inspection interval with some safety factor taken into consideration. Based on representative coupon test data, the optimal durability analysis can be selected from crack initiation models as well as LEFM models implicitly in the EBA approach, and the optimal damage tolerance analysis can be selected from LEFM models implicitly in the EBA approach, as shown in Figure 3-3.

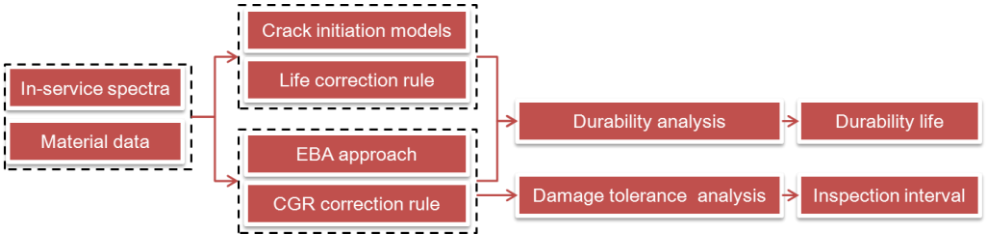

Figure 3-3 Flow chart of procedure of DaDT analysis

Case study

Case study of some bulkhead representative coupon fatigue test data is reviewed where the implementation of generalized correction methodology has been comprehensively examined and validated, and the optimal model for DADT analysis is each selected.

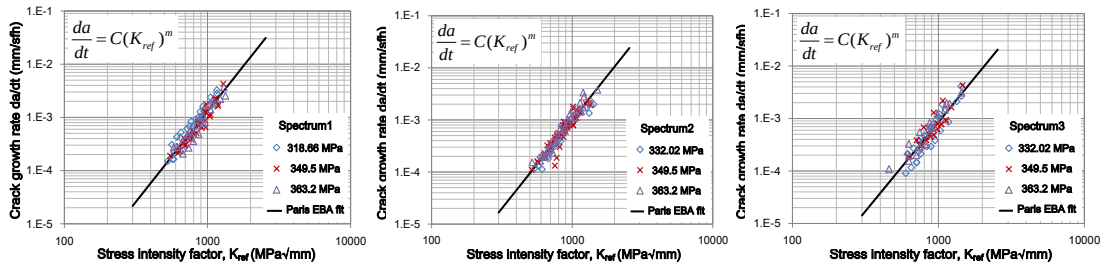

Figure 3-4 CGR vs Kref for the representative coupon data

Experimental CGR fit of Paris-type EBA are given in Figure 3-4. It is shown that EBA model gives a reasonable representation of the experimental CGR, and EBA model parameters are insensitive to stress level compared to load sequence.

For the totally 32 prediction cases, *ε–N* approach and EBA3 approach (i.e. Walker equation with Closure model implicitly in EBA model) should be selected for durability analysis and EBA3 approach for damage tolerance analysis. Figure 3-5 is correlation plot of predicted life and test life.

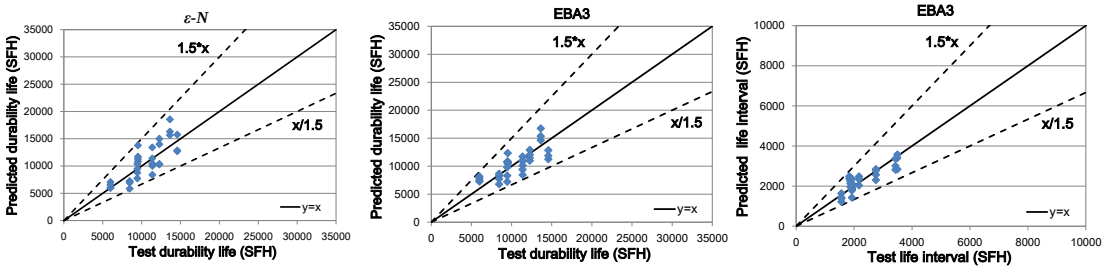

(a) Durability life by *ε–N* approach (b) Durability life by EBA3 approach (c) Life interval by EBA3 approach

Figure 3-5 Correlation plot of predicted life and test life

It has proved that the prediction accuracy of generalized correction methodology is largely dependent on the selection of DADT models. The generalized correction methodology proposed in this study is anticipated to provide highly accurate and reliable structural service life assessment for agile fighter aircraft under operational load spectrum.

3.2 Research on the Airworthiness Compliance Strategy of Composite Structure[1]

This research analyzes some regulation requirements closely related with composite and proposes a technical road map of the development and verification of composite structure.

Regulation compliance analysis

Material requirements. Based on the data provided by the material supplier for initial screening, material screening test could be conduct to prepare the draft material specifications. Then, the applicant could implement PCD Audit, material pre-identification for accessing comprehensive material performance data. Based on the data, the first draft of material specifications is established for preliminary design. If the applicant formally submits the type certification application, it is necessary to submit the specification and the data to authority in accordance with the FAR25.603, and prepare the material qualification test plan, carry on the test, form the formal material specification, approve into the QPL. Material specifications and materials that meet the requirements of FAR25.603 can be used for detailed structural design and validation.

Process requirements. According to the design characteristics of specific structural parts to choose the applicable process methods, the applicant could prepare the process specifications. The parameters in the process specification obtain through element tests, such as composite laminate suction and curing temperature, time and pressure. The porosity and mechanical properties are measured, and the curing process parameters of the materials are determined.
Then, within the requirements determined by the process specification, through the study of the

[1] Shanghai Aircraft Design and Research Institute of COMAC. LI Weiping: liweiping@comac.cc.

manufacturing process of specific structural parts (including the molding process method, the mold scheme, the process scheme and the forming process of each part), the process procedure of the parts is compiled. the manufacturing study, pre-part manufacturing (PPM), the thermal distribution test, cutting, mechanism testing and other tests are conduct to optimize a variety of molding process parameters.
Synchronously, non-destructive inspection (NDI) the standard block is developed.
Finally, the various formal process specifications and process procedures are established. The applicant submits the certification test plan of process specifications. After certification test, the process specification can be effective and implemented. Then the prepared various types of process procedures and PPM implementation plans are submitted to the authority. Only the results combine with the prediction, a manufacturer can formally produce certain types of parts in accordance with the approved process procedures, thus completing the compliance with FAR25.605.

Material allowable value. The typical layups of laminate are selected to test according to the Test Standard of airworthiness approval. The material allowable values (FAR25.613) are obtained on the statistical analysis of testing data, and used for structural design and strength analysis. The results are generally required a comparison with the relevant test data of the material supplier to ensure consistency between the processing process method of the user and the supplier.
Structural design value. After the material and process is determined, some typical design detail and structural element are tested for design value considering the stable and qualified manufacturing. The results should be approved by authority and the determined allowable value (FAR25.613) for specific details are used in structural design and strength analysis.

Test planning of composite main structures

The recommended compliance strategy of composite structure is building block. The development and verification building block could be divided into development tests for design/manufacturing and airworthiness tests for verification.

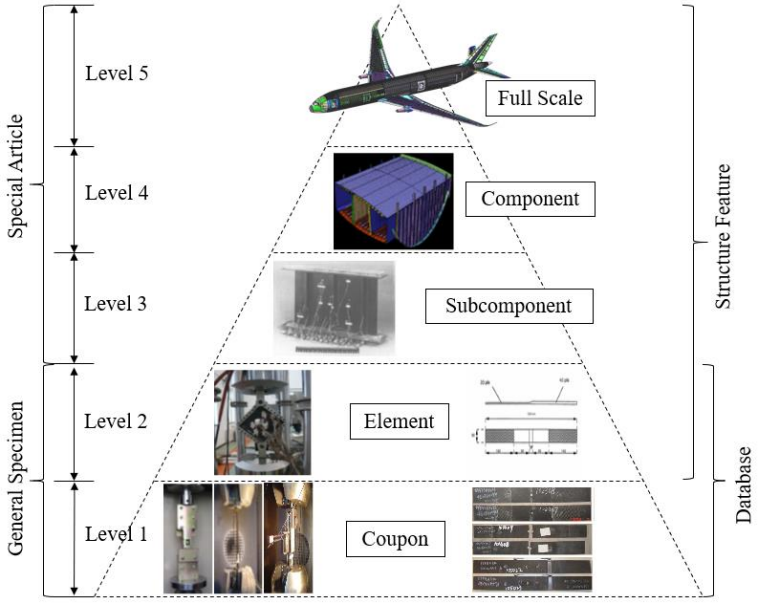

Figure 3-6 Building block test level

Development tests for design and manufacturing.

In the development of composite structure, engineering research and development test must be carried out as follows.
Material research: material screening and process selection are inextricably linked and must be carried out together. It is the responsibility of the material supplier to ensure that the user has the correct knowledge of the process. The supplier shall provide performance data for the processing of selected materials under the technological conditions of its plant facilities. And the user will process and test the selected materials under the conditions in which they are actually used for production, compare the data, and ensure consistency between the process conditions of the user and the supplier.

Process research: On the basis of preliminary determination of process specifications, the process parameters are determined through testing. The formal process specifications and NDI specifications are established.
Pre-Parts Manufacturing: For all kinds of structural parts, the molding process are researched. The mold design and manufacture needs to be studied and controlled. Thermal distribution measurement and cutting test are carried out according to the types of structure configurations.
Structural parts research and development: This parts contains series of structural parts configuration selection test, including panels (plane and curved plate), stringer, frame, beam and so on. The results are applied for structural detail design and selection, including all kinds of joints and integrated structure details, analysis method research and verification.
Allowable values and design values: Before the process study is completed, a batch of mapping tests can be carried out for structural design, taking into account a variety of use environmental factors. When the process specification is determined or approved, a comprehensive allowable value test is carried out for detailed structural design and validation.
Damage tolerance: The load spectrum of composites was compiled, and the low-load truncation value is determined by sample fatigue test. The damage characteristics of various structural parts are researched, including the introduction of manufacturing defects and impact damage. The type, size, location and energy of the damage need to be obtained through test and statistical analysis, and all kinds of damage in service must be covered. The goal is to verify the structural capability of 5 types of damages (BVID, VID, LVID, discrete source damage, abnormal damage) and manufacturing defects of various structural parts. In this process, the acceptance requirement of composite part manufacturing and structural inspection outline is established.
Repair considering: The repair requirement should be considered to select repair materials, repair process, repair design, repair analysis, repair tolerance, and repair during maintenance through the repair test. All above repair method and strength recovery should be verified.

Airworthiness verification test. According to the conformity analysis of the airworthiness regulations, the airworthiness verification test is carried out for each clause, and the requirements of AC20-107B are followed. It should pay attention that the strength verification test of composite structure can not only rely on full-scale test. It needs to plan the building blocks of various levels of validation tests according to structural characteristics and process methods. All airworthiness verification tests are subject to approval by the authority, manufacturing conformity inspections, on-site witnesses, approval processes, and eventually obtaining airworthiness approvals for the closure of the terms.
Materials: The applicant should prepare specifications and invite the authority for on-site PCD audit. During PCD audit, the material qualification test plan should be approved and the test procedure should be witnessed.
Process: The applicant should prepare process specifications, submit the verification test plan to authority for approval, and conduct process verification test by authority on-site witness.
Parts manufacturing: For all kinds of structural parts, full-size parts and integral molding structural parts of the pre-production verification Test (PPV). This procedure should invite the authority on-site review. The results should be stable and accepted by the authority.
Allowable value: After the process specification is determined, the tests of the allowable value are carried out. It is necessary to consider the influence of various environments.
Structural verification: Validation tests are carried out for each structural detail, typical structural parts, and full-scale structural components.
Damage tolerance: During the structural validation, it should be verified at the same time that the ability of 5 types of damages identified by each component and the acceptable manufacturing defect/.
Repair: The repair method for each component (repair material, repair process, repair design, repair analysis, repair allowance) is validated and incorporated into the repair manual, which can be carried out

in conjunction with structural verification.

Conclusion

Through an analysis of the airworthiness requirements of composite structures, it is concluded that there is sufficient experimental support, controllable manufacturing process, continuous maintenance of proven configuration state is the fundamental guarantee of product quality and stability of composite structural parts, and is also an important prerequisite for the design and manufacture of composite structural parts to obtain approval from the authority. Therefore, it should pay attention to the integrated development ideas of materials, process, design, analysis, manufacture, testing, verification and maintenance of composites, and plan the test tasks of various specialties, according to the building block of development and verification.

3.3 Damage Tolerance Research on Composite Material[1]

With the gradual application of composites in the main structure, COMAC began to study the damage tolerance assessment technology of composite main structures. The main work carried out are damage threat, manufacturing defect impact research, composite fatigue analysis method, composite damage tolerance analysis method and damage tolerance verification research.

In the damage threat: COMAC has analyzed 25,000 aircraft damage data in nearly 7 million flight hours, and the energy level of Type I damage has been determined according to the zone division. COMAC has investigated the unexpected impact incident data and runway foreign object from 4 Class 4C, 4 Class 4D, 4 Class 4E, 2 Class 4F, a total of 14 airports in nearly 10 years. Damage resistance test, impactor equivalence simulation test and dent rebound test were carried out to determine the energy level that may occur in the operating environment.

Figure 3-7 Ground Vehicles around aircraft

Figure 3-8 Impact Damage on Slat induced by Maintenance Tool

[1] Shanghai Aircraft Design and Research Institute of COMAC.

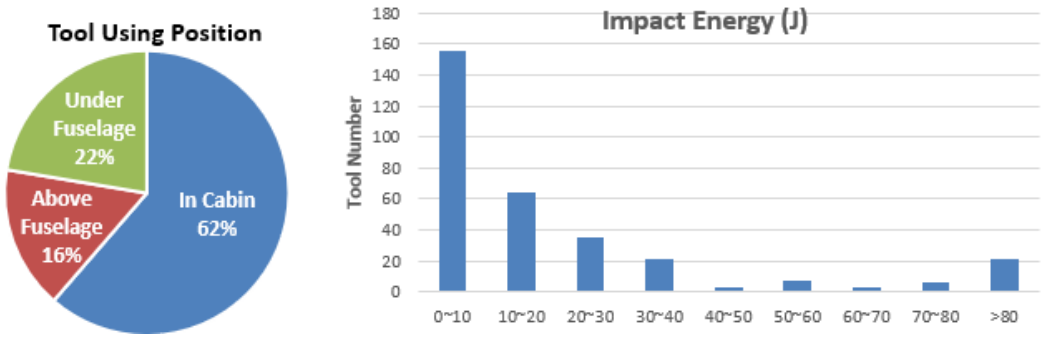

Figure 3-9 Maintenance Tool Statistical Analysis

In the manufacturing defects: In recent years, the statistics analysis of manufacturing defects introduced in the whole manufacturing process has been completed, and the measurable indication has been studied, and the detectable and acceptable limits have been determined.

So far, COMAC has carried out more than 30,000 fatigue and residual strength tests with manufacturing defects and impact damage in types of laminated plate, stringer compression, shear tie pulling, frame compression, frame four point bending, co-bonding interface four point bending, co-bonding interface eight point bending, stiffened panel compression and shear, curved panel under combined load, etc.. The propagation characteristics of initial manufacturing defects and damage under repeated loads are studied, and the residual strength of the structure is determined. It was used as the input of avoiding harmful damage expansion or non-extended design in the design. The above test results are used to support the development of composite structure fatigue analysis and residual strength analysis method. The fatigue analysis method of damaged structure under in-plane loading has been completed.

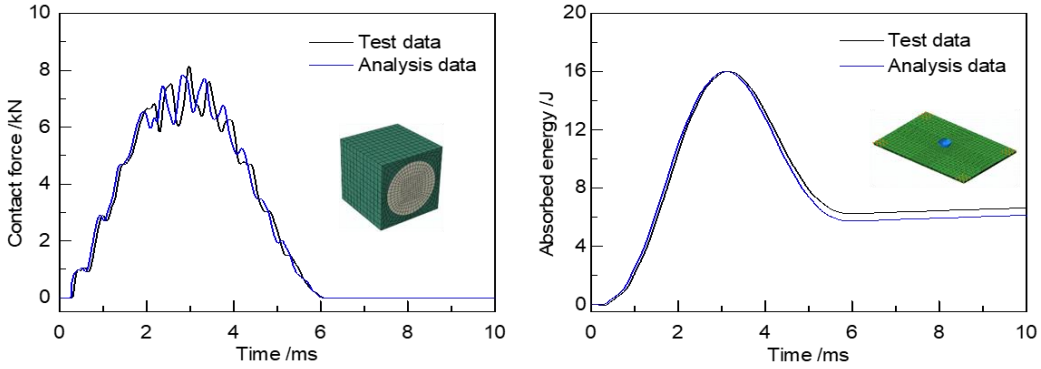

Figure 3-10 Impact Analysis versus Experiment

COMAC has completed the research on Damage tolerance verification based on AC20-107B, which is used to guide the setting of inspection threshold, the method of inspection and the determination of inspection interval, and the analysis and test matrix of damage tolerance, and verification method of composite structure are worked out.

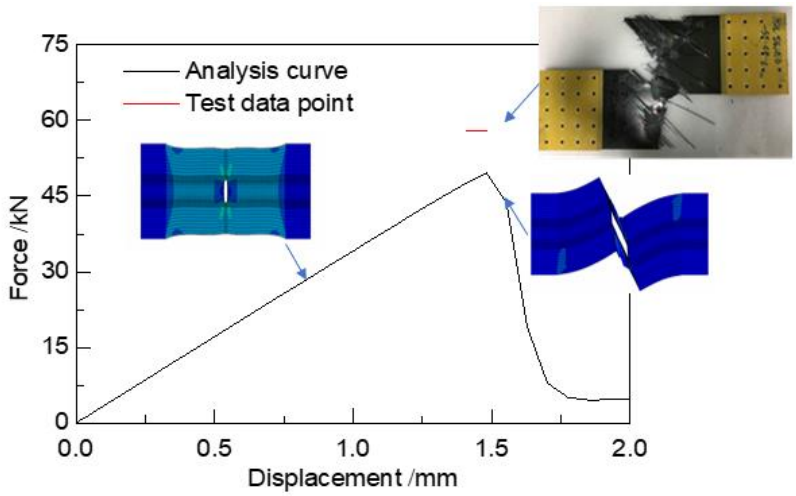

Figure 3-11 Tension on sample with gap

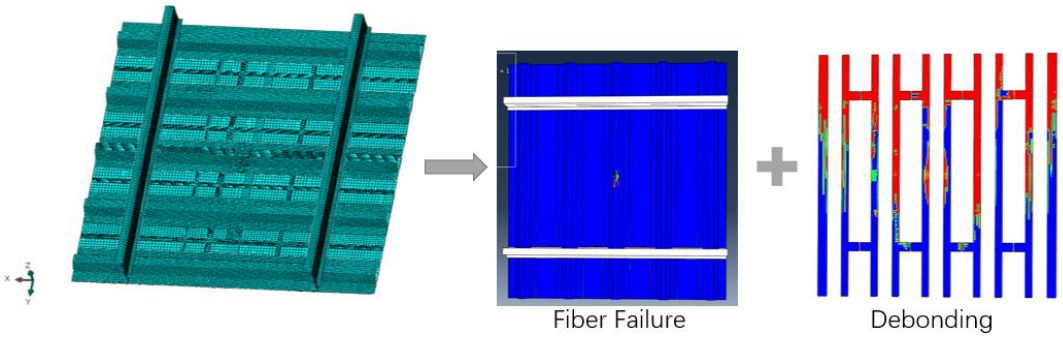

Figure 3-12 CAI Model of Fuselage Panel

3.4 Temperature Control Parameter Demonstrating of Helicopter Rotor Drag-hinge Fatigue Test[1]

The Drag-hinge applies self-lubricating bush material made by POM. While the helicopter was flying, Drag-hinge was oscillating periodically with producing a lot of heat (Figure 3-13). The heat caused the self-lubricating bushing to rise and the damping value changed drastically. Through the establishment of a helicopter drag-hinge self-lubricating friction heat generation\heat transfer model, calculated the total heat of the drag-hinge (Figure 3-14). The heat distribution is calculated on the assumption that the maximum temperature of friction pair contact surface is equal. Applying the commercial finite element software steady-state solution simulated the heat transfer process, obtained the temperature distribution of the friction pair of the drag-hinge when the helicopter rotor was running, Analyzed of heat dissipation equivalence of fatigue-durable test equipment for self-lubricating bushing, Finally determined the temperature control parameters of the test device. The results provide parameters for the design and demonstration of the fatigue durability test of the helicopter's drag-hinge self-lubricating bushing, and provide reference for frication heat generation calculation and temperature distribution calculation of articulated rotor configuration helicopter self-lubricating bushing (Figure 3-15 and Figure 3-16).

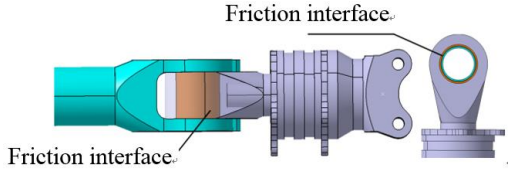

Figure 3-13 Schematic diagram of friction heat generation

[1] AVIC Harbin Aircraft Industry Group Co, LTD. MA Zhanqi: pziq8@163.com.

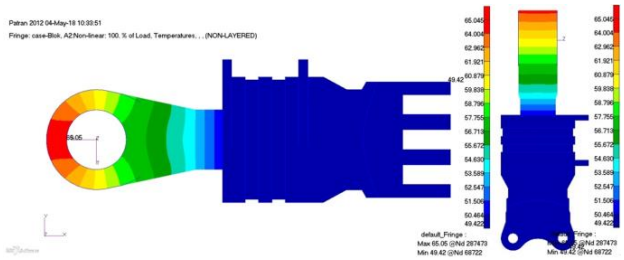

Figure 3-14 Overall temperature distribution result

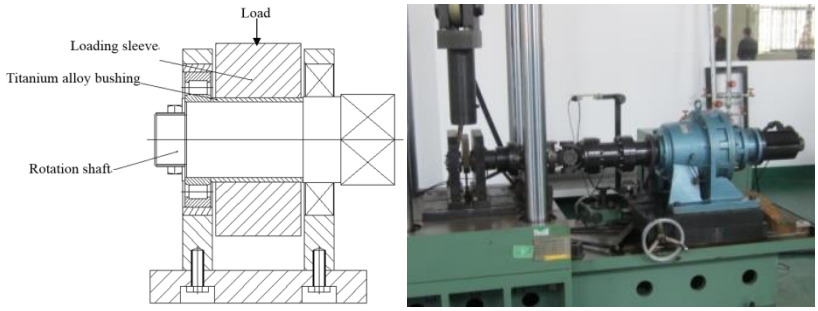

Figure 3-15 Schematic diagram of test device

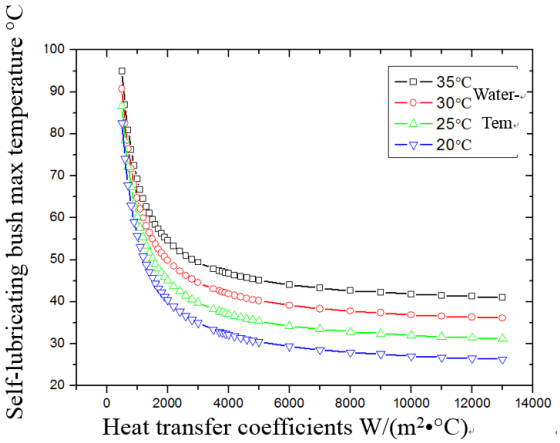

Figure 3-16 Temperature distribution titanium alloy bushing under different heat transfer coefficients

3.5 Research on Buckling Fatigue Behavior of Fuselage Stiffened Panel[1]

During the catapult launch and the arrested landing process for carrier based aircraft, buckling waves of tension field at fuselage panel will induce additional tension or bending stress, which significantly decreases the fatigue behavior of structure and changes the fatigue failure position. Buckling fatigue test was conducted through three-point bending specimen with tension-field spar to study the fatigue behavior under repeated buckling. Critical buckling load measured from the test matches well with that obtained from engineering tension field theory. Then, load to fatigue life curves were derived based on buckling fatigue test under three different load levels. Finally, buckling level using tension field factor can be determined during design process of stiffened panel by adopting the buckling fatigue test results and the design service goal of the aircraft. This job accumulated beneficial data for buckling fatigue of carrier based aircraft during catapult launch and arrested landing.

[1] AVIC The First Aircraft Institute. LI Xiaopeng: merlxp@163.com.

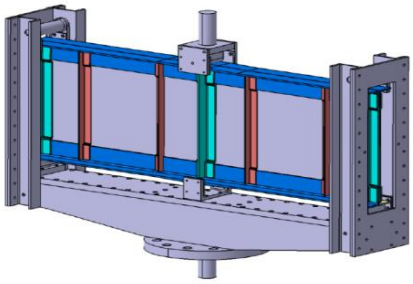

Figure 3-17 Three-point bending load view of specimen for tension field spar buckling test

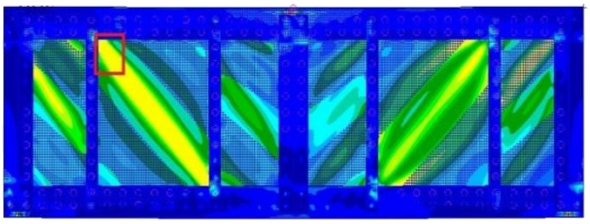

Figure 3-18 FE buckling analysis of test specimen

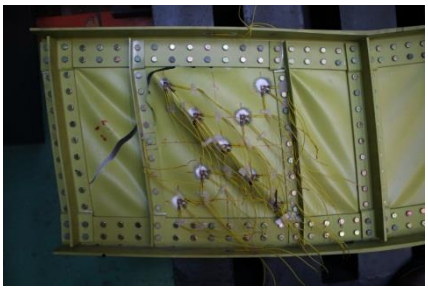

Figure 3-19 Failure feature of test specimen

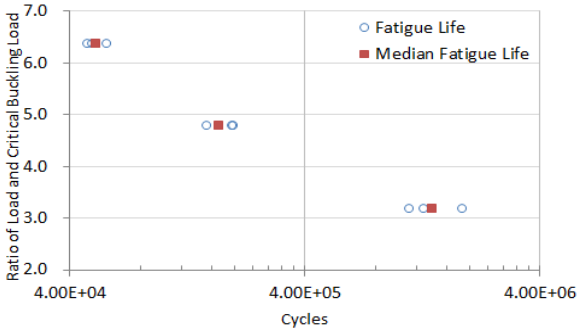

Figure 3-20 Curve for ratio of load and critical buckling load to cycles (t=1.5mm，R=0.1)

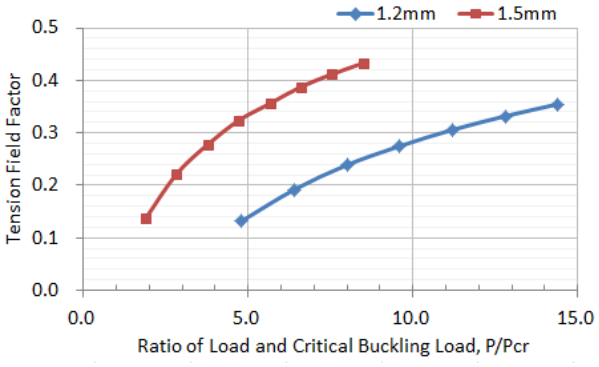

Figure 3-21 Relationship between load and tension field factor

3.6 Design and Verification Technology for Damage Tolerance of Large Size Integral Structure[1]

Application of the integral structure has become the trend of aircraft structure design. There exists big difference of large size integral structure and the traditional assembly structure in the design, due to the absence of fatigue sources such as rivet holes and thus stronger fatigue performance compared to riveted structures. However, there is no crack-arrested element such as rivets, which brings weak damage tolerance performance to the integral structure. Thus, special attention of damage tolerance characteristics should be paid on the integral structure design.

However, these deficiencies can be improved through the detailed design of the integral structure, so that the integral parts may even surpass the assembled structure in terms of damage tolerance performance. Due to the good fatigue and improved damage tolerance of the integral structure, it has been used and promoted by many aircraft with long life (such as large transport aircraft, etc.)

Based on the conventional cracking mode, a finite element model for calculating the Stress Intensity Factor (SIF) of the integral structure was established by static analysis and stress field analysis of the cracked structure. In view of the numerous possible matching structural parameters in the integral structure, the sensitivity of the damage tolerance characteristic parameters of the integral structure to the SIF was analyzed and studied by using the global sensitivity analysis method and the local sensitivity analysis method starting from the weight reduction and effective utilization rate of the structure. According to the calculation boundary, a model including optimization objective, structural parameters and constraint conditions was established, and the optimization analysis of the structure was then carried out. At the same time, the technology of determining the minimum area of the crack-arrested bar on the wing spar in the design of the integral structural was put forward. Damage tolerance analysis method of large size integral structure was verified by fatigue and damage tolerance test combined with available analysis models. Finally, the fatigue and damage tolerance performance of the wing box section of large transport aircraft were evaluated by using this method.

[1] AVIC The First Aircraft Institute. ZHANG Yanjun: sakerzyj@163.com.

Figure 3-22 Damage tolerance test of integral wing lower panel

Figure 3-23 Fatigue and damage tolerance test of integral wing spar

3.7 Influence of Bonded Crack Retarders on Damage Tolerance Performance of Aircraft Fuselage Panel[1]

The effect of bonded crack retarders on fatigue crack growth behavior and residual strength of fuselage panels was studied through the tests of 3 baseline panels (JZ-1, JZ-2 and JZ-3) and 3 reinforced panels (SR-1, SR-2 and SR-3). The baseline panels were curved fuselage panels with 7 stringers and 5 frames. As for the reinforced panels (Figure 3-24), crack retarders made of Glare-2 2/1 0.3 were bonded to the skin under each stringer and between adjacent stringers, along the direction of stringers. An initial circumferential skin crack with a length of 25.4mm was introduced in the middle of each panel. Fatigue crack growth tests were conducted at axial constant amplitude loads till the crack tips approached the adjacent stringers. Static tests were performed as well to determine the residual strength of the panels with two-bay skin crack. Significant retardation was found for the reinforced panels with bonded crack retarders, as shown in Figure 3-25. With the same skin stress, the average fatigue crack growth life of reinforced panels (SR-1 and SR-2) was about 2.7 times of that of baseline panels. The residual strength of reinforced panels was over 37% higher than that of baseline panels.

The fatigue crack growth behavior was also predicted based on finite element model and virtual crack closure technique. The residual strength was analyzed based on modified net-section criterion. Good consistence was found between prediction and experimental results. The mechanism of crack retardation and the influence of the location of bonded Glare straps were identified.

[1] AVIC Aircraft Strength Research Institute. ZHANG Haiying: haiyingzh13@126.com.

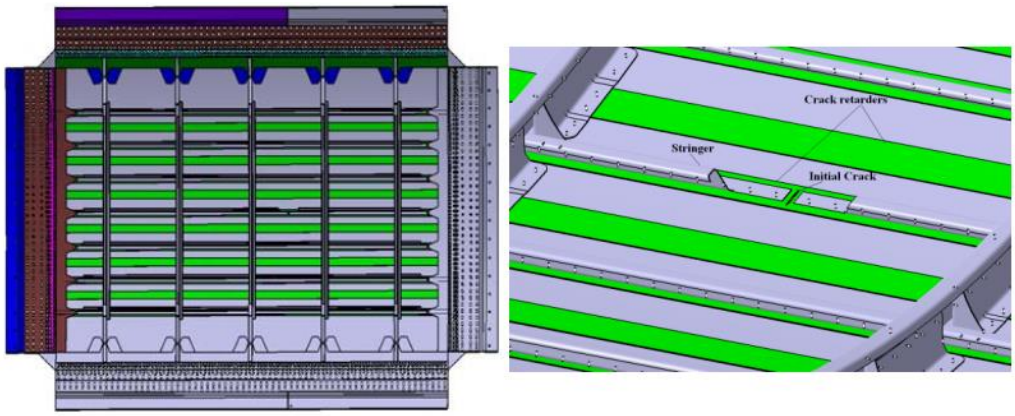

Figure 3-24 Configurations of test panel with bonded crack retarders

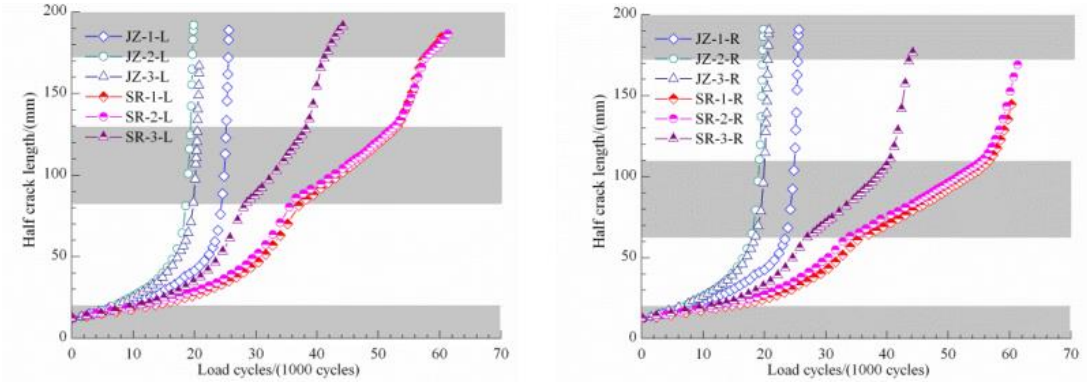

(a) Left side (b) Right side

Figure 3-25 Half crack length vs. load cycles (the grey areas represent retarder locations)

3.8 Fatigue Behavior Prediction and Validation of Wing-fuselage Connection Structure[1]

The wing-fuselage connection structure is an important loading path of the aircraft, and its fatigue reliability directly governs the flight safety. In the present work, the fatigue behavior of wing-fuselage connection structure is predicted on the basis of the finite element method and validated resorting to the fatigue testing. The general static analysis is used to calculate the stress distribution and load transfer of the wing-fuselage connection structure. Subsequently, the value of detailed fatigue rating (DFR) with respect to the structural detail is calculated for the purpose of predicting its fatigue life. The following formulae are used to predict the most dangerous location of the wing-fuselage connection structure, and the corresponding fatigue lives are determined to guide actual fatigue testing:

$$\begin{cases} DFR = DFR_{base} \times A \times B \times C \times D \times E \times U \times R_c \\ N = 10^{\left(5-\frac{\lg Y}{\lg S}\right)} \\ Y = \dfrac{\left(S_{m0} - 0.53DFR\right) S_a}{0.47DFR\left(S_{m0} - S_m\right)} \end{cases}$$

Five details of the structure are evaluated to determine the critical location, as shown in Figure 3-26 and

[1] Avic Aircraft Strength Research Institute. FAN Junling: fanjunling@mail.dlut.cn.

Figure 3-27. The analytical result shows that the most dangerous position is located around the hole of number 2 due to the higher pin load and reference load, as shown in Figure 3-28. Table 3-1 shows the fatigue reliability life with reliability of 95% and confidence of 95%. Experimental result shows that the fatigue life of the structure is in good agreement with the predicted results, with an error of 30.4%.

Fatigue testing is carried out on the MTS testing machine, and the variable stress amplitude is applied on the structure. Experimental result shows that the fatigue life of the structure is in good agreement with the predicted results, with an error of 30.4%, as shown in Table 3.2. The failure location is right around the hole of number 2, which demonstrates the accuracy of the present approach. Figure 3-29 shows the failure of the wing-fuselage connection structure.

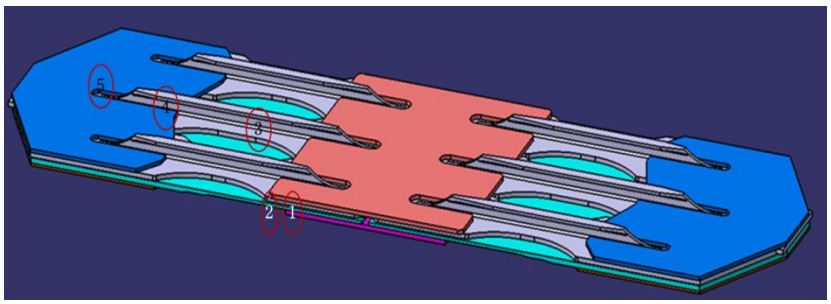

Figure 3-26 Details of the structure

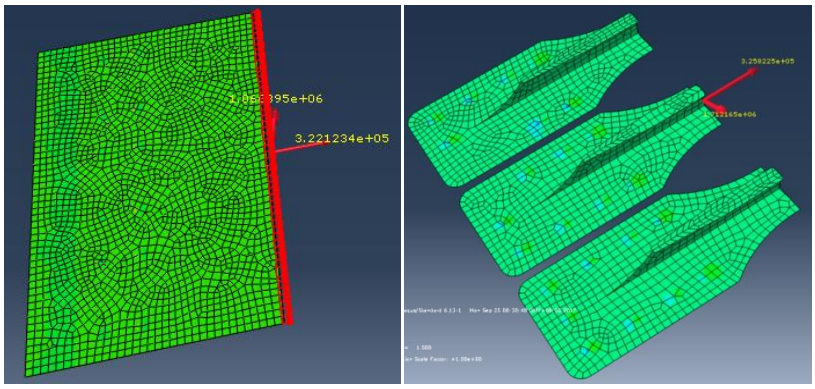

Figure 3-27 Load distributions of the stringer and skin

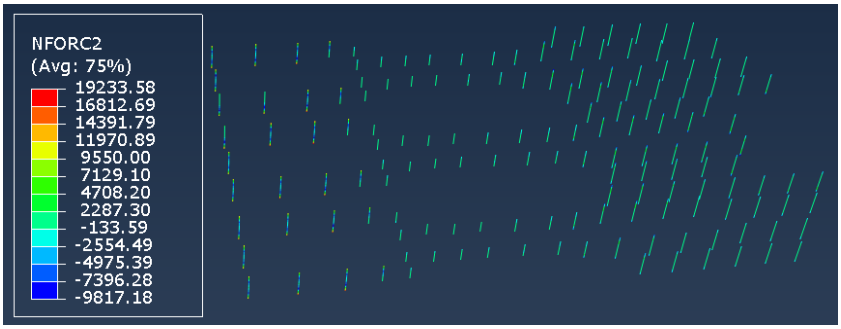

Figure 3-28 Load distribution of the fastener

Table 3-1 Fatigue reliability life of the details

Detail No	1	2	3	4	5
$N_{95/95}$	761613	459577	2426572	7213291	47920345

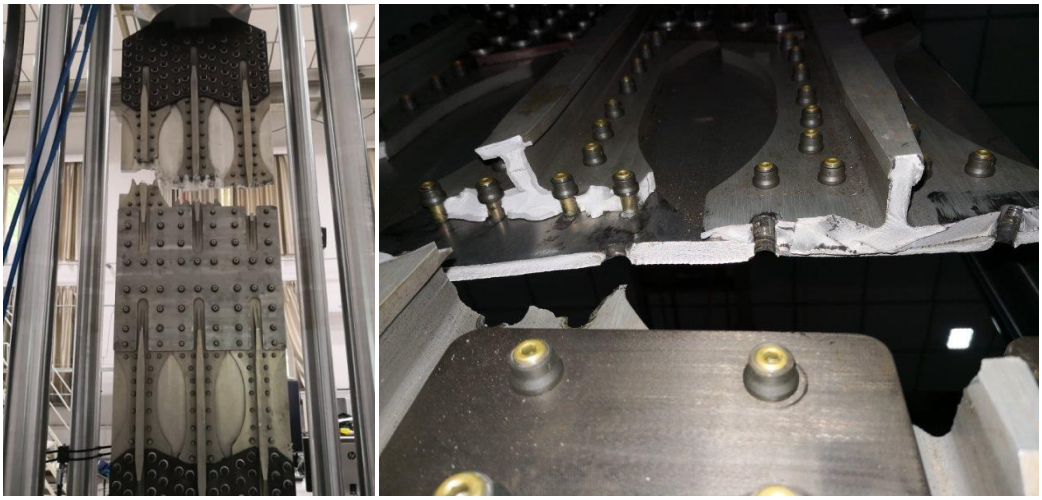

Figure 3-29 Failure of the structure

Table 3-2 Comparison between FEM analysis and fatigue testing

	FEM	Test1	Test2	Error1	Erro2
Characterized life / Block	403	579	309	-30.4%	30.4%

3.9 Vibration Monitoring and Analysis of Accessory Gearbox of Aero-engine in Flight Tests[1]

The accessory gearbox of aero-engine is used to fix and transmit power to the fuel pump, lubricating oil pump and alternator .etc. which is essential for operation. The accessory gearbox has many vibration exciters and is impacted by engine vibration introduced by accessory drive shaft. Therefore, the accessory gearbox appears fatigue crack, bearing and gear wear easily. Several times, these fault lead to lubricating oil leak or transmission failure in flight tests, which result in fight shutdown of aero-engine finally.

Key Techniques

A vibration monitoring has been researched to monitoring the broadband vibration and the component vibration of accessory gearbox, and which data was used to analyze the vibration exciters of accessory gearbox in different states. In addition, the vibration baseline in flight was established for fault warning. In the project, the following techniques were addressed: (a) a real-time calculation method of vibration characteristic quantities of accessory gearbox has been established; (b) a vibration monitoring system has been researched, which can adapt to high-frequency vibration signal; (c) a analyze method of vibration exciters has been established for accessory gearbox; (d) a establishment method of vibration baseline in fight has been developed.

Application effect

The vibration monitoring system has been installed in an aircraft and the broadband vibration and the component vibration of accessory gearbox has been obtained in flight tests, which frequency range is 5Hz~10kHz, the processing error ≤10%(including senor error), the output delay is 0.82s, and the

[1] Chinese flight test establishment. LEI Xiaobo: 627983062@qq.com.

broadband noise can be filtered by system. Figure 3-30 is system working principle diagram, Figure 3-31 is system physical map.

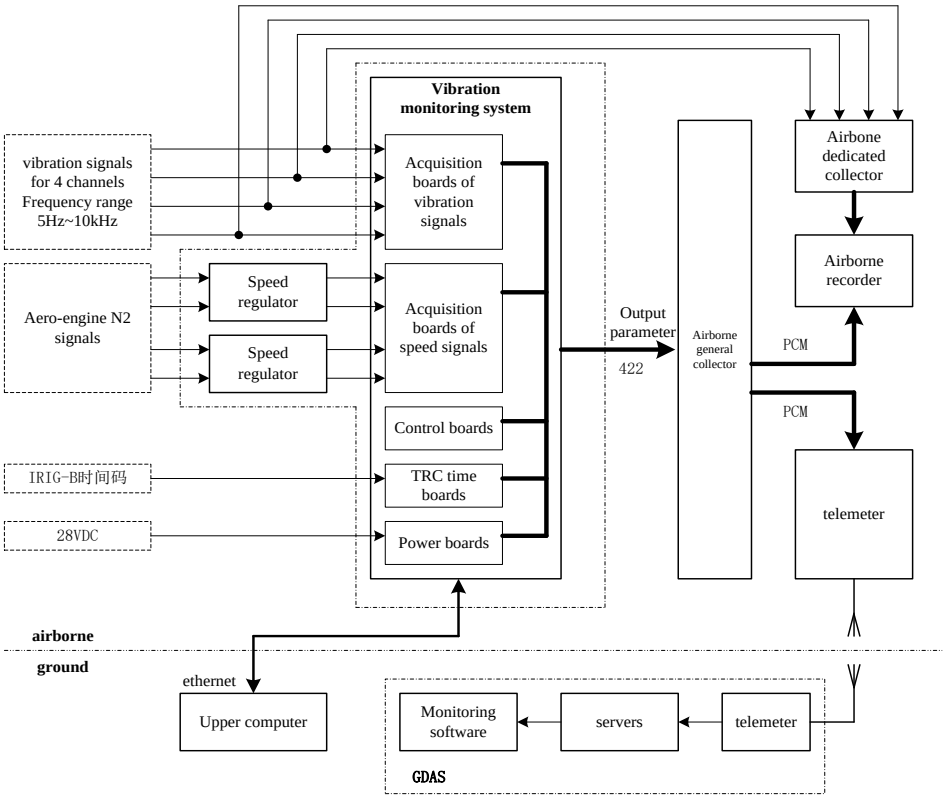

Figure 3-30 System working principle diagram

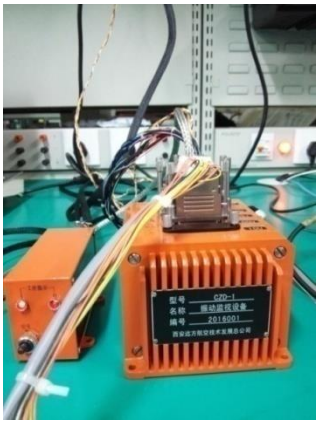

Figure 3-31 System physical map

Figure 3-32 is system physical map the changing curve between the vibration characteristic quantities of accessory gearbox calculated by system and flight altitude and speed of aircraft and the speed of engine high pressure rotor (N2). The rule can be defined that the characteristic quantities mainly change with N2, but they will increase with flight altitude slightly. In addition, the data has been used to find the gear set which is the main vibration exciters of accessory gearbox in various operating conditions. The data analysis can be seen in Figure 3-33.

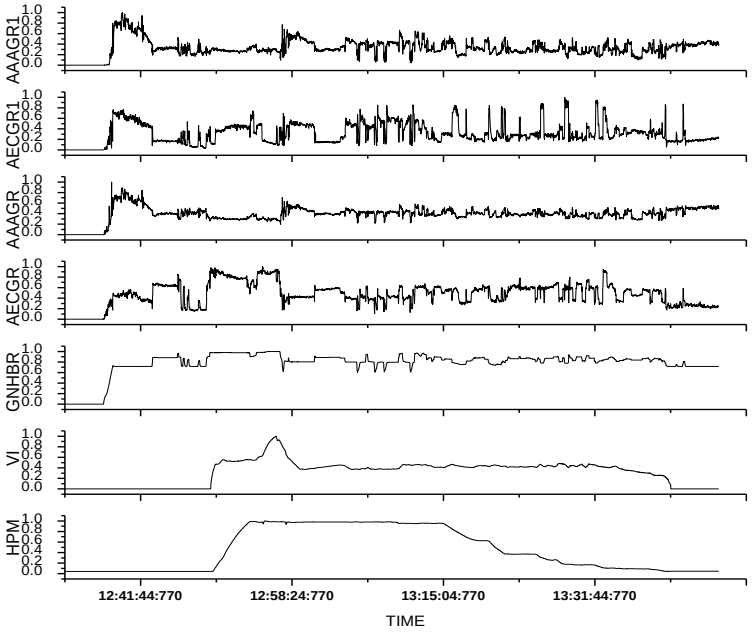

Figure 3-32 The changing curve between several parameters

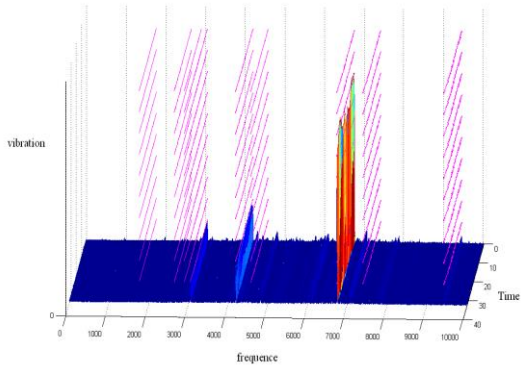

Figure 3-33 Data analysis chart

Finally, the flight tests data in different vehicles and altitudes have been used to established the vibration baselines of accessory gearbox in flight (shown in Figure 3-34), which can be used to fault warning.

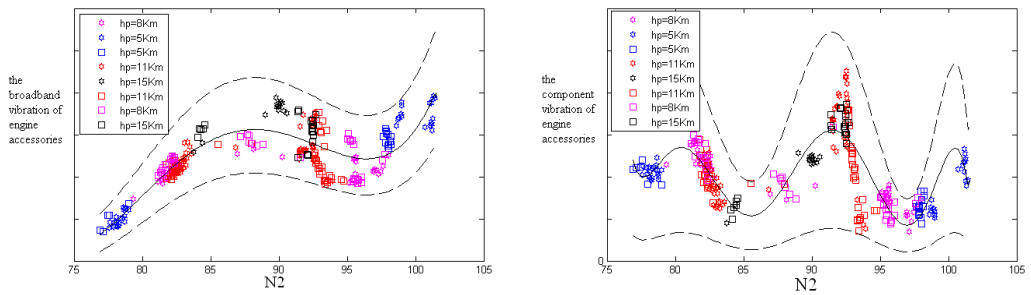

(a) The broadband vibration of engine accessories (b) The component vibration of engine accessories

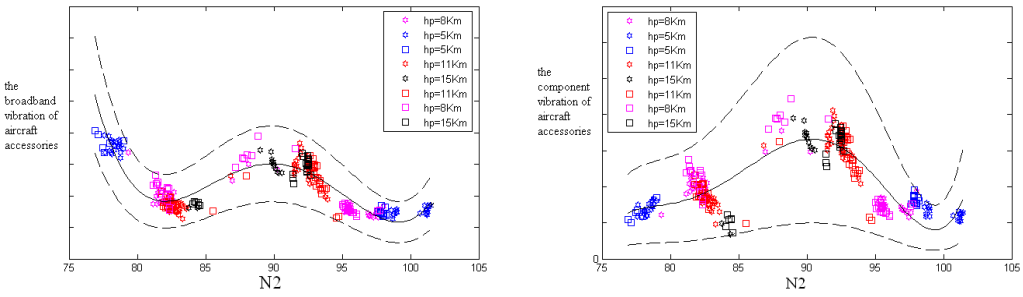

(c) The broadband vibration of aircraft accessories (d) The component vibration of aircraft accessories

Figure 3-34 The vibration baselines of accessory gearbox

4. RESEARCHES ON WIDESPREAD FATIGUE DAMAGE

4.1 Fatigue Crack Growth Prediction and Verification of Aircraft Fuselage Panels with Multiple Site Damage[1]

Widespread Fatigue Damage (WFD) is recognized as one of the biggest threats on structural integrity, especially for aging aircraft. Its evaluation provides a tough challenge for typical aircraft damage tolerance design and analysis because of many structural detailed differences in stress levels, local loading and assembly forms. Three main factors should be considered in multiple site damage (MSD) problems: crack cracks interference, inner-stress redistribution and overlap between cracks. Independent cracks propagation analysis will induce incorrect results in MSD prediction, and the traditional engineering method face the difficulties to obtain stress intensity factors and interference effects of multiple cracks. Comparatively numerical simulation methods are favoured by aeronautical engineers owing to its independence of crack geometries. Engineers mainly apply Finite element method to evaluate the airworthiness of metallic structure in Civil Aircraft, yet how to build a modelling to analyse the coordinating and automatic propagation between multiple cracks is the key and complicated point to predict MSD life.

Based on the secondary development function of ABAQUS, this paper will provide an efficient modeling to analyze the fatigue cracks growth life of aircraft fuselage panels with MSD, besides the test approach of panels subjected to internal pressure load is studied to verify the feasibility of the proposed modeling.

Based on linear fracture mechanical theory, the crack pre-growth length Δa for MSD structures is limited as $\Delta a \geq \Delta a_{\min}$ .The propagation length of each crack is:

$$\Delta a = f(\min_{i=1}^{n} \Delta N)$$

where ΔN is the cycle number when every crack propagate the minimum step length; $f(x)$ is crack propagation function; n is the number of crack tips .

The stress intensity factor K of structures under constant spectrum loading can be considered as constant in small propagation length; Conversely, K depends on loading value for the structures under random

[1] AVIC Aircraft Strength Research Institute. SU Shaopu: shaopu_su@sina.com.

spectrum. In order to decrease the numerical calculation amount, K can be obtained as following:

$$K_{j+1} = \frac{\sigma_{j+1}\sqrt{a_j}}{\sigma_i\sqrt{a_i}} K_i$$

where σ_{j+1} is the current loading stress; σ_i is the loading stress at step i (when FE crack modelling created); a_j is the total crack length after loading stress σ_j ; a_i is total crack length at step i; K_i is stress intensity factor at step i. This algorithm can quickly calculate the stress intensity factor at random loading stress, and reduce the crack length calculation.

Considering the effect of I-II mixed type stress intensity factors on the growth rate of multiple cracks, we propose the following crack growth model to predict MSD life:

$$\frac{da}{dN} = ce^{\beta\left(\frac{2}{\pi}\arctan\left|\frac{K_I}{K_{II}}\right|-1\right)}(\Delta K_{eq})^n$$

where ΔK_{eq} is the effective stress intensity factor, $\Delta K_{eq} = \sqrt[0.25]{\Delta K_I^4 + 8(\Delta K_{II})^4}$; c,n,β are material parameters; K_I, K_{II} are respectively I-type and II-type stress intensity factors. This crack growth model has been verified by CT model test.

If the crack growth length and crack path direction at step i are respectively Δa and θ_c , the new crack tip location at step i+1,written as ($x_{i+1,-1}, y_{i+1,-1}$) in Cartesian coordinate system, can be obtained as following:

For the cracks in plane:

$$\begin{cases} x_{i+1,-1} = x_{i,-1} + sign(x_{i,-1} - x_{i,-2})\Delta a\cos\theta_c \\ y_{i+1,-1} = y_{i,-1} + sign(x_{i,-1} - x_{i,-2})\Delta a\sin\theta_c \end{cases}$$

For the cracks in curve (described in Figure 4-1):

$$\begin{cases} x_{i+1,-1} = x_{i,-1} + sign(x_{i,-1} - x_{i,-2})\Delta a\cos\theta_c\cos(\frac{\Delta a\cos\theta_c}{R}) \\ y_{i+1,-1} = \sqrt{R^2 - x_{i+1,-1}^2} - R\cos(\frac{L}{R}) \\ z_{i+1,-1} = z_{i,-1} + sign(x_{i,-1} - x_{i,-2})\Delta a\sin\theta_c \end{cases}$$

where $x_{i,-1}, y_{i,-1}$ are the coordinates of crack tip at step i; $x_{i,-2}$ is the coordinate of the point with the minimum distance with crack tip; L is half arc length of fuselage curve panel.

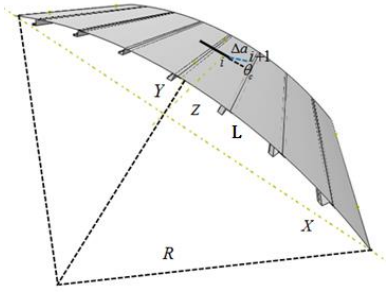

Figure 4-1 Description of crack coordinates in curved panel

The plane with MSD and the curved panel with two cracks are also analyzed by test to verify the

modelling. The testing details are described in Figure 4-2. The test rig has been proposed to realize the internal pressure loading for curved panel. It can well simulate the pressure load with uniform distribution. The circular load owning to boundary limitation can also be eliminated in the process of increasing pressure load. The test rig gives a good support for the design of new type civil aircraft.

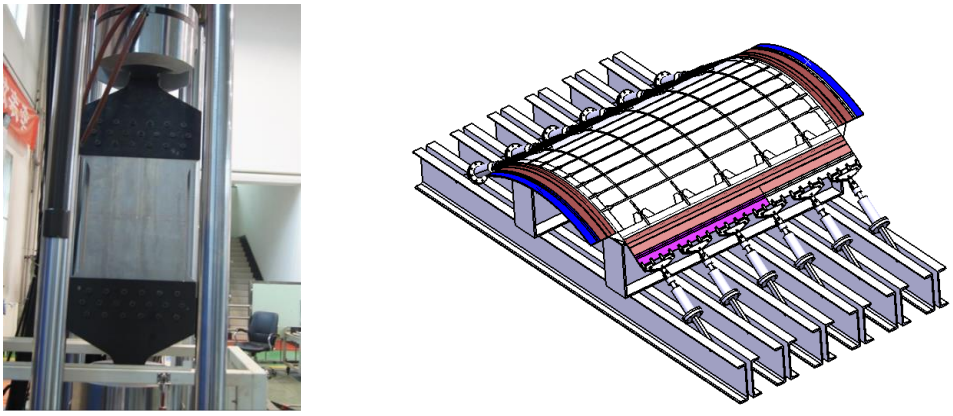

(a) Test rig of the plane with WFD (b) Curved panel subjected to inner pressure loading

Figure 4-2 Test rig in horizontal type

Compared with crack growth path and life, the numerical simulations by FEM model have a good agreement with the test results. For the plane with MSD, The average test result of crack propagation life is 245542 cycles, and the numerical result is 250395 cycles; For the curved panel with two cracks, the test result is 97000 cycles and the numerical one is 95038 cycles. In view of engineering application, the analytical model can give a good prediction for the aircraft panels with multi-cracks.

4.2 A Probabilistic Damage Tolerance Analysis Method of Multiple Site Damage for Structure Containing Holes [1]

The calculation method of multiple cracks stress intensity factor of MSD structure contains holes is studied. Taking the Paris crack propagation model as the research object, the crack propagation rate parameter is used as a random variable to simulate the randomness of crack propagation. A prediction model is established. The comparison between the relevant examples and the experimental data shows that the prediction model can accurately calculate the crack propagation life of MSD structure containing holes, and the reliability analysis of the sampling calculation results of structural crack propagation life is carried out. The model is used to calculate and analyze the crack propagation life of structure containing holes with several different MSD modes, and some conclusions are given.

[1] AVIC Aircraft Strength Research Institute. SUN Hanbin: sunhanbin623@163.com.

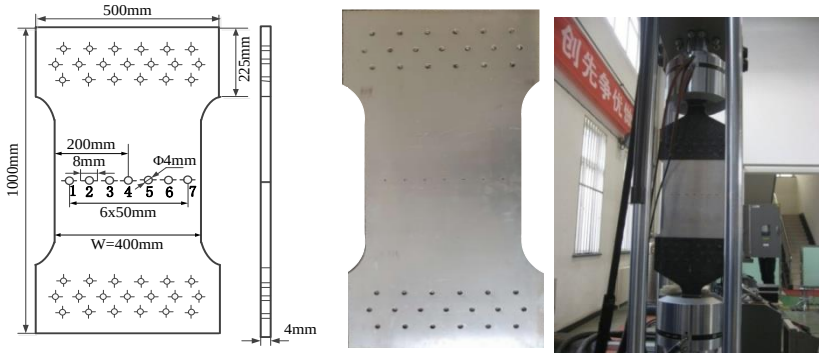

Figure 4-3 Components Design and Tests

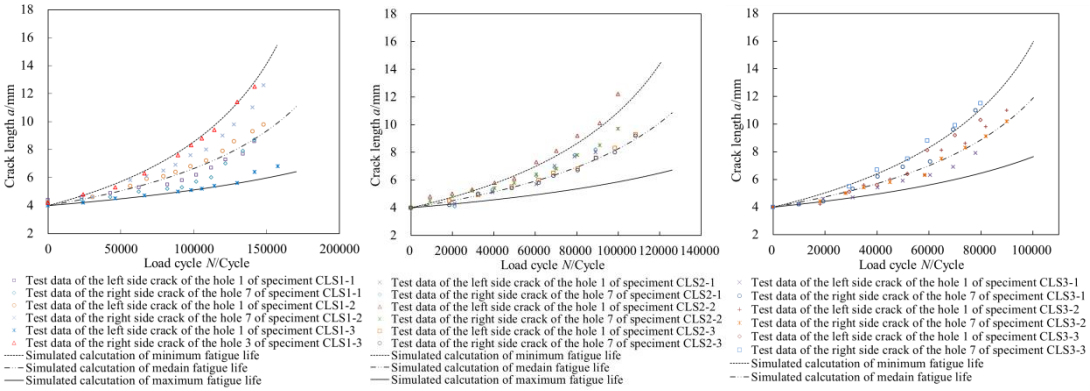

Figure 4-4 The comparison between the relevant examples and the experimental data

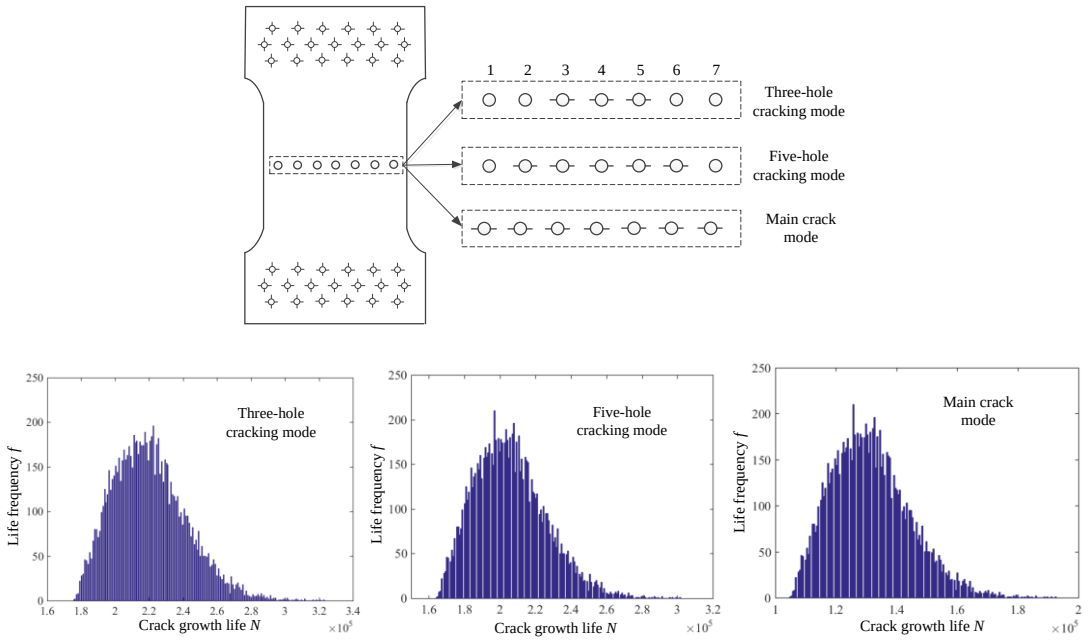

Figure 4-5 the crack propagation life prediction of kinds of MSD structure containing holes

4.3 An Engineering Calculation Method of Probability Distribution of Crack Initiation Life for Widespread Fatigue Damage[1]

An engineering calculation method of predicting probability distribution for crack initiation life of structures susceptible to widespread fatigue damage is proposed. Through a study of the crack initiation mechanism, the incident that crack initiation life of multiple detail structure taking a certain value is transformed into the intersection of three independent incidents. The probability of occurrence of the former incident is the product of the probability of occurrence of the latter three independent incidents, which is derived from the probability distribution function of crack initiation life of single detail structure. Thus, the detailed formulae of probability density functions of initiation lives for cracks appearing in turn in multiple detail structure are obtained. Making use of these detailed formulae, the calculation formula of median rank of initiation life is derived. It is only related to failure order and total number of details. Through the value of median rank, the initiation life with reliability of 50% can be achieved. Thus, an engineering calculation formula of probability distribution of crack initiation life is gotten. Crack initiation test of specimens with a single hole notch and multiple holes notches were carried out. The model is used to estimate crack initiation lives of the multiple holes notched specimens. The predicted results are in good agreement with the testing results, which show that this model is effective.

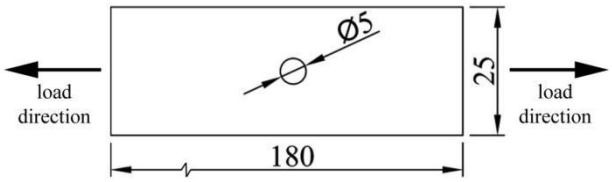

Figure 4-6 Sketch map of single hole notched specimen

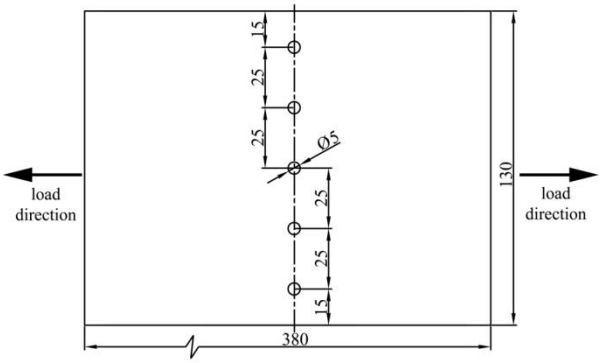

Figure 4-7 Sketch map of five holes notched specimen

[1] COMAC Shanghai Aircraft Design and Research Institute. XI Wei: xiwei@comac.cc.

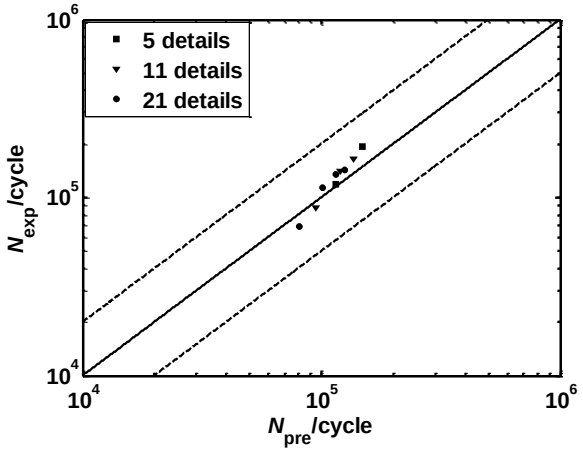

Figure 4-8 Comparison between predicted and experimental results

4.4 WFD Research in Civil Aircraft[1]

FAA issued amendment Nos. 25-132 in November 2010, which requires that design approval holders of transport category airplanes should establish a LOV for airplane to avoid the occurrence of WFD. CAAC compiled a special condition about WFD requirement according to amendment Nos. 25-132 during the certification of XXX.

Commercial Aircraft Corporation of China, Ltd. (Hereafter referred to as COMAC) has paid efforts in the prediction of widespread fatigue damage average behavior, determination of residual strength criterion of widespread fatigue damage and the determination of LOV since 2009 in order to implement the requirement of special condition for widespread fatigue damage on XXX aircraft, including crack initiation and residual strength test on coupon specimen with multiple open holes, crack initiation and residual strength test on coupon specimen with multiple rivets, fuselage panel MSD/MED test and lower wing panel MSD/MED test. The fuselage panel and wing panel tests will last until 2020.

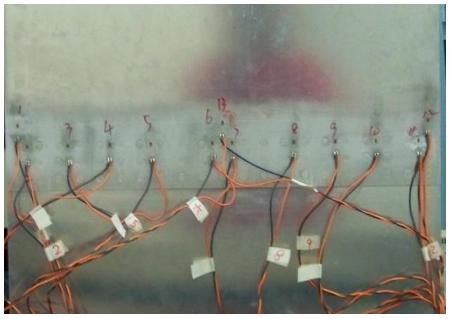

Figure 4-9 MSD test of skin lap joint specimen

[1] Shanghai Aircraft Design and Research Institute.

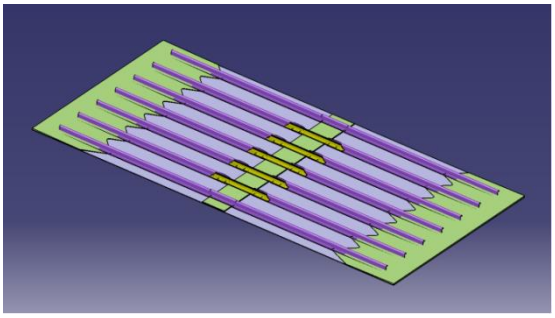

Figure 4-10 MED test of stringer joint specimen

In the prediction of widespread fatigue damage average behavior, Monte Carlo method is used to simulate the first and second fatigue crack initiation life of structures with multiple similar details, based on which the relationship between the second crack initiation life and the first crack initiation life under different similar details is deduced. The second crack initiation life with 50% reliability is conservatively assumed to be WFD average behavior. Regard to the verification of WFD average behavior analysis method and residual strength method for WFD susceptible structures, COMAC was devoted on validating WFD analysis method by sub-component tests, and the test matrix and test methods were determined for XXX aircraft.

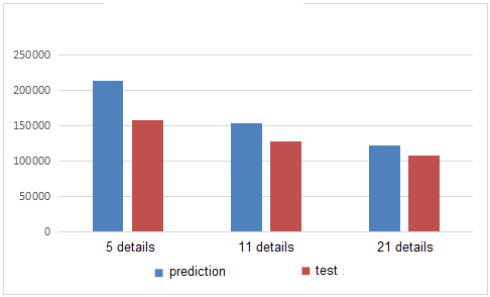

Figure 4-11 Life comparison between predicted and test results

4.5 Analysis and Test Research on Multiple Site Damage in Longitudinal Fuselage Lap-joints [1]

Finite element analysis of the multiple site damage crack propagation behavior was carried out by Franc3D (Figure 4-12), including the crack growth rate and the interaction between cracks. Reliability and Monte-Carlo probability method (Figure 4-13) was used to analyze the probabilistic behavior of multiple site damage crack initiation and failure. The results show that the structural failure criterion used has a great influence on the analysis results when using the reliability analysis method. Monte-Carlo analysis results show local damage and multiple site damage. Three-row rivet lap-joints test (Figure 4-14) was carried out, and the process of crack initiation, crack propagation (Figure 4-15) and structural failure were recorded, and the results were firstly analyzed by the life dispersion coefficient method.

[1] Civil Aviation University of China. Mao Yike: maoky_aw@163.com.

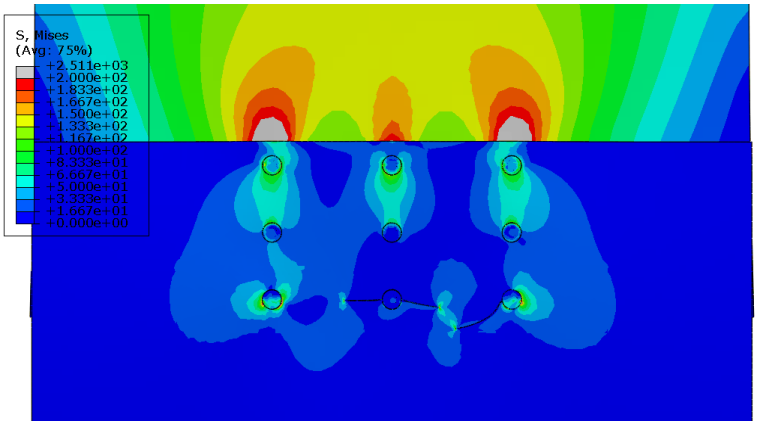

Figure 4-12 Propagation Path of MSD Cracks

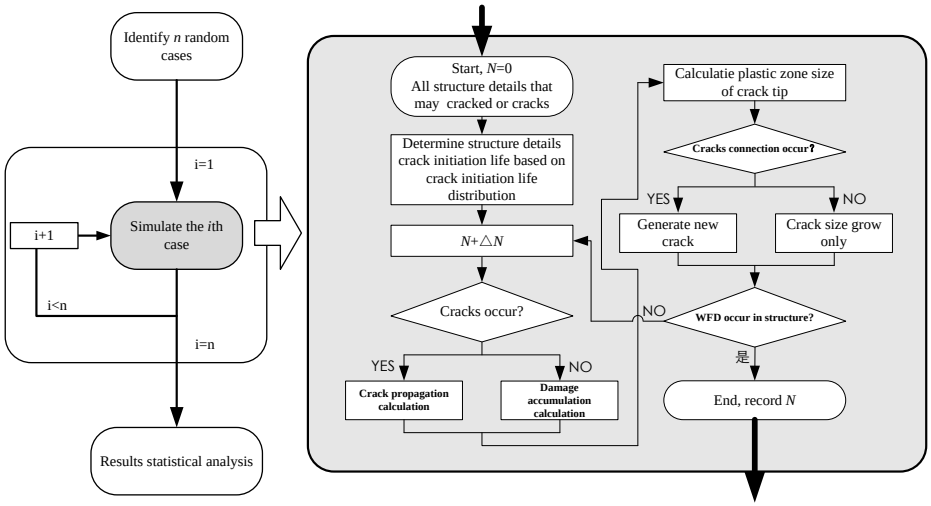

Figure 4-13 Monte-Carlo Process

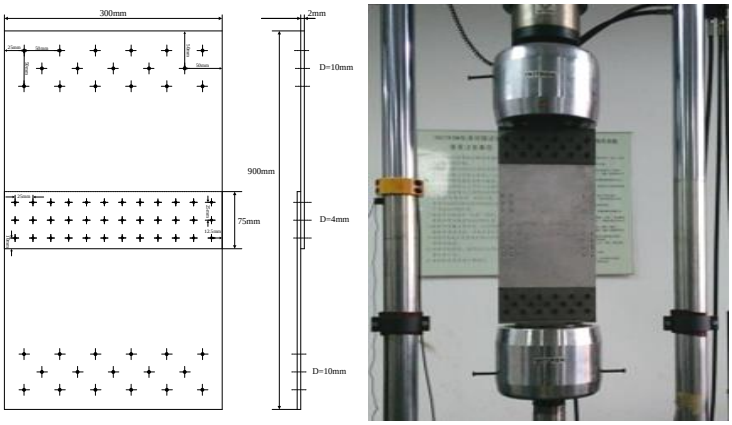

Figure 4-14 Test Specimen and Fixture

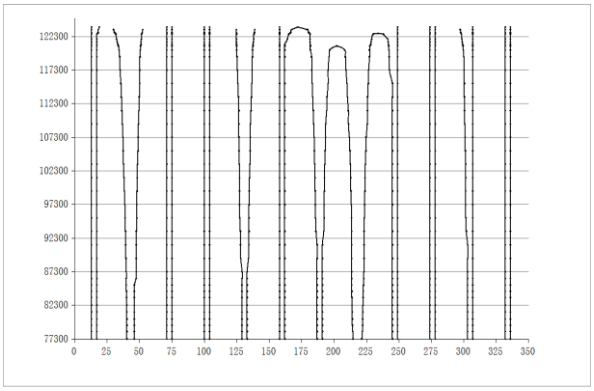

Figure 4-15 Schematic Diagram of Crack Propagation Process

4.6 WFD Evaluation of a MED-susceptible Structure Based on the Test Data[1]

To research one civil aircraft fuselage damage tolerance and judge the widespread fatigue damage(WFD)，one fuselage isometric section fatigue test was done (Figure 4-16). During the aircraft isometric section of fuselage fatigue test, many cracks were inspected on the frames, some frames broken down at almost the same place (Figure 4-17). The structure of every frame is same and has the similar stress distribution, so the fuselage test specimen belongs to the multiple element damage(MED)-susceptible structure of WFD structures. The frames' WFD average behavior could be obtained by analyzing the frames, fatigue test data and because the frame structure is detectable (Figure 4-18), so we could calculate the inspection start point (ISP) and the structural modification point (SMP), after these, the evaluation of a MED-susceptible structure of WFD structures was finished (Table 4-1).

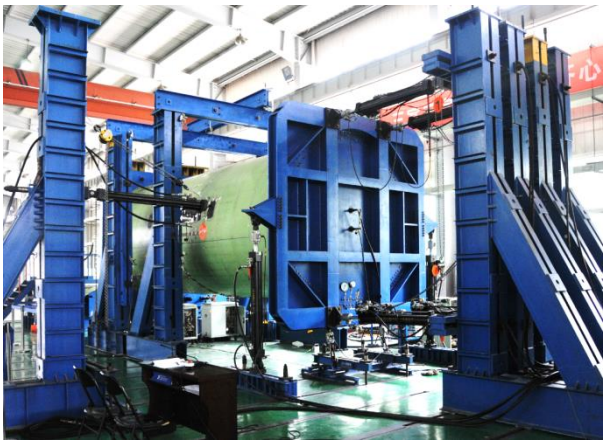

Figure 4-16 The fuselage isometric section test

[1] AVIC Xi'an Civil Aircraft Industry Company LTD. LIU Haitao: sea574839@163.com.

Figure 4-17 Photo of the damaged frames

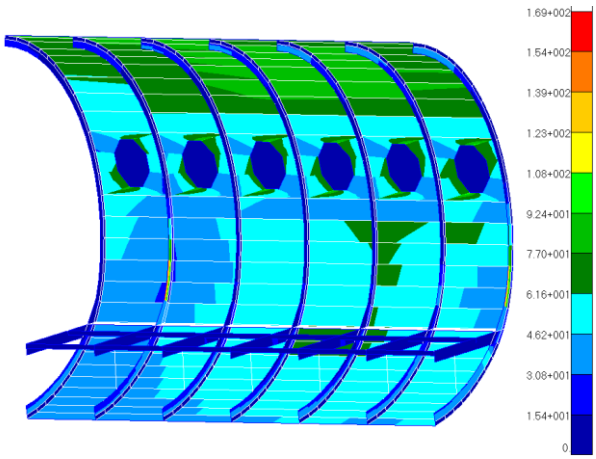

Figure 4-18 The stress distribution after many frames broken

Table 4-1 ISP and SMP

	Left frame	Right frame
ISP	18380	19711
SMP	27571	29567

4.7 Impact Analysis of Long Crack on Residual Strength of Adjacent Components[1]

The influence of long crack on residual strength of adjacent components is studied. Based on the connotation of the residual strength, key points of the residual strength analysis in the composite structures are listed. The effect of long cracks on adjacent elements is discussed. It is shown that the residual strength of structures is changed by internal force distribution. Moreover, Multiple Element Damage (MED) example regarding residual strength analysis of adjacent components is given.

[1] AVIC Aircraft Strength Research Institute. CHANG Wenkui: cwk623@126.com.

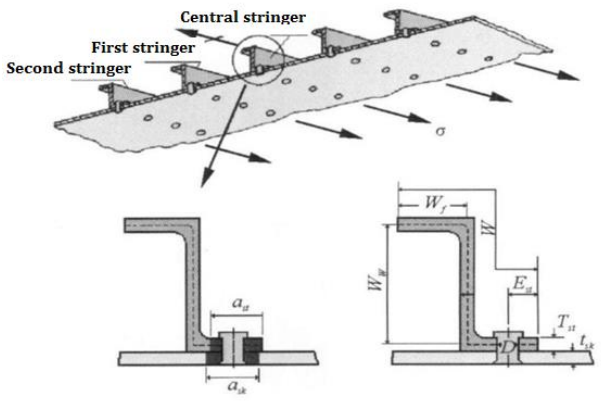

Figure 4-19 Structure Model

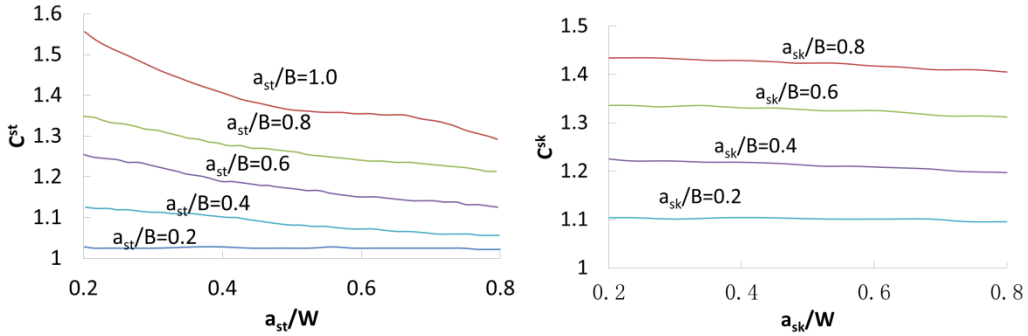

(a) String (b) Skin

Figure 4-20 Interaction factors of crack on string/skin for MED structures

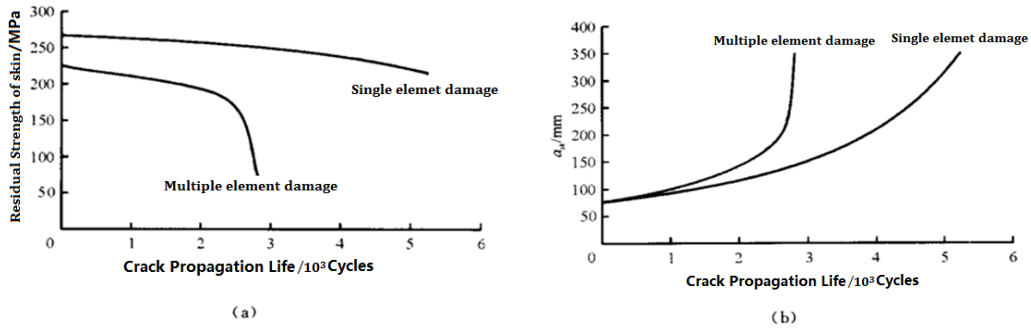

Figure 4-21 Comparison of skin crack propagation life and residual strength

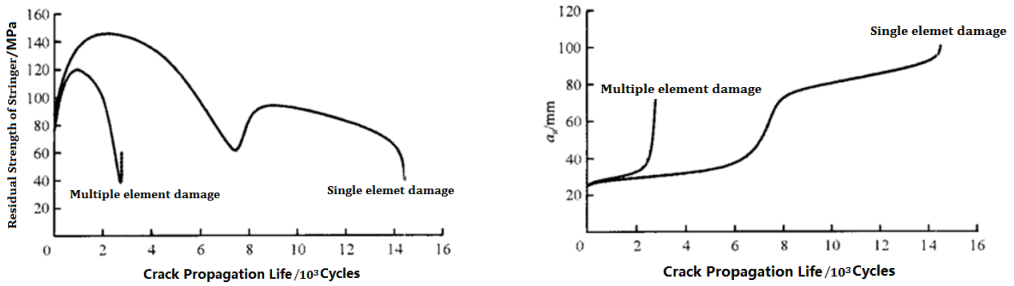

Figure 4-22 Comparison of string crack propagation life and residual strength

5. RESEARCHES ON LOAD MEASUREMENT AND LOAD SPECTRUM

5.1 Design Practice of Dynamic Load and Load Spectra of Aircraft[1]

After years of predictions and related researches in FAI (the First Aircraft Institute), especially through the engineering models' such as JH7 series、ARJ21、KJ-2000、Y-20、KJ-600 application and development, A large amount of experience and data have been accumulated in the fields of plane dynamic load calculation, design load spectrum(equivalent load spectrum, flight by flight load spectrum) and measured load spectrum compiling. Combining with a large number of measured data of aircrafts', the discrete gust equivalent load spectrum of civil aircraft has been improved, and a large number of verification tests are planned, forming complete design, verification process and method. Relying on the technical renovation project of the institute, FAI plan to establish a complete、 applicable software system for different types load spectrum of aircrafts.

According to the military specifications, FAI compiles the design spectrum for the military aircraft. For the aircraft with measured data, the measured data are compiled according to the representative flight method. For the civil aircraft, the equivalent load spectrum of the mission segment is compiled for durability analysis, and the random load spectrum is compiled for full scale fatigue test.

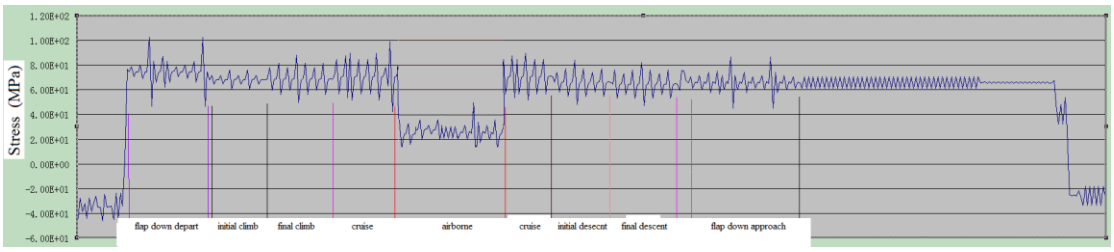

Figure 5-1 Airborne mission profile load spectrum

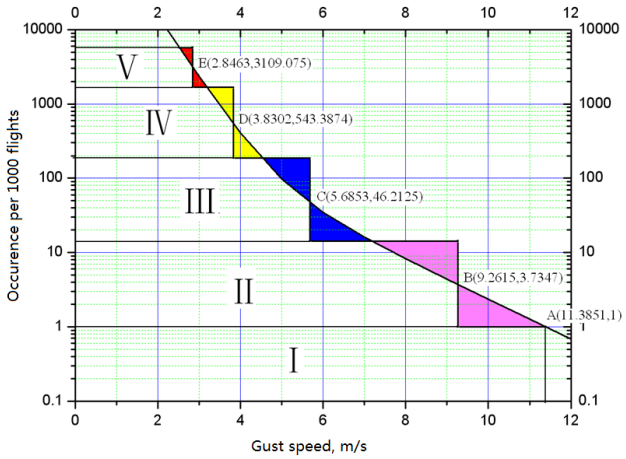

Figure 5-2 Discrete gust load spectrum

[1] AVIC, the First Aircraft Institute. MIN Qiang: 13679187219@163.com.

5.2 Load Spectrum Enhancement Method with Around-air-ground Invariance of Aircraft Metal Structure[1]

Full-scale fatigue test is an essential link in the process of aircraft development ,but its long test cycle has become the bottleneck of aircraft development .In this paper ,the load spectrum Enhancement method with ground-air-ground and the life prediction method are presented .This method is used to aggravate the small load in equal proportion，the cycle of excess ground-air-ground load after enhancement remains unchanged. Using this method can improve the damage of each block spectrum, deduced the life of the original spectrum by using of the Enhancement spectrum. At the same time, reduce the number of the total circulation blocks and shorten the test period at the same time holding the line of ground-air-ground invariance.

In this paper, a certain type of MA600 is selected to carry out the verification test at the outer wing. Under the condition of 1.2 times heavier, the test time is about half of the time under the original spectrum. The original spectrum fatigue life is deduced by using the Enhancement fatigue life, the error between the result of life prediction and the result of test is within the acceptable range of engineering. The damage position is the same as that under the original spectrum. Figure 5-3 is outboard drain port test scene; Figure 5-4 and Figure 5-5 are comparison of the results of the test. Figure 5-6 is the photo of MA600 full-scale fatigue test.

Figure 5-3 Outboard drain port test scene

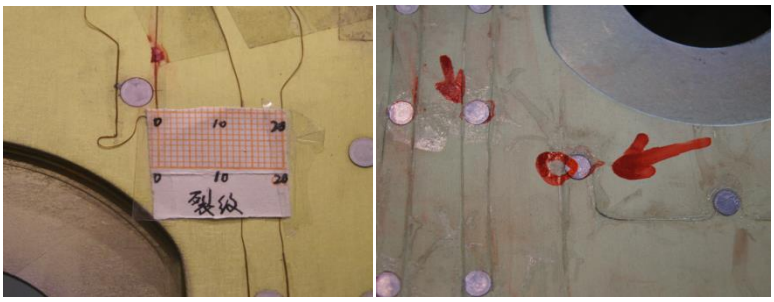

(a) original spectrum (b) enhanced spectrum

Figure 5-4 flap crack under two random spectrum

[1] AVIC Aircraft Strength Research Institute. CHEN Li: 2416806709@qq.com.

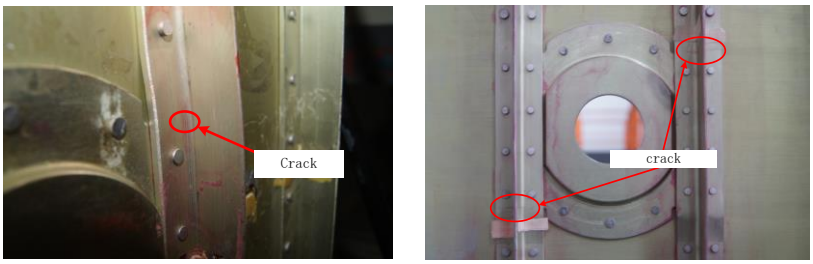

(a） original spectrum (b) enhanced spectrum

Figure 5-5 Stringer crank crack under two random spectrum

Figure 5-6 MA600 full-scale fatigue test

5.3 The Structural Health Monitoring and Spectrum Research for Heavier Air Tanker[1]

This paper makes a preliminary analysis of the existing data of a small quantity of fire fighting, and gives the problems existing in the existing fire fighting load spectrum and related influencing factors. The existing data of a small quantity of fire fighting shows that the fire fighting load spectrum is related to the maximum takeoff weight and average flight time of the aircraft. On this basis, the relative damage percentage of fire extinguishing was evaluated by taking the lower panel of a large extinguishing aircraft as an example. In view of the limitation of the existing measured data, the particularity of the fire fighting task and the quantitative comparison analysis of small overload caused large damage, the structural health monitoring program for all tanker was proposed, and the related requirements of the fire fighting task flight measured parameters and sampling frequency were clarified.

Key Techniques

the present study has focused on evaluating aerial firefighting spectra and using a relative damage methodology to define preliminary operational loads spectra for aircraft operating in the air tanker and lead aircraft roles. Based on the low quality and quantity of data available, the spectra that are proposed are conservative and rely in part on operational data acquired in similarly demanding low-altitude missions, such as aerial survey work. Should additional data from SHM (Structural Health Monitoring) programs become available, the proposed spectra could be reviewed and updated as appropriate.

---

[1] AVIC China Aviation Industry General Aircraft Co., Ltd. WANG Xiangsheng: 18688191081@163.com.

Effect of MTOW on Load Spectrum Severity

While there appears to be a trend that might support the hypothesis that the severity of the usage spectrum is related to aircraft weight, there are two areas in figure5.7 that suggest that such an inference cannot be drawn without further information. The MTOW for groups 1 and 2 is 26,300 lb. However, rather than their exceedance curves being coincidental, their exceedance curves are quite distinct. Similarly, while groups 5 and 6 contain aircraft in a similar weight category (MTOWs of 106,000 and 126,000 lb, respectively) their exceedance curves are also quite distinct. Before a relationship between MTOW and severity of spectrum can be established, it will be necessary to determine the weight of each aircraft at the time a given exceedance occurs.

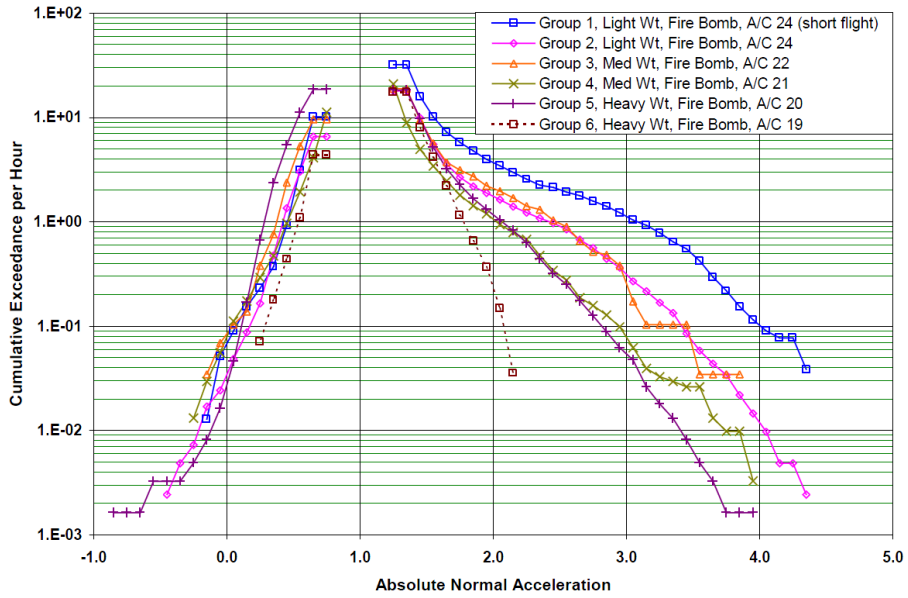

Figure 5-7 Exceedance Plot for Different MTOW Firebombers

Incremental and cumulative damage

The results presented in this section are based on the calculation of cumulative damage (Σ (n/N)) between n = 1.1 g's through to n = 4.4 g's. The incremental and cumulative damage values are normalized using the calculated total damage to give a total damage of 1.0 for all cases. A typical result for a heavyweight air tanker is shown in figure 5.8. The cumulative curve in figure5.8 indicates that approximately 50% of the accumulated damage comes from g-level excursions with a maximum g-level of 2.5 g's or less. The incremental curve indicates that the maximum amount of damage is attributable to g-level excursions with maximum g-levels in the 2.0- to 2.25-g range.

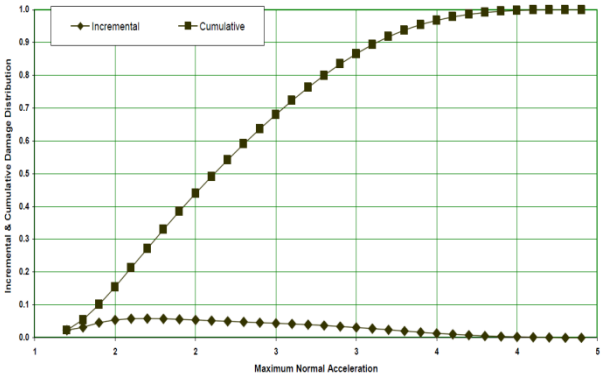

Figure 5-8 Incremental and Cumulative Damage for The Heavier Tanker

Structural Health Monitoring

Relative damage calculations indicated that there is significant variation in both the air tanker and lead aircraft loads environments. For air tankers, the cyclic (fatigue) loads that are responsible for the majority of the cumulative damage sustained by an aircraft structure appear to be related to aircraft size. Damage sustained by larger, heavier aircraft (in excess of 80,000 lb) is principally attributable to large numbers of relatively low-level loads. Conversely, the damage sustained by smaller, lighter aircraft (less than 30,000 lb) is primarily attributable to smaller numbers of relatively high load cycles. These factors have a number of implications for future Structural Health Monitoring (SHM) programs implemented on air tanker and lead aircraft. These include, but are not necessarily limited to, the following: (a) Implementing Individual Aircraft Tracking (IAT) programs on all air tanker and lead aircraft. While initial sampling programs can be used to establish preliminary spectra for air tankers and lead aircraft, significant variations in usage between aircraft operating in nominally the same role appear to exist. Consequently, it will be necessary to track individual aircraft to ascertain exactly how they are being operated and adjust their associated inspection and maintenance schedules accordingly. (b) Exercising considerable care when defining the resolution (granularity) of parameters such as Nz and strains for use in SHM programs. Resolutions used to monitor aircraft in more conventional/design intent roles may result in load cycles that contribute a significant amount of cumulative damage to the structure being overlooked. This is particularly true for larger, heavier aircraft used in the air tanker role. (c) Segmentation of the various phases of the air tanker and lead aircraft roles through the use of discrete signals/markers to ascertain whether the variability in the data is primarily due to the loads experienced in the immediate vicinity of the fire. If this proves not to be the case, other factors such as crew training, pilot technique, and terrain should be investigated to establish whether or not the data variation that has been observed is inherent to the aerial firefighting role.

5.4 High Temperature Load Measurement for Nozzle Component of Aero-Engine[1]

T4 link is the critical load-bearing component for nozzle element of a certain engine. Whether the nozzle load meets the requirements or not at high temperature is the key factor in the structural integrity of the nozzle unit. It's analyzed that strain response of the T4 link was resulted from mechanical load, thermal

[1] AVIC Chinese flight test establishment. WEN Min: wenmin05040205@163.com.

gradient and material parameter using the thermo-solid coupling method. The T4 link load at high temperature was measured with the high temperature strain gauge on bed test. The process for bonding and assembling the high temperature strain gauge was developed, the equation extension method of the load calibration was deduced, the measurement method containing load calibration, thermal correction, and data processing for the high temperature load was established. The aero-engine bed test shows that the variation tendency and value of the thermal-output strains vary much between different T4 links. The maximum error for T4 link is 0.27kN. The maximum measured tension is 62.1% of the designed load value, the maximum pressure is 58.46% of the designed load value, and the structural strength design of T4 link meets the operating requirements.

Research ideas and Achievements

Refitting technology of high temperature strain gauge

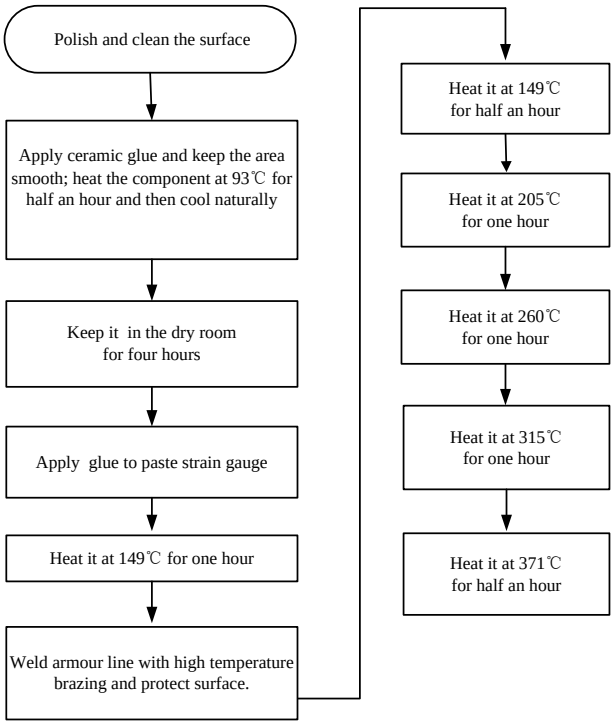

Figure 5-9 Refitting process

Figure 5-10 Refitted components

Load calibration test of nozzle components at normal temperature

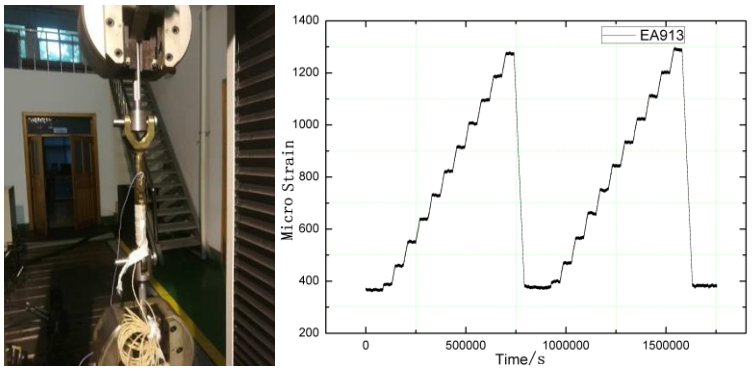

Figure 5-11 Load calibration test site and test curve

Temperature correction test of nozzle components under unloaded condition

Principle of temperature correction ：

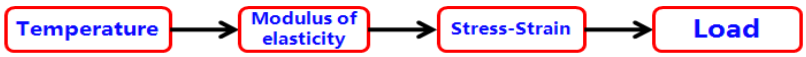

Tension and compression load: $F_p = f(E,\ T)\varepsilon_p A$

Bending moment load: $M_b = f(E,\ T)\varepsilon_b W_z$

Torque load: $N_t = f(E,\ T)\varepsilon_t W_p$

Shear load: $F_s = f(E,\ T)\varepsilon_p A_{bs}$

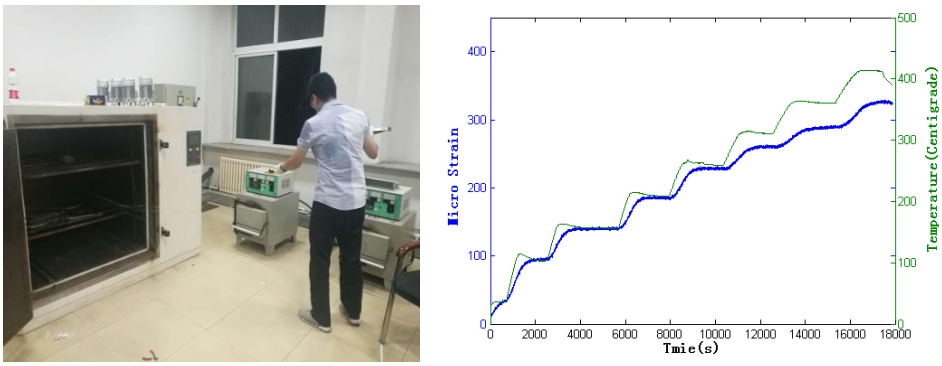

Figure 5-12 Testing site and data

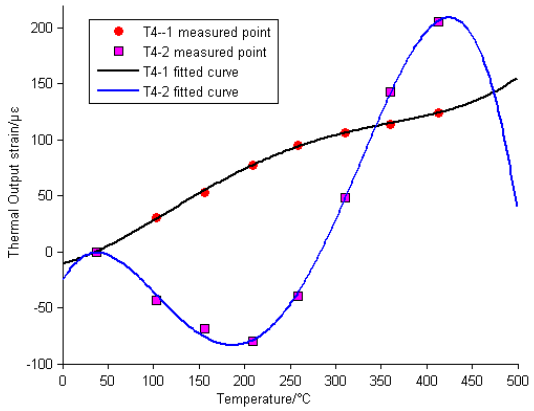

Figure 5-13 Strain fitting curves of different thermal components

Bench test of nozzle load measurement for ground machine

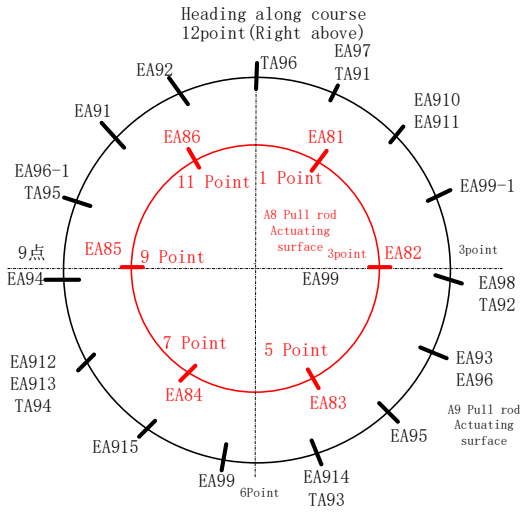

Figure 5-14 The whole machine assembly

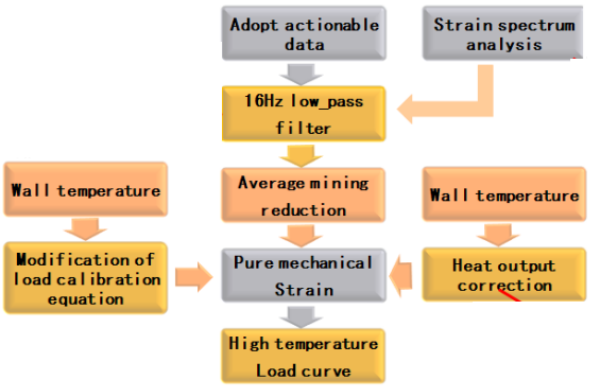

Figure 5-15 High temperature load determination method

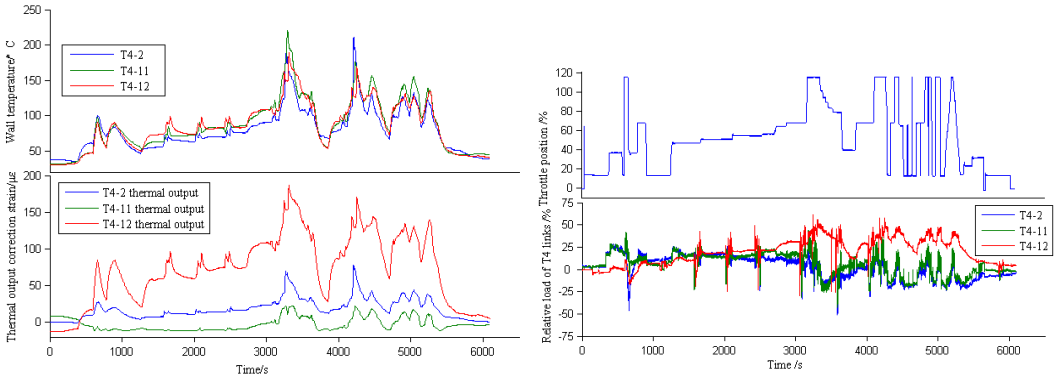

Figure 5-16 Test results of High temperature load measurement

5.5 In-flight Measurement of Three-axis and Four-angle Motion of Rotor Blade in Space[1]

As the main lift system of helicopter, the flapping angle, shimmy angle and variable pitch angle of the rotor determine its motion state, directly affect the intension, performance, quality and have great significance to analyze the law of helicopter rotor motion, the dynamic modeling and the development of blades. Those parameters are alternating and random uncertain, therefore, the theoretical calculation error is large, which can only be measured by prototype. This technique is very complex and high tech, which realizes the synchronous and dynamic measurements of spatial triaxial motion parameters of rotor blades.

The technology has several key points shown as follows.

Firstly, single chip PSD and micro LED are used, and a non-contact rotor motion measurement system based on the principle of visual angle imaging is developed. The system solved some problems which are the dynamic measurement of rotor blade flapping angle, pendulum angle, variable pitch angle, azimuth angle in helicopter flight.

This system composition is shown in Figure 5-17. The PSD is selected as detector, which measure the two-dimensional position of the luminescent markers in the moving plane. Two LED luminescent points were placed on both ends of the axial of the profile of the blade to measure the variable pitch angle, as shown in Figure 5-18. The method is based on the principle of visual imaging measurement. Figure 5-19 shows the measurement principle of blade flapping angle and pendulum angle.

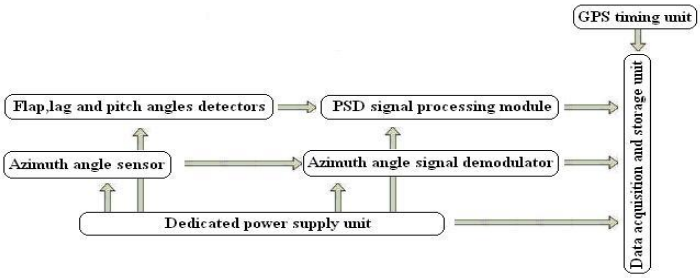

Figure 5-17 Composition of flight test system of rotor motion parameters

[1] AVIC Chinese flight test establishment. CHENG Weizhen: avicavic@eyou.com.

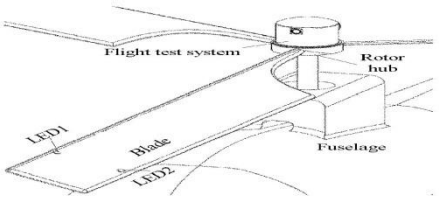

Figure 5-18 Schematic diagram of measurement principle

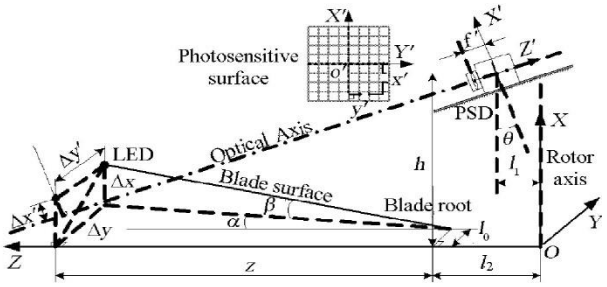

Figure 5-19 Schematic diagram of the imaging measurement method

Secondly, the decomposition technique of rotor blade static simulation is proposed, which solves the problem of automatic control and loading of rotor blade triaxial motion in ground calibration test. And also a program-controlled ground calibration system of rotor motion state is developed, which can improve the calibration precision.

The first one is that this system consists of mobile electric gantry frame, three axis servo loading platform, microcomputer controlled servo loading system, lifting platform and so on, as shown in Figure 5-20 and Figure 5-21. Ground calibration system for rotor motion parameters is divided into 3 major aspects:

The three axis servo loading platform includes a macro loading system and micro loading system as well as a blade backing platform. The load applied by the macro loading system is transferred to the micro loading system. The micro loading system is connected to the preset section of the blade by the blade backing platform, the applied load is transferred to the blade through the blade backing platform, and also protect the blade. Such a load transfer route can effectively solve the problem of blade loading profile follow-up. The other parts of the ground calibration system are microcomputer controlled servo loading system and mobile electric gantry frame and its auxiliary equipment.

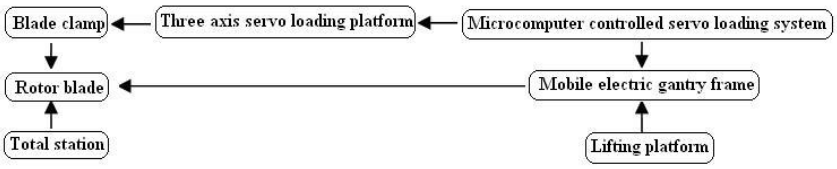

Figure 5-20 Module function block diagram of ground calibration system for rotor motion parameters

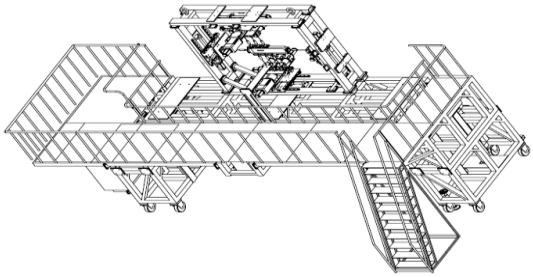

Figure 5-21 Integrated graph of ground calibration system for rotor motion parameters

The flight test system of rotor motion parameters is mounted on the top of the rotor hub. In accordance with the flight test outline, the test machine was equipped with sensors and airborne equipment required for test flight and completed all test flight subjects specified in the flight test outline. The flight test results are shown in Figure 5-22 and Figure 5-23. Figure 5-22 is a time history diagram of hover state, while Figure 5-23 is a time history diagram of horizontal flight state. It can be seen from the figures that the periodicity of the measured results is obvious, which accords with the spectrum analysis of the blade.

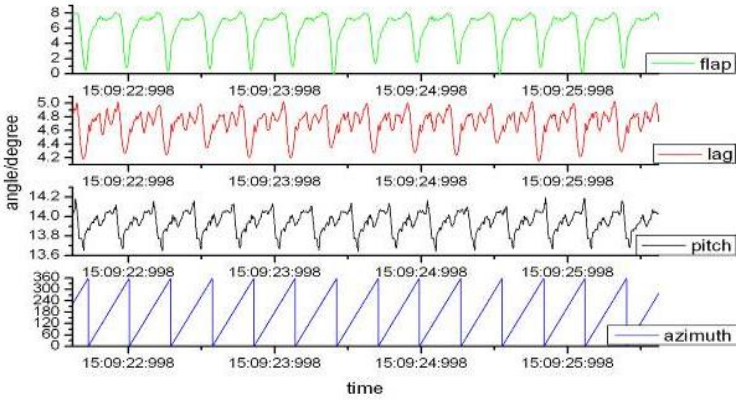

Figure 5-22 Hover state

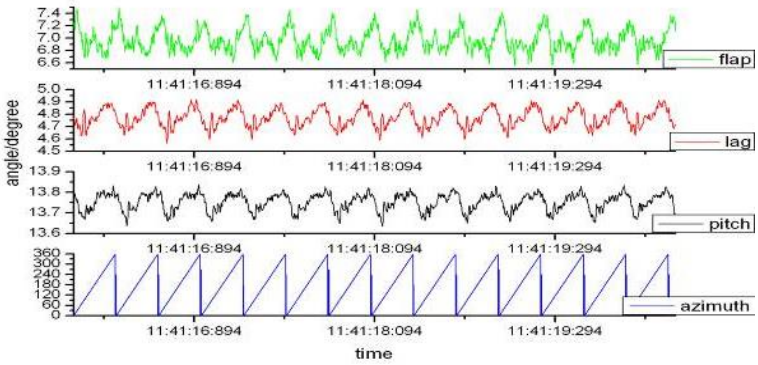

Figure 5-23 Horizontal flight state

5.6 Flight Test Technique for Blade Structural Load of a Coaxial Helicopter [1]

The research of helicopter rotor load is one of the most fundamental and significant, also one of the most

[1] AVIC Chinese flight test establishment. CHENG Weizhen: avicavic@eyou.com.

difficult and complex subjects about the helicopter theory and technology. Blade structural load is significant for improving calculation model of load, determining the value of a fatigue test, compiling load spectrum, estimating fatigue life and etc. Starting from the actual structural layout of the coaxial helicopter system, the mechanical model of load calibration test for upper and lower rotor was established, the non-airfoil blade root was selected as blade measurement section for strain bridge design, the blade load equations of upper and lower rotor were obtained by the blade load calibration test of unidirectional loading method. This paper presents a load measurement scheme for coaxial rotor; accordingly, an airborne test system based on small telemetry strain measurement technology is developed and applied to field test flight. The flap-wise moment, shimmy moment and torque of the coaxial rotor blade were obtained by flight measurements in real atmospheric environment. Small telemetry strain measurement technology was successfully applied in the flight test of a coaxial helicopter, and the structural load of coaxial rotor blade measured by which, is of great significance to the research of coaxial helicopter.

The measurement of blade flight load usually adopts the strain measurement method, and the optical fiber measurement method. There are generally 4 methods for signal transmission: electron inducing ring, liquid electron inducing machine, wireless telemetry, a solid-state acquisition recorder, and, recently, an electro-optical transmission. Compared with the ordinary single rotor, the coaxial anti-rotation of the upper and lower rotors makes the synchronous dynamic measurement of the load of upper and lower rotors of the coaxial helicopter more difficult in engineering. After comprehensive consideration of various factors, the load measurement scheme of the coaxial rotor blade system is shown in Figure 5-24. The upper and lower rotor collectors are independent and unified to form a whole. The collector A measures the load of the upper rotor blade and sends a wireless signal, which rotates to the left synchronously with the fixed connection of upper rotor; The collector B measures the load of the lower rotor blade and sends a wireless signal, which rotates to the right synchronously with the fixed connection of lower rotor; receiver is fixed on the back of the fuselage and receives the wireless signals off the collector A and collector B, and has the function of data storage; the ground controller has the function of monitoring collector A , collector B and wireless receiver.

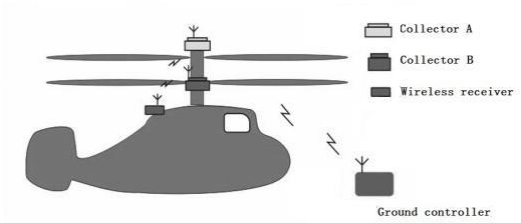

Figure 5-24 The measurement solution of the blade structural load of coaxial rotors

According to the above measurement, a coaxial rotor load test system is developed. The airborne test system adopts micro-power short-range telemetry strain measurement technology with dual wireless redundancy design, small telemetry strain measurement technology for short, including left rotating part(collector A， rice cooker structure), right rotating part(collector B， ring structure), and fixed part(wireless receiver). both left rotating part and right rotating part are consist of strain senser, MCU data acquisition module, dual channel wireless communication module, GPS timing module, power supply module; at the end of each channel is a variable gain amplifier; High-speed data collection is adopted, 16 times every millisecond, and then the signal is removed by hopping point and the average value is filtered to filter the noise. The overall architecture of the system is shown in Figure 5-25, the

fixed parts uses the telemetry receiver to simultaneously receive the wireless signals of the left and right rotating parts and store. The system uses reasonable wireless frequency band for data communication, and the air transmission rate meets the test requirements. All telemetry signals transmitted are encrypted, the signal power and communication distance are small, preventing it from being received by the outside world. In order to reduce the bit error rate of communication, dual wireless redundancy design is used, and different frequency points are used to send signals at the same time, so as to improve the reliability of communication. In the helicopter electromagnetic environment and high-speed rotation environment, there is great uncertainty about the reliability of small power wireless communication. Through the analysis and comparison of the measured data, the wireless signal transmission is proved to work stably in this environment, with the bit error rate less than 1%, meeting the test requirements. Each part uses GPS as time synchronization signal source and introduces GPS timer to facilitate data comparison among airborne equipment.

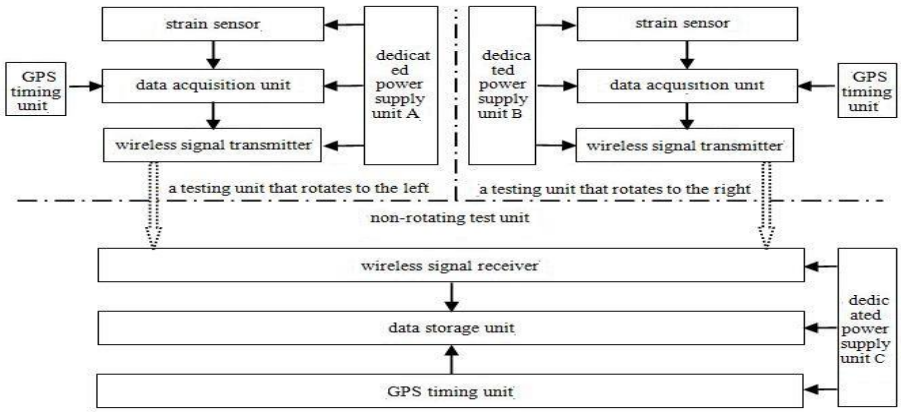

Figure 5-25 The airborne testing system of the blade structural load of coaxial rotors

According to the requirements of the flight outline, the test aircraft is equipped with sensors and airborne test equipment required for test flight. Completed all test flight subjects specified in the test flight program. Take the measured flight data M_β of upper and lower rotor blades, Figure 5-26 is a time history diagram of out ground effect hovering state at a height of 25m from the ground, fig.4 is a time history diagram of a flight state at a air pressure attitude of 1500m, 120km/h airspeed. The analysis shows that M_β of upper and lower rotor blades changes periodically with time, and corresponding phenomena of positive and negative pulses appear. This is due to the aerodynamic interference between the upper and lower rotor, resulting in positive and negative pulses on upper and lower rotor blades. By comparing Figure 5-26 and Figure 5-27, it can be seen that in horizontal flight state, M_β of upper and lower rotor blades are not significantly different, while in hover state the differences are obvious, which is caused by the greater aerodynamic interference in the hovering state than in the horizontal flight state.

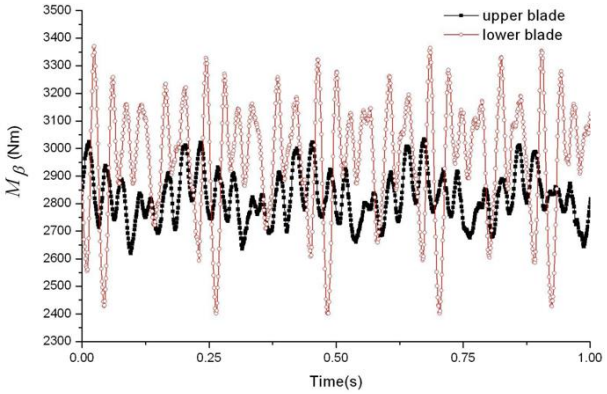

Figure 5-26 Time history diagram of the blade flapping moment in OGE hovering

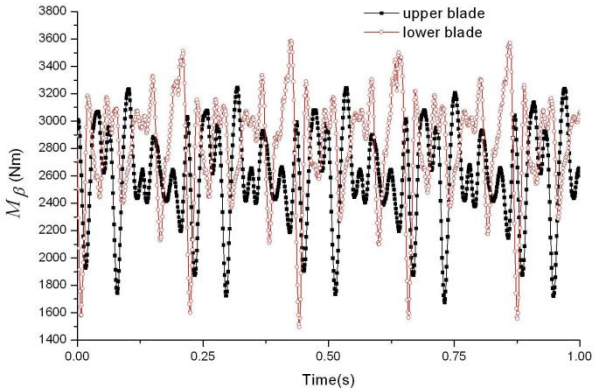

Figure 5-27 Time history diagram of the blade flapping moment in flat flight

5.7 Loads Calibrations Test Technique of Aircraft Components under the Stiffness Adjusting Condition [1]

The loads calibration of aircraft is the key technique in flight loads measurements and loads spectrum compilations. It was widely used in aircraft structural fatigue and integrity fields while founded in 1950s'. From then on, a large number of researches were conducted and practiced on method of the loads calibration by the flight loads engineers. More technical details were extend and modified, making it become more precision and economics in flight loads measurements. The paper dissertates the stiffness-changing

In this study, a wing adjusting-stiffness test bench (WASTB) was designed and manufactured in order to evaluate differences of wing stiffness in various aircraft and local stiffness change on the wing。By adjusting the stiffness of the test bench，wing loads calibration methods in large deformation and high loads conditions was realized. Discovered influence factors of coordinate load system control parameters due to local stiffness change to optimize parameters configuration. The vibration problem which is generated due to coupling of wing stiffness and loading frequency in loads calibration test has been solved。Multi-points coordinate loading method also researched in this paper.

Key Techniques

[1] AVIC Chinese flight test establishment. YU Jianhu: yjhtiger@163.com.

Design and manufacture the wing adjusting-stiffness test bench (WASTB). Several of wing stiffness and local stiffness change could be simulated through stiffness-adjusting equipment. The calibration test loads was applied at different stiffness in order to study load calibration test method for high loads and large deformation wing. The wing vibration problem due to the coupling of local inherent frequency in the wing and coordinate loading frequency has been resolved.

Technique Targets

The targets of the developed device, the wing adjusting-stiffness test bench (WASTB) are respectively described in Table 5-1 and Table 5-2.

Table 5-1 Basic index

Types	Targets
Scope of wing deformation	-0.5~1.5m
Capacity of load	-1000~2000kN
Capacity of actuator	104
Load factor	3.0

Table 5-2 Expected load and deformation in different stiffness type

Stiffness Type	Maximum expected Load （kN）	Maximum expected deformation（mm）
Type1	500	30
Type 2	500	200
Type 3	500	500
Type 4	500	750

Wing stiffness simulate

Theoretically, the wing could be simplified as a cantilever beam. The deformation along span wise was plotted using the data from design and statics test, and the local stiffness change could be obtained through linear fitting. In practice, a rigid beam frame was designed to simulate wing box, a stiffness controllable spring was mounted on the frame to simulate the stiffness change, the loading points were the same as in calibration test in order to simulate real wing loads calibration test. The test loading system adjusting and validating were finally achieved.

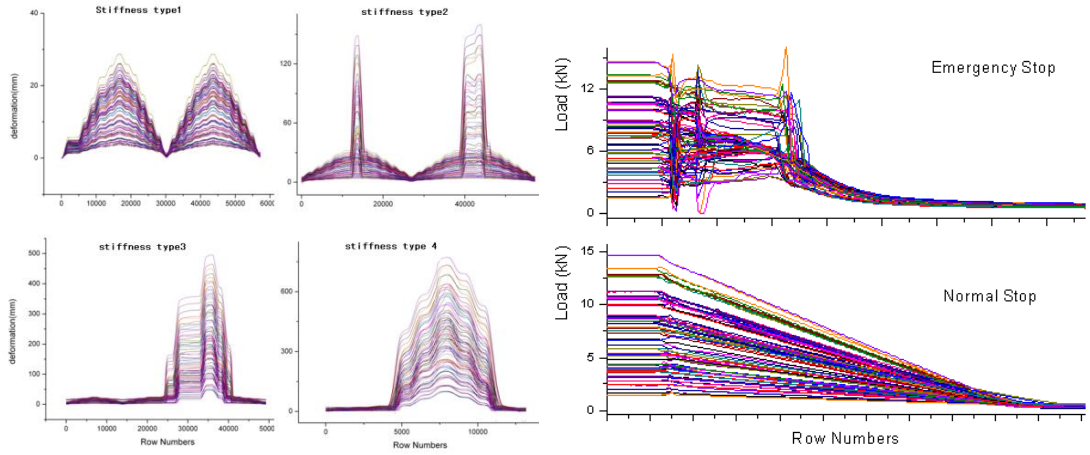

Figure 5-28 Loads under different wing stiffness and parameters

Test Device

By adjusting stiffness, the WASTB are applied to simulate the mechanical characteristic of wing in real circumstance. After the device were installed and debugged, the test of Multi-points coordinate loading can be executed under the high load and large deformation, the affection of stiffness change to control parameter configure will be researched and the solution will be come up, all of above is the technical preparing for the aircraft loads calibration. The WASTB is described in Figure 5-29.

Figure 5-29 Wing adjusting-stiffness test bench(WASTB)

5.8 Off-line Calibration Technology for Landing Gear Loads [1]

The test flight of landing gear load is an important item of new aircraft finalizing design or qualified test flight. The ground calibration test of load must be carried out before load measurement by strain method, which is the premise and key of load measurement, and is an important link related to whether the result of load measurement is correct or not. The conventional online calibration method has severe limitations in loading conditions, small loading magnitude, high risk of balance, constraint and fixation of the whole machine, and large potential safety risks of human and machine, which cannot meet the needs of landing gear calibration test with complex structure and heavy load. Gear off-line load calibration technology.

[1] AVIC Chinese flight test establishment. TANG Ani: tangani@sohu.com.

Off-line calibration test of the landing gear is carried out by detaching the landing gear from the aircraft and fixing it on the specially developed ground platform, and applying the hydraulic automatic control system to load the landing gear, which effectively solves the problem of landing gear calibration with complex structure and large load.

Key technology

Development of general off-line calibration test equipment: the key of off-line calibration test is to free the landing gear from the aircraft support structure and fix it on the ground support structure for loading. The ground support structure, equivalent to the fuselage/wing simulator, is the core component of the test equipment. The ground support structure should simulate the landing gear installation in real aircraft to ensure that the landing gear installation is exactly the same as that in real aircraft. The universal design is realized on the basis of satisfying the requirements of off-line gear calibration test.

Landing gear mounting: landing gear mounting is the premise and basis of off-line calibration. Landing gear must be mounted on the platform exactly as it would be on a real aircraft, including the mode of connection, attitude, stiffness, etc.

Deformation coordination loading technology of space multidimensional combined force system: during the calibration test, the landing gear loads are decomposed in an orthogonal way, and the load components are the course load, vertical load and lateral load which are perpendicular to each other. The landing gear load points are in the center of the wheel or the tire contact point. At the same point on the landing gear to apply loads in different directions, if the design is not reasonable, easy to cause landing gear deformation drag, serious, causing damage to the landing gear; Another consequence is that the loading equipment deformed and stuck, resulting in damage to the loading equipment, affecting the safety of the test, and even the safety of the landing gear.

Modeling technology of complex structure landing gear: in the landing gear load calibration, the ideal situation is to find some single response positions, but in fact, it is difficult to find these positions of complex structure landing gear, the response of strain gauge is the integrated effect of multiple load output. This brings great difficulty to load modeling. For such a structure, a model of multiple input and multiple output loads is established on the basis of sufficient physical tests.

Technical objectives

Using this method can effectively improve the landing gear calibration test ability; improve the test safety and loading accuracy, more consistent with the real landing gear under load state. Its technical objectives are as follows: (a) calibrate the loading order to reach 100% load limit; (b) simulate the real load of the landing gear, and apply the combined load of complex working conditions to the landing gear; (c) the test process is safe and controllable to achieve complete automatic loading; (d) multi-input and multi-output modeling technology for landing gear of complex structure based on multi-dimensional loading.

Test equipment

Gear off-line calibration technology test equipment is shown in Figure 5-30.

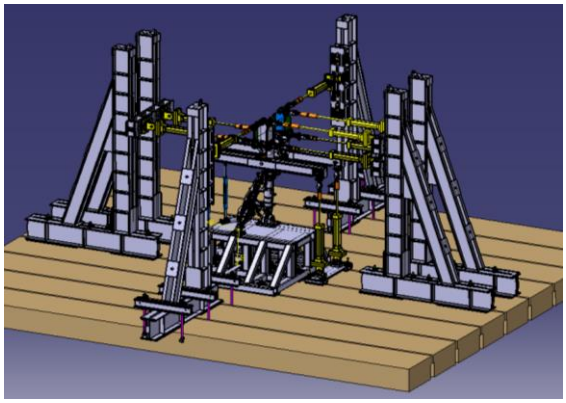

Figure 5-30 Off-line calibration test

Calibrate the measured results

Compared with conventional online calibration methods, offline calibration technology has significant advantages. The results of the two calibration methods are shown in Figure 5-31.

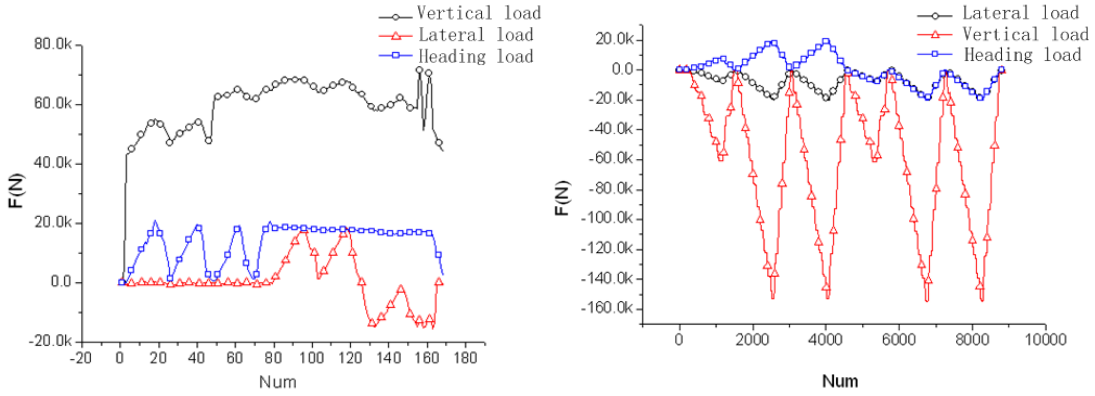

(a) Online results (b) Offline results

Figure 5-31 Results of load calibration test

In the conventional online load calibration, since the test object is the whole aircraft, in order to ensure the safety of the aircraft, the vertical load is usually applied first, and then the load in other directions is gradually applied. The loading effect is shown in Figure 5-31 (a). In addition, limited by the field conditions of the test, part of the landing gear can't be implemented under real loading conditions.

In off-line calibration, the landing gear is tested separately, and the calibration loads in each direction can be applied independently to completely simulate the various actual loading states of the landing gear. In combination loading, the landing gear can also be applied at the same time according to the actual different proportions, which can effectively improve the loading accuracy of the calibration test.

5.9 Research on the Scatter of Structural Load-time History in a Fleet[1]

It is necessary to consider all of the variability factors to access the reliability life of a structure. The variability factors mainly fall into two major categories, one is related to the structural characteristics, the other is about the load-time histories. The variability of structural characteristics consists of material

[1] AVIC Chengdu Aircraft Design & Research Institute. LI Tang: litang@buaa.edu.cn.

properties, processing methods, structure assembly, etc. There are already some relatively mature analysis methods of the problem. On the other hand, structural load-time history in a fleet scatters a lot due to the climate, weather, runway, pilot flying intelligence, etc. Even for one aircraft with the same flight mission, the actual load-time histories from different flights may have some difference. Recently, many researchers and engineers have tried to describe the scatter of load-time histories in a fleet. Most of the researches have focused on the normal acceleration (Nz) spectra or the load spectra of main components, e.g. the wing root load spectrum. However, there are few researches focusing on the scatter of load spectra of structural details, which directly relates to structural service life of agile fighter aircraft. In addition, load-time histories at different critical locations of one component may also differ. If the scatter factor of the fatigue life is more comprehensively determined, fatigue life prediction for aircraft structures will be more reliable.

Concept

To study the scatter of structural load-time histories, four typical structural details of 12 aircrafts from a fleet are chosen as case study. First, operational load-time histories at four critical locations in question of each aircraft are obtained according to the flight-data based load equation and transfer function relating the monitored load to the critical location stresses. Then, the fatigue notch coefficient in local stress-strain method is calibrated and validated by representative coupon test data and then used to calculate fatigue damage under different structural load-time histories of each aircraft. Finally, statistical analysis of the fatigue damages is conducted and scatter factor are obtained.

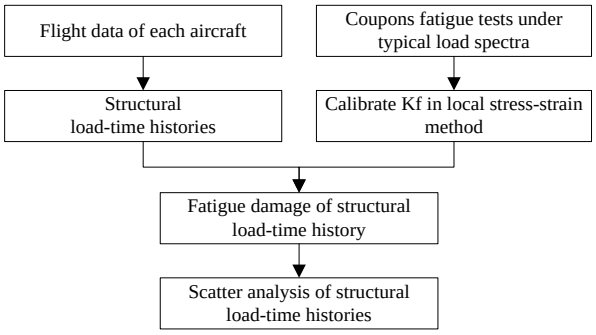

Figure 5-32 The flowchart of procedures

Case study

Representative coupons of the four typical structural details are designed. Fatigue tests of each coupon under three representative load spectra have been carried out. According to the test results, local stress-strain method can be calibrated. According to the flight-data based load equation and transfer function, four typical structural load-time histories of 12 aircrafts in a fleet are developed. Then the fatigue damage of every load-time history is evaluated by the calibrated local stress-strain method above and statistical analysis is performed. Nz spectrum is also analyzed as the benchmark. The five kinds of samples have good fitness to log-normal distribution, which are shown in the following figure.

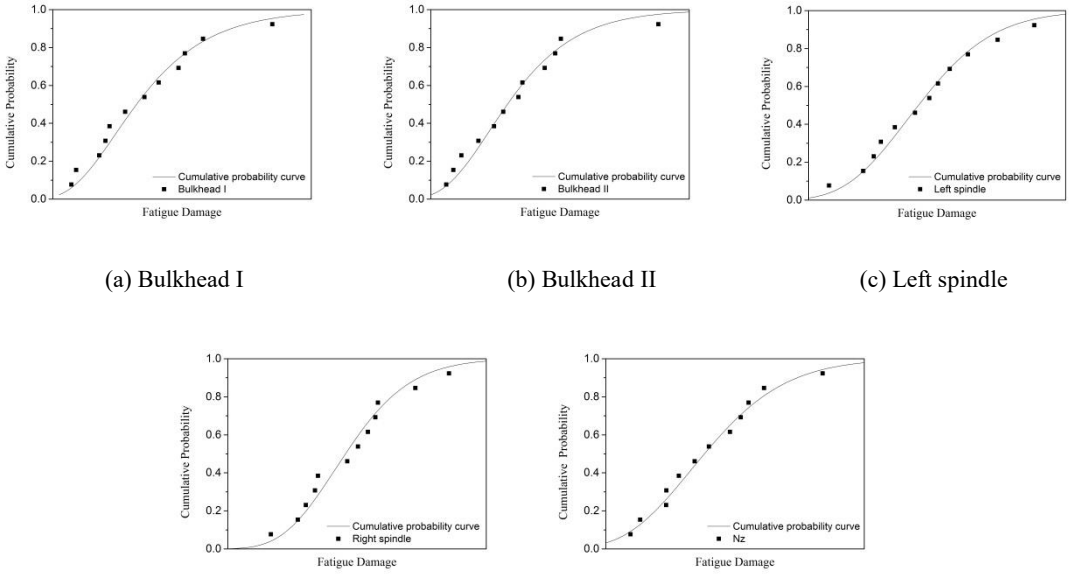

(a) Bulkhead I (b) Bulkhead II (c) Left spindle

(d) Right spindle (e) Nz spectrum

Figure 5-33 The fitness of samples to log-normal distribution

Table 5-3 Scatter Factor of different load-time histories

Structure	Log-normal Standard Deviation	Scatter Factor
Nz	0.084	1.79
Bulkhead I	0.1679	3.20
Bulkhead II	0.1468	2.77
Left spindle	0.0742	1.67
Right spindle	0.0802	1.74

Then, the logarithmic standard deviation and scatter factor are obtained, listed in flow table. Here, the reliability level is 99.9%.

Conclusion

Scatter of structural load-time history of aircrafts in a fleet has been analysed in this research and case study of operational load spectra at four typical structure details of 12 aircrafts is given. The result shows that there are significant differences in scatter factor of different structures. Thus, it may be advisable to fully consider the differences of scatter factor among different structures in structure fatigue life assessment.

5.10 Flight Tested Data Analysis of Helicopter[1]

Based on the characteristics of structure and load transfer, the origin, amplitude, frequency, phase and distribution regularity of helicopter rotor shaft moments were investigated. After that, the flight test data effectiveness of actual random spectrum was analyzed and abnormal data was distinguished. The actual random loading spectrum was developed, which provides a technical support for fatigue assessment in helicopter structures. The life of hub and shaft meets the target requirements with the measured rotor shaft moments spectrum.

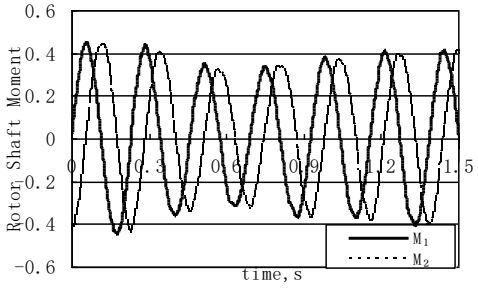

Figure 5-34 Time domain of two rotor shaft moments interval 90 degree angle circumferential

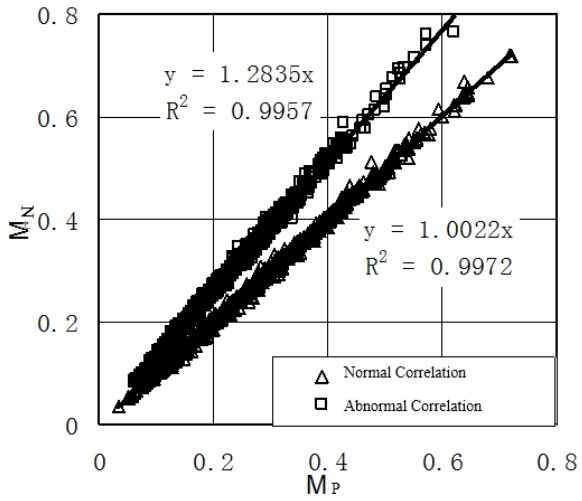

Figure 5-35 Correlation analysis of two rotor shaft moments amplitude at different circumferential angle

5.11 Uncertainty Evaluation of Wing Flight Loads Measurement [2]

Flight load measurement plays an important role in the whole flight test, which can verify whether the aircraft structure is reasonable or not. In flight load measurement, the accuracy analysis of measurement results is very important. In the field of measurement, the general method is to give the standard uncertainly an extended uncertainty based on the uncertainty evaluation theory.

Key Techniques

Through the analysis of the wing loading test each link may affect the measurement results, the

[1] AVIC China Helicopter Research and Development Institute. CHEN Yaping: cyp28503059@avic.com.

[2] AVIC Chinese flight test establishment. YAN Wenhui: fourse@126.com.

uncertainty evaluation theory is introduced into the load analysis of measurement results, The mathematical model for the evaluation of the uncertainty of the load measurement test is calculated used by two kinds of method, including the uncertainty of transmission method and Monte Carlo method, and the calculation is made based on the wing load measurement data of a certain type of aircraft.

Technique Targets

For the measured wing load of a certain type of aircraft, the standard uncertainty calculation model of wing load is established, as shown in Eq. 5.1：

$$u_c(L)=\sqrt{\begin{aligned}&(\beta_1*u(\mu_1))^2+(u(\beta_1)*u_1)^2+(u(\mu_1)*u(\beta_1))^2+(\beta_2*u(\mu_2))^2\\&+(u(\beta_2)*u_2)^2+(u(\mu_2)*u(\beta_2))^2+\ldots+(\beta_m*u(\mu_m))^2+(u(\beta_m)*u_m)^2\\&+(u(\mu_m)*u(\beta_m))^2+2\sum_{i=1}^{m-1}\sum_{j=i+1}^{m}(r(\beta_i\beta_j)*u(\beta_i)*u_i*u(\beta_j)*u_j)\end{aligned}} \tag{5.1}$$

For the load Eq. 5.2, the probability distribution model of equation coefficient and strain bridge response as shown in Table 5-4, was established for Monte Carlo sampling calculation.

$$L=[\beta_m][\mu_m] \tag{5.2}$$

Table 5-4 Input probability

	β	μ
Probability distribution	Multidimensional normal distribution	Uniform distribution
Multidimensional expectation	$[\beta]$	μ
The variance	$K_R^2*S^2(\mu^T\mu)^{-1}$	$\frac{(1\%\mu)^2}{12}$

The uncertainty of wing flight test loads

For the wing load measurement test of a certain aircraft, GUM and MCM methods were used to calculate the uncertainty of shear force and moment load under a certain measures section, The results are shown in Figure 5-36 and Figure 5-37.

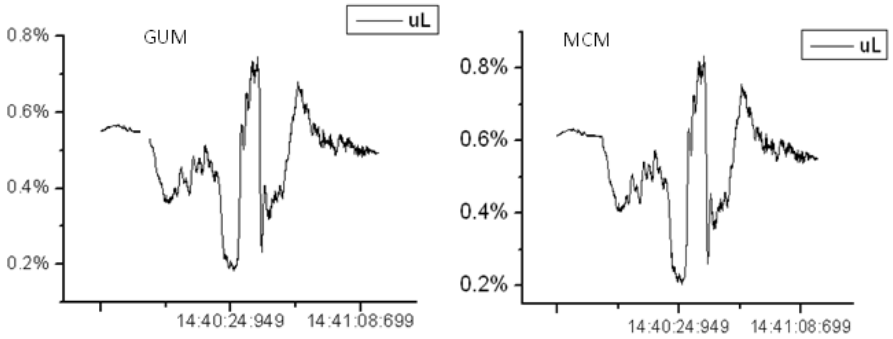

Figure 5-36 Uncertainty of shear force

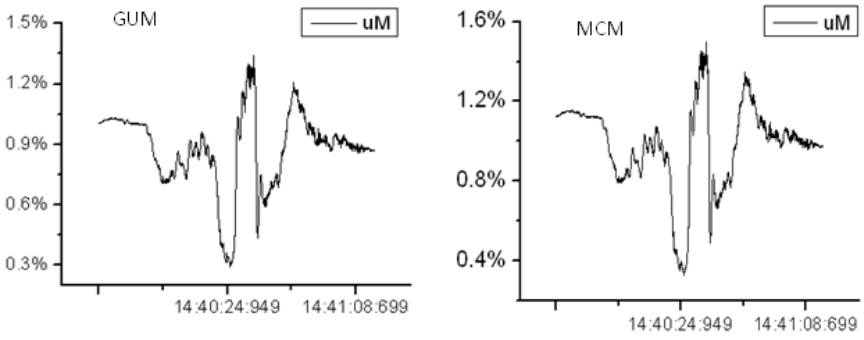

Figure 5-37 Uncertainty of bending moment

For shear force and bending moment of uncertainty, the uncertainty of relative to the load maxima is small, the size of the peak value is less than 1.5%, the measurement is relatively accurate, the uncertainty of MCM generally greater than GUM uncertainty, which dues to the calculation model of the GUM department set up as shown on the type of equation 3.1 when the factors of uncertainty of measurement caused by the merger, simplified.

5.12 Research on Virtual Load Calibration Test Technology[1]

Virtual load calibration test uses CAD/CAE as tools to simulate the load conditions. By applying virtual load to the finite element model and extracting the virtual strain, relationship between virtual strain and virtual load, as known as load equation, is established. Firstly in this paper, based on the virtual test method, the wing root load calibration method of the underwing landing gear layout aircraft was studied. By spinning of the influence of the landing gear load, the load equation was established. And the correctness of the method was checked using the model. Then we studied the relationship between the load equation precision and load condition numbers and load condition selection, based on virtual calibration test. The optimization design scheme was proposed to improve the test efficiency, precision and economical efficiency.

There are three key techniques in the present research, which are: (a) model building and model verification technology of virtual load calibration test; (b) the wing root load calibration method of the underwing landing gear layout aircraft based on virtual load calibration test; (c) study on the optimization design scheme of the load calibration test based on virtual load calibration test.

There are six technique targets in the present research, which are: (a) establish the finite element model of the aircraft wing; (b) design and build the strain gage of the virtual test based on the real strain modification scheme; (c) design the constraint and calibration load of the virtual test model based on the real load calibration test scheme; (d) modify the virtual test model based on the real load calibration test results; (e) based on the virtual test method, the wing root load calibration method of the underwing landing gear layout aircraft was proposed. By applying calibration load on the virtual model, the load equation was established and the correctness of the method was checked; (f) the optimization design scheme was proposed.

[1] AVIC Chinese flight test establishment. MENG Min: 510659780@qq.com.

Research results

The first one is the virtual test model building and modification technology, which includes virtual strain building technology, virtual test model building technology and virtual test model correction technology, as shown in Figure 5-38.

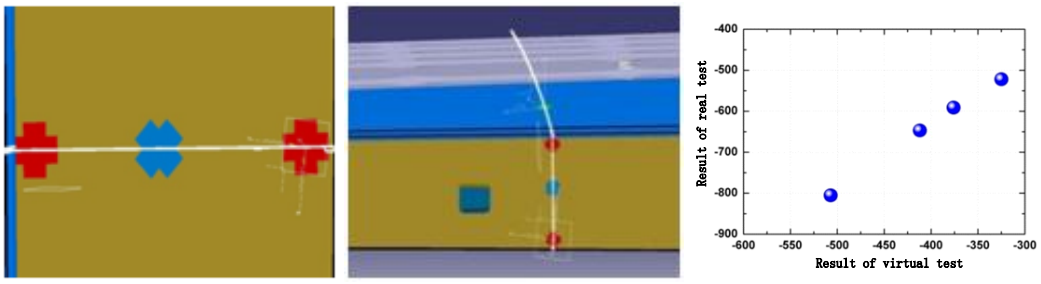

(a) (b) (c)

Figure 5-38 (a) Virtual strain building technology, (b) Virtual test model building technology (c) Virtual test model correction technology

The second one is the wing root load calibration method of the underwing landing gear layout aircraft based on virtual test. Using the virtual test, the decoupling condition of landing gear load was designed, and the constraint load was decoupled successfully. The virtual test was designed to build a load equation. It solved a worldwide problem, which was the wing root load calibration test of the underwing landing gear layout aircraft.

The third one is the optimization technology of load calibration condition based on virtual test. Based on virtual test, the key factors of load calibration test scheme, such as the number of building model condition and the selection of building model conditions, were studied to improve the test efficiency, precision and economical efficiency.

The summary of virtual load calibration test process is shown in Figure 5-39.

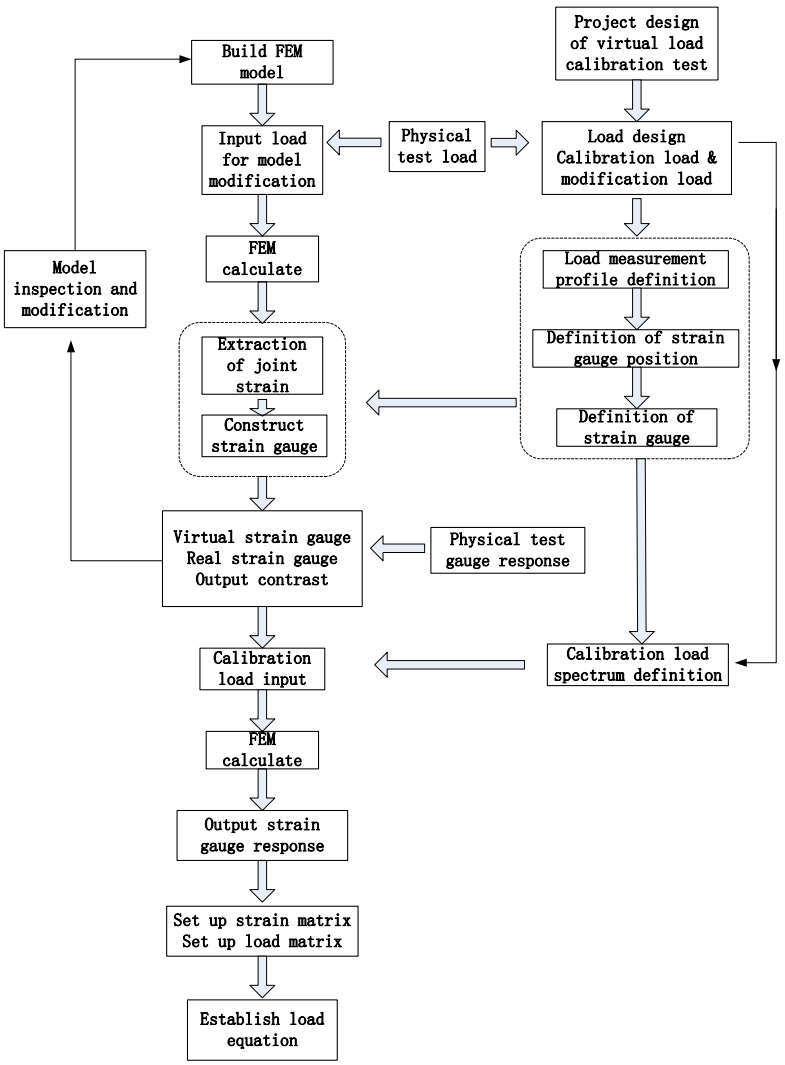

Figure 5-39 The flow chart of virtual load calibration test process

5.13 Research on Flight Load Pattern Recognition Methods and Applications[1]

Load data of engine such as heat, pressure and structure are important basis for reliability design of engine structure and data source for structure failure analysis of engine components. With the development of engine design towards refinement and pure probability, simple data statistics can no longer meet the design requirement, it is urgent to master the distribution law of various load parameters and the extreme value under a certain degree of reliability to carry out the reliability research of components and the whole machine. To solve this problem, extreme value prediction based on nonparametric estimation has been applied in recent years. However, the disadvantage of non-parametric estimation method is that it is impossible to obtain the distribution probability model of samples, which brings new problems to the reliability test of engine components. Therefore, how to accurately obtain the law of sample distribution and how to predict the extreme value of these sample data is a problem to be solved in the study of flight load spectrum.

[1] AVIC Chinese flight test establishment. LEI Xiaobo: 627983062@qq.com.

Key Techniques

In consideration of unknown to aircraft/aero-engine load parameter probability distribution modes, the method of using general distributions and correct pattern recognition was established to get the nearest distribution to the sample, and then the extreme value of the sample could be predicted using high accurate calculations of distribution parameters. The analysis and comparisons were carried out by use of using Mahalanobis distance, fuzzy nearness and weighted distance methods, and the results show that weighted distance method could correctly recognize the nearest distribution to the sample. Analysis results show that the maximum value of normal overload is expressed by Weibull distribution on load pattern recognition method, the conclusion is proved to be correct by K-S test. The weighted distance method and the method of extreme value prediction provide important methods for aircraft and aero-engine reliability research.

Technique Targets

The targets of the method are gaining the probability distribution of one parameter through analyzing the sample. Considering that the probability models commonly used in engineering research have extensive universality and strong data fitting ability, this paper proposes a weighted distance discrimination method to identify the best probability model of the sample. It differs from the traditional distance method in that different distances are multiplied by a weighting coefficient. Due to the probability of sample data appearing in different intervals or the degree of distribution density is not equal, so the contribute of the difference between two patterns in a certain interval to pattern recognition should also be unequal. The greater probability density of the intervals is, the greater the proportion of the difference value contribution of the interval should be, and vice versa. Here, the probability of the actual sample interval distribution is used as its weight coefficient, and the specific expression is

$$Q(A_i, B) = \sum_{k=1}^{m} B(x_k)\left|A(x_k) - B(x_k)\right| \tag{5.3}$$

where m is the number of intervals divided, when

$$Q(B, A_i) = \min\{(B, A_1), (B, A_2), \ldots (B, A_n)\} \tag{5.4}$$

Then the distribution probability model of the sample B is closest to the model of A_i.

In order to verify the correctness of the method, Matlab random number generation function is used to generate random number samples subject to various probability distributions, the sample size is set at about 200. In this paper, three load pattern recognition methods are compared and analyzed by taking samples of normally distributed random numbers, log-normally distributed random numbers and three-parameter Weibull distributed random numbers as examples. In order to increase the difficulty of identification, most of the sample values are set within the same range when generating random numbers with the above distribution. In this paper, the range of statistical interval is set at 0~9, and a small number of data points also exist in other intervals.

A logarithmic normal distribution random number sample conforming to μ=0.8，σ=0.5 is generated. The weighted distance method identifies the sample as closest to the logarithmic normal distribution, while both markov distance method and fuzzy recognition algorithm identify errors. The lognormal distribution parameters estimated by the weighted distance algorithm are μ=0.8021，σ=0.5164, and the relative errors are 0.263%、3.28%, it can be seen that the predicted value is of high precision.

Extreme value pattern recognition and prediction of aircraft normal overload

The maximum normal overload value of 118sorties of an aircraft was obtained by outfield statistics. Figure 5-40 shows the histogram of the maximum value of normal overload N_z.

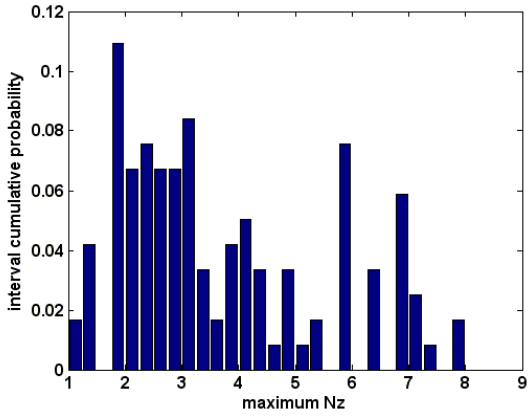

Figure 5-40 Maximum values histogram of normal overload

The distribution probability model fitting method in the probability model library is used to sample the maximum overload value, and the interval step is 0.5. The probability density distribution of each probability model is shown in Figure 5-41. As can be seen from the probability density distribution in Figure 5-41, the normal distribution and Rayleigh distribution are obviously different from the other four probability models, but the probability density changes with the interval are generally consistent.

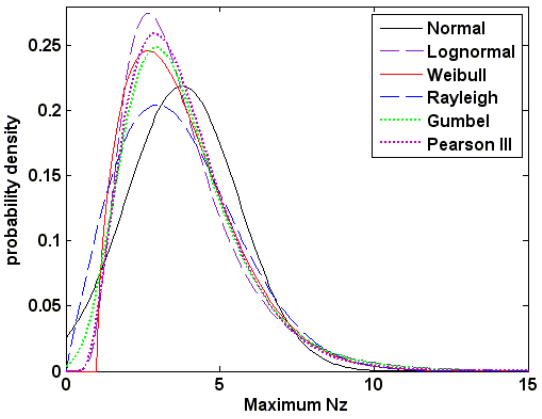

Figure 5-41 Probability density curves of different distributions

The weighted distance method was used for pattern recognition of the maximum normal overload samples. The recognition results showed that the maximum normal overload samples of the aircraft were closest to the weibull distribution, and the correlation coefficient R between the fitted value and the measured value of the weibull distribution reached 0.984. The expression of the cumulative distribution of the maximum normal overload is

$$F(N_z)=1-e^{-(\frac{N_z-1.052}{3.03})^{1.53}} \tag{5.5}$$

In order to further test whether the maximum normal overload value obeys the three-parameter weibull distribution, Kolmogorov-Smirnov(K-S) method in the non-parametric test can be used to test. Set the distribution function of measured samples are $F(x)$, the distribution function of reference samples are $R(x)$, both the measured sample size and the reference size are N_1, the distance between the two samples is calculated according to equation 11.

$$D = \sup_{-\infty<x<+\infty} \left| F_{N_1}(x) - R_{N_1}(x) \right| \tag{5.6}$$

The observation $\hat{D}$ of statistic D in given α, if $\hat{D} < D_{\alpha,N}$, then the actual samples and reference samples belong to the same population, in this α=0.05,look up the table and get the threshold $D_{0.05,118}$=0.1235, observed value $\hat{D} = 0.1030 < 0.1235$. Therefore, the maximum normal overload samples follow the three –parameter weibull distribution listed in formula 10, Table 5-5 shows the maximum normal overload of different reliability predicted by each distribution model.

Table 5-5 Maximum values of normal overload of degrees of reliability

distribution	R_D=90	R_D=95	R_D=98	R_D=99	R_D=99.9
Normal	6.115	6.777	7.521	8.018	9.409
Lognormal	6.264	7.466	9.096	10.377	15.008
Weibull	6.209	7.141	8.256	9.035	11.353
Rayleigh	6.363	7.258	8.294	8.999	11.021
Gumbel	6.260	7.325	8.704	9.737	13.151
P-Ⅲ	6.113	7.057	8.232	9.082	11.760

6. RESEARCHES ON FULL SCALE STRUCTURAL TEST

6.1 Structural Health Monitoring for Aircraft Structure Ground Test[1]

At present the structural integrity detection in aircraft structure ground test mainly depends on the nondestructive testing (NDT) techniques and strain monitoring by strain gauge. However, these NDT techniques need the complex testing equipment, and are time-consuming. For some unreachable aircraft structure, it even requires component disassembling. These NDT techniques are also influenced by human factors, which would cause the damage to be undetected. Structural health monitoring (SHM) technology offers an alternative means to detect and monitor damage in aircraft structure ground test.

For the SHM in aircraft structure ground test, the researches include strain monitoring by Fiber Bragg Grating (FBG), damage monitoring by the guided waves-based damage monitoring (GWDM) technology and acoustic emission (AE) technology, and SHM system integration.

Strain monitoring by FBG

The FBG technology is used to strain monitoring in aircraft structure ground test. Then using the strain of aircraft structure, the stress/load history of aircraft structures can be reversed, and the structural integrity of aircraft structures could be assessed. Figure 6-1 shows the strain monitoring of fuselage using FBG.

[1] AVIC Aircraft Strength Research Institute. LIU Guoqiang: gqliu1984@163.com.

Figure 6-1 Strain monitoring of fuselage using FBG

Damage monitoring by the GWDM and AE

The GWDM and AE are used to monitoring the aircraft structure damage. Using the relationship between the aircraft structural damage and monitoring signal characteristics, the damage location, size and type are identified by information processing, algorithm and pattern recognition. Figure 6-2 shows the damage monitoring of fuselage using GWDM. Figure 6-3 shows the damage monitoring of landing gear joint using AE.

Figure 6-2 Damage monitoring of fuselage using GWDM

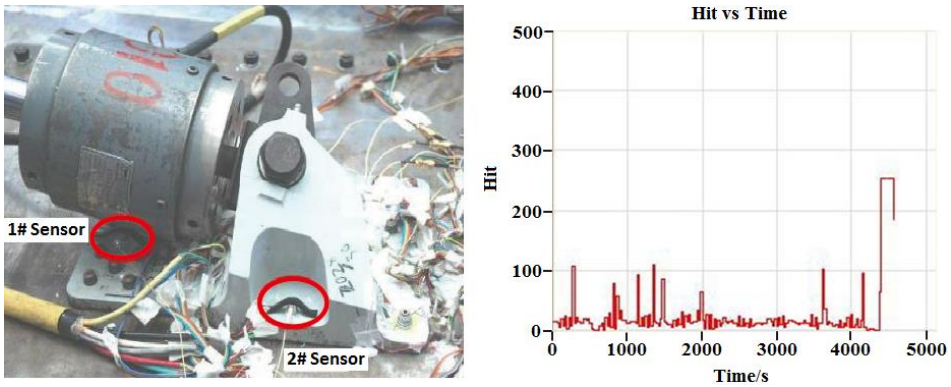

Figure 6-3 Damage monitoring of landing gear joint using AE

SHM system integration

Figure 6-4 shows the SHM integrated system applied in the aircraft wing test.

Figure 6-4 Developed SHM integrated system

6.2 Damage Tolerance Test on Straight Section of MA700 Aircraft[1]

In this Damage tolerance test, a Self-balancing frame is designed which integrates support, load, hydraulic pressure pipeline, inspection platform and other systems. The test was conducted for the following purpose, verify topical crack propagation characteristics of fuselage wall panel, evaluate the two-span crack and verify the residual strength of the fuselage structure, to study and verify the nondestructive inspection characteristics of structures, in order to study and verify the typical fuselage wall panels, frames and other structural design concepts and analysis methods, the strain, displacement and deformation of the structure under static design condition have also been studied.

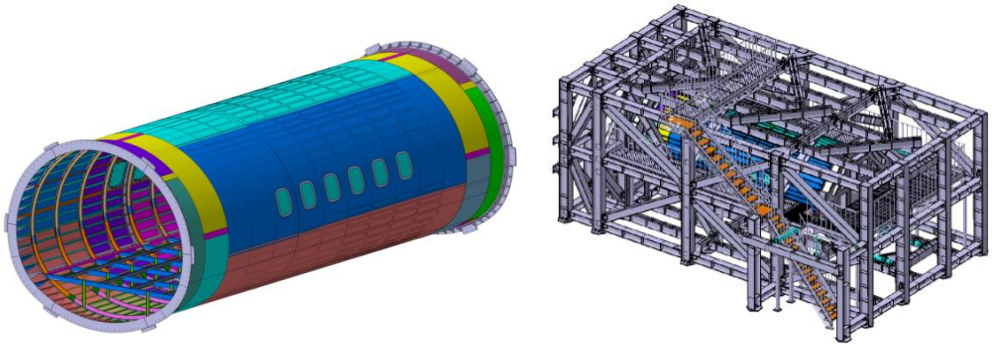

Figure 6-5 Schematic diagram of the straight section structure and the Self-balancing frame

The test items include static test and damage tolerance test. The damage tolerance test included a crack growth test that doubled the design service target (60000 flight cycles).

[1] AVIC Aircraft Strength Research Institute. ZHANG Huifeng: zhanghfeng@126.com.

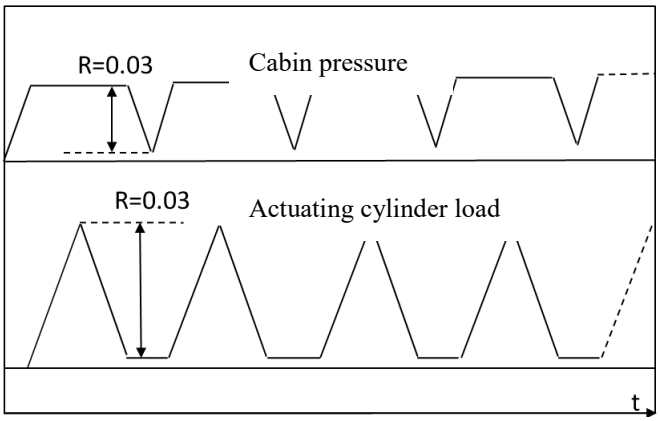

Figure 6-6 Schematic diagram of Damage tolerance test load

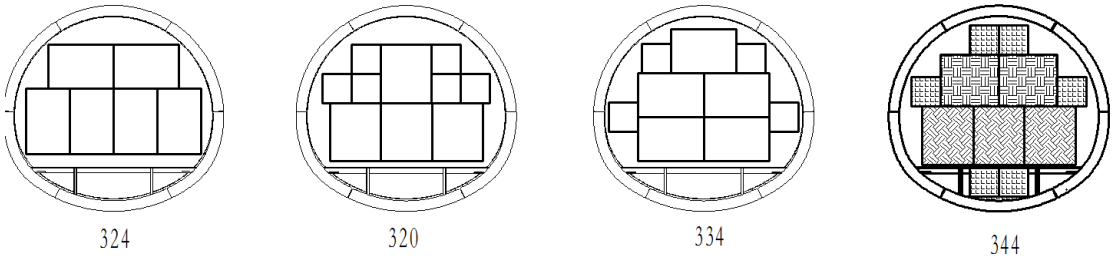

Figure 6-7 Two sizes of filler achieve 70% space filling

Thirteen cracks were prefabricated on the straight section test piece of the fuselage with a diameter of about 3m for damage tolerance test. Space filling, multi-way filling and unloading, active pumping and other ways are adopted, which greatly shorten the test period and improve the test efficiency. After experiencing one lifetime (60000 cycles) fatigue load, the precast crack has expansion. Except for the prefabricated cracks, extensive damage occurred in the frame at the 3-4 long piles upward on the floor on both sides of the fuselage.

Figure 6-8 Self-balancing overall support loading framework

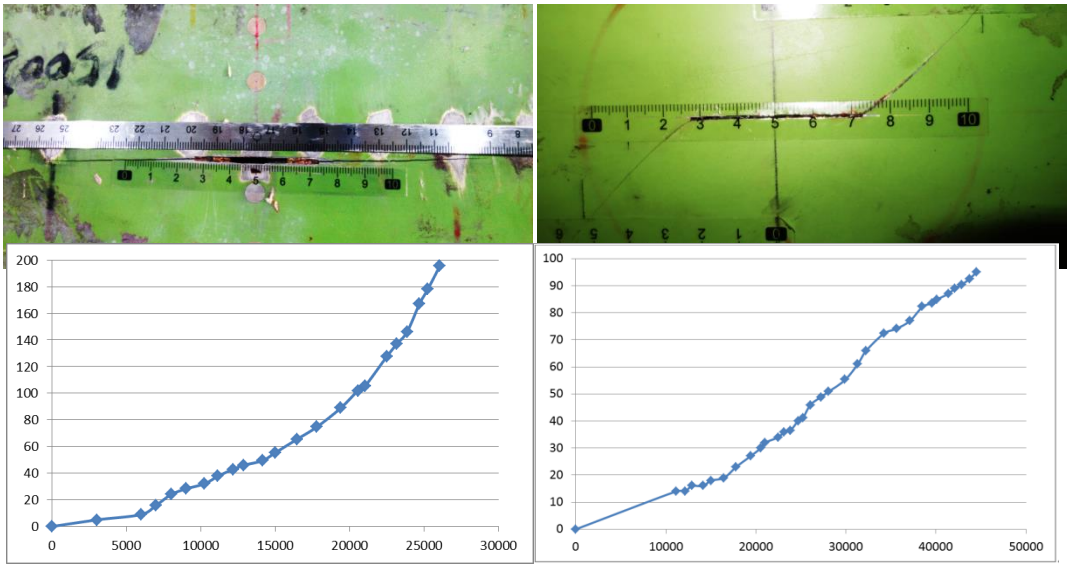

Figure 6-9 Precast crack growth condition and crack growth curve

Figure 6-10 WFD of the fuselage frame

6.3 Strength Test of the Mid-rear Fuselage [1]

The fuselage structure is one of the key components of the whole aircraft structure, applying the fuselage load in a different way is directly related to whether the test can simulate the true load cases of the fuselage structure, and thus affect the effectiveness of strength test. The inertial load of cargo and passengers is the main load borne by the fuselage of civil air craft. The load ACTS on the floor structure of the cabin and warehouse inside the fuselage, and then is transferred to the fuselage shell structure through the floor structure.

[1] AVIC Aircraft Strength Research Institute. SHAO Qian: shaoqian623@163.com.

Figure 6-11 The Mid-rear fuselage stiffness and strength test

At the component level in the static test, the test structure loading is more concerned about the details of each part, and the cabin and cargo loading way is based on four fuselage frame standard load applied. There are some problems, such as the position load of each fuselage frame cannot be distributed according to the actual load, and the position of resultant force point of cabin load and cargo load is not coincident.

In the component level static test, there are usually a variety of test cases, and the proportion of the load in each frame and the position of the resultant force are also change accordingly. To truly simulate the loading, the lever ratio should be adjusted according to the requirements of test cases. Therefore, connection holes corresponding to loading positions in different test cases are set up on the first lever to install and adjust the position of the second lever. The third lever is equipped with two rods for extracting the load, and the outside of the fuselage is connected by an external loading lever. It is worth noting that the span of two rods covers the position of resultant force under all test cases. In this way, the load can be applied to each frame in proportion to the position of the resultant force on the external loading lever

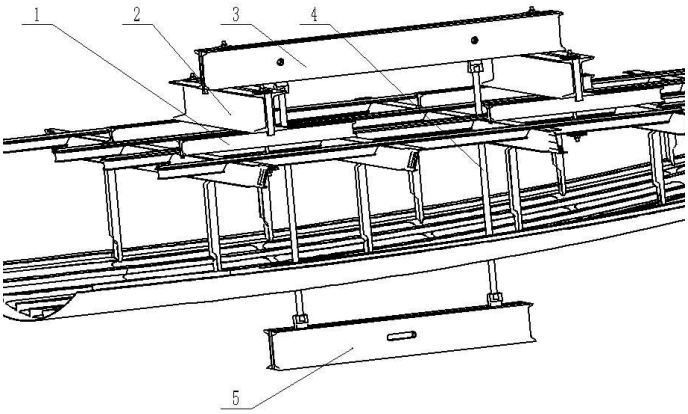

1-The first lever, 2-The second lever,3-The third lever,4-The rod,5- External loading lever

Figure 6-12 Loading Schematic Diagram

In the strength test of the mid-rear fuselage continuous opening zone, the above method is used for internal payload loading, which solves the problem that it is difficult for the fuselage load to be applied to each frame according to the theoretical value. Through the separation and extraction of the loading method, the problem of the failure to apply the theoretical load to each case was solved. The loading

method has less influence to the fuselage, reducing the centralized loading of the fuselage panel, and the process from bucking to damage can be clearly observed in the full-size large part test. In the test, the measurement date is transmitted simultaneously, and the tester can compare the real-time data with the calculated value, and find the abnormal situation in time.

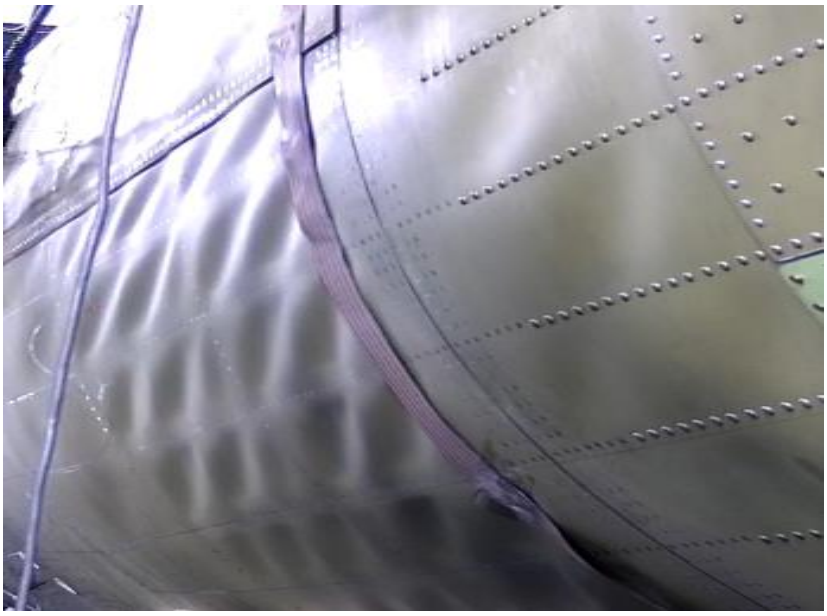

Figure 6-13 Fuselage skin buckling tension field

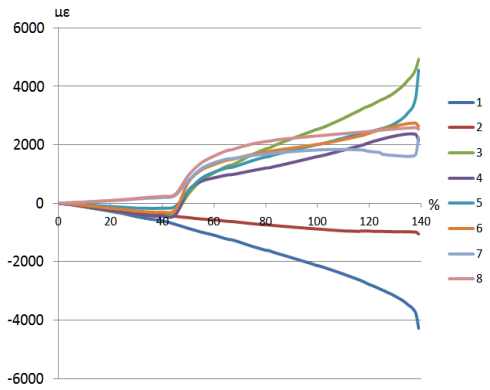

Figure 6-14 Strain measurement curve

6.4 Static Test of Typical Box Structures in Horizontal and Vertical tails[1]

The box structure of horizontal and vertical tails is an important structure form of aero-transport and its mechanic performance has a direct influence on the security and economy of aircraft. In the research of tail design, it's the foundation of structure configuration selection, structure design and modification.

Key Techniques

This test evaluated the static load capacity of typical box structures in horizontal and vertical tails. The load working states include the local load state, abrupt pitching maneuver and rolling maneuver due to the yaw motion. The emphasis and difficulty of abrupt pitching and rolling maneuver tests lie in how to simplify the actual wing load and transform it from wing panels to ribs according to the moment balance theory. In the actual testing, the characteristic of loading apply was adopting lock boards to replace the traditional loading methods, such as canvas-pad, which will cause damage to the surface of specimens in the grinding stage.

[1] AVIC Aircraft Strength Research Institute. YANG Jun: tex1110@163.com.

Test Device

Figure 6-15 shows the local load test which occurs in the joints of vertical tail. Figure 6-16 shows the loading apply of abrupt pitching and rolling maneuver tests.

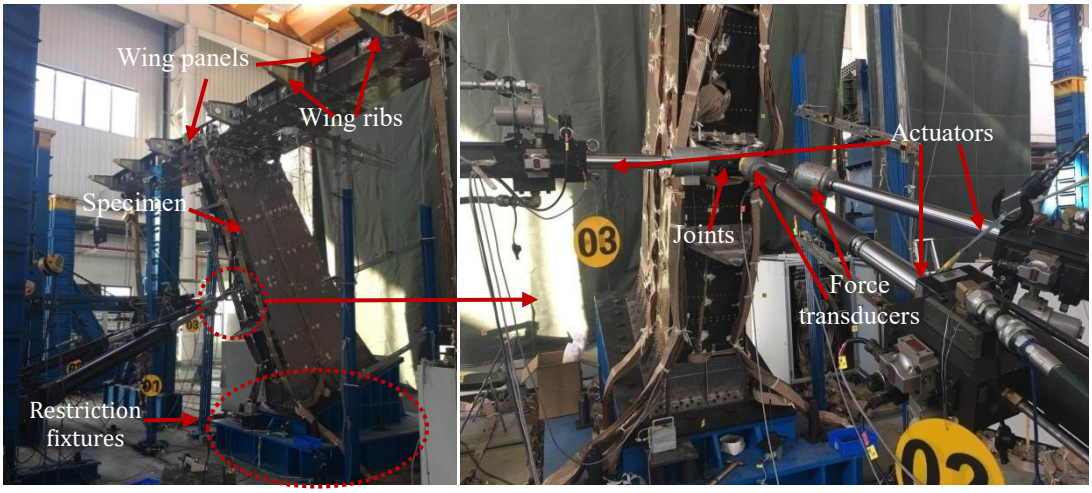

Figure 6-15 Local load test of horizontal and vertical tails

Figure 6-16 Abrupt pitching and rolling maneuver tests of horizontal and vertical tails

6.5 Airworthiness Validation Technologies for Fatigue of General Aviation Aircraft Improved Structures and Engineering Application[1]

Civil aircraft must conduct fatigue airworthiness according to requirements published by airworthiness authority. Full-scale fatigue tests are the most reliable method for establishing the fatigue performance of a structure. When testing a complete airframe, a crack develops on some structure. Applicants choose to repair the cracked structure and continue the test, improved design for the local structure. Since do not conduct full-scale fatigue tests or spectrum loading component level tests on improved design structure, this paper researches relevant fatigue airworthiness documents published by FAA, and then discusses

[1]AVIC Harbin Aircraft Industry Group Co.Ltd. LI Yulian: Liyulian1980@163.com.

some key airworthiness validation technologies for analysis supported by test evidence of general aviation aircraft improved structures (Figure 6-17 - Figure 6-19), based on an engineering application of fatigue airworthiness validation for a general aviation aircraft. This method provides some guidance for general airplane design airworthiness validation technologies for fatigue of aircraft improved design structures.

Figure 6-17 Full-Scale Fatigue Test of general aviation aircraft

Figure 6-18 Crack at the rivet hole in spar

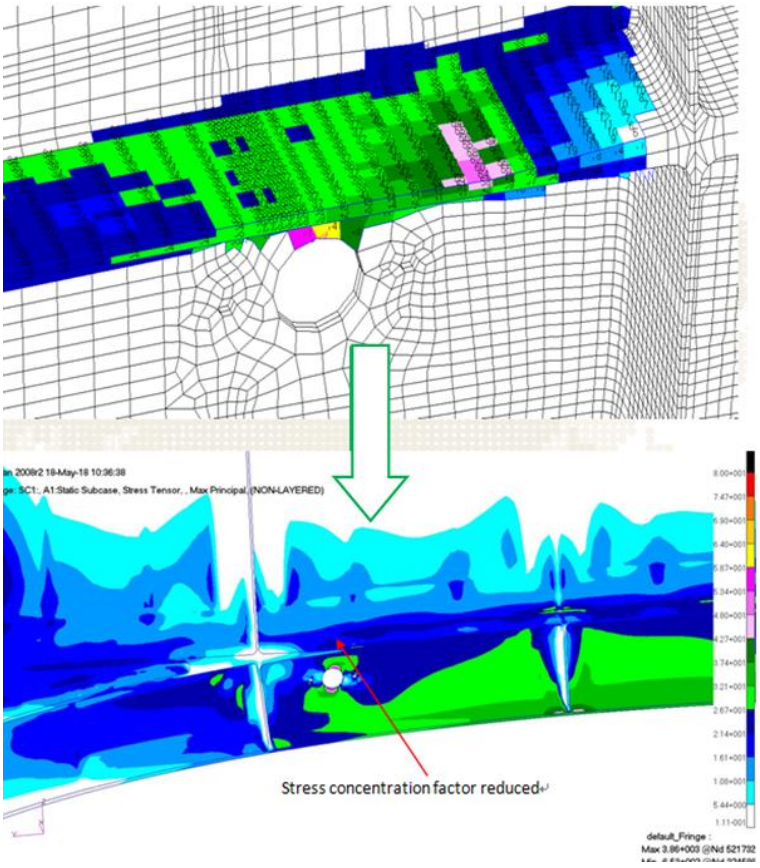

Figure 6-19 Stress comparison

6.6 Experimental Techniques of Ground and Air Resonances of a Helicopter Excited by a Fly-by-wire Flight Control System [1]

In helicopter ground resonance and air resonance experiment, through the fly-by-wire flight control system is adopted to improve the motivation of excitation signal directly injected into the flight control system of the main oar steering gear, and through the three steering gear coupling output helicopter, and the longitudinal and transverse cycle variable distance and rotor total distance incentives, to complete the key mode of incentive to the body and rotor helicopter. The dynamics characteristics of the rotor and the airframe structure under different conditions are obtained, and the problems of difficult excitation input control, unpredictable input and high safety risk in the ground and air resonance tests of the helicopter are solved.

The driving principle diagram of the fly-by-wire flight control system is as follows:

[1] AVIC Chinese flight test establishment. LI Xiaolu: 89233848@qq.com.

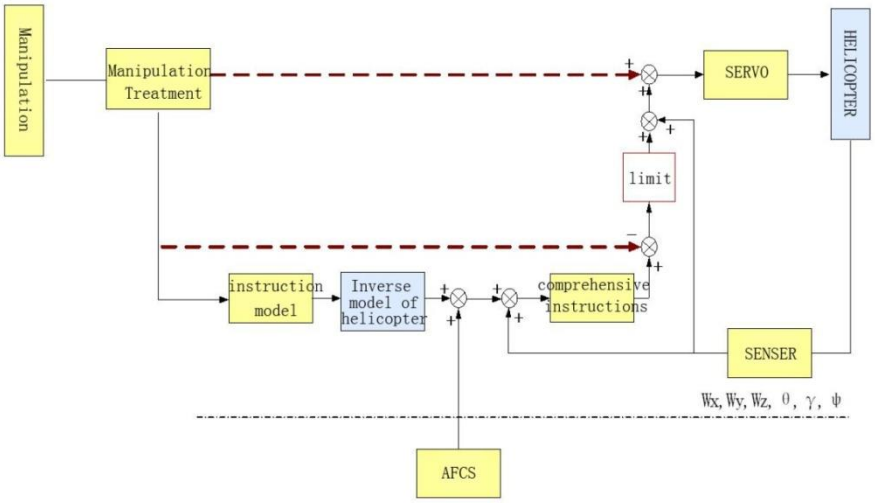

Figure 6-20 The driving principle diagram of the fly-by-wire flight control system

The working principle diagram of the helicopter excitation system is as follows:

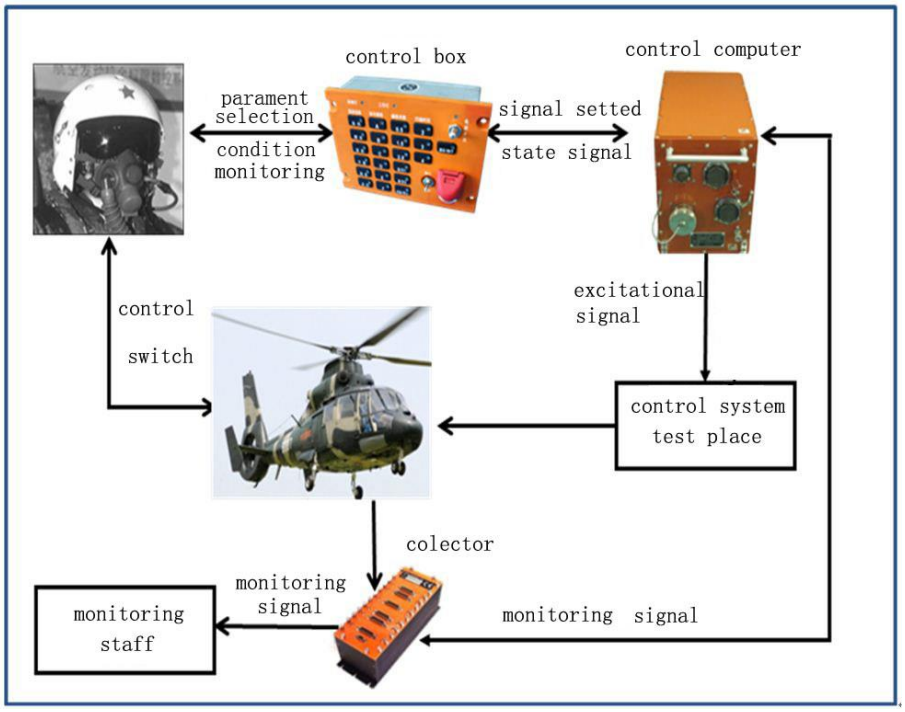

Figure 6-21 The working principle diagram of the helicopter excitation system

Excitation signal design includes: (a) constant frequency sinusoidal signal; (b) equal amplitude sinusoidal linear sweep signal; (c) sinusoidal logarithmic sweep signal; (d) variable amplitude and frequency compound linear sinusoidal signal; (e) multistage frequency conversion sinusoidal linear sweep excitation signal; (f) exponential excitation signal; (g) pulse excitation signal.

The excitation test results are shown in the figures below.

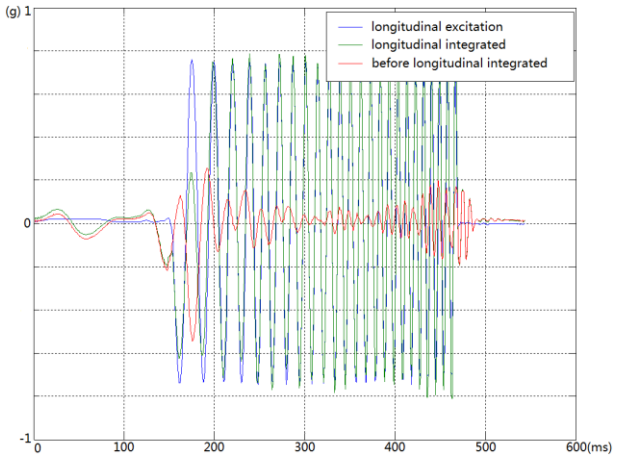

Figure 6-22 Input and output time domain diagram of pitch variable pitch angle

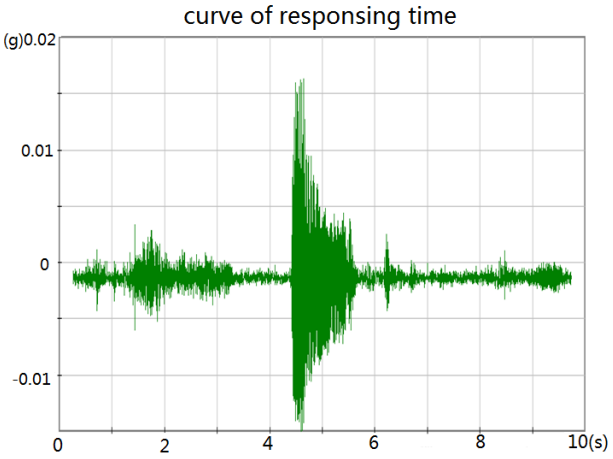

Figure 6-23 Time domain diagram of vibration sensor response at hub of helicopter propeller

6.7 Landing Gear Shimmy Flight Test Technology [1]

Landing Gear shimmy is a harmful self-excited vibration phenomenon during aircraft taxiing. It is shown that the wheel swing part rotates alternately around its directional axis, and the tire and ground contact part deforms alternately. Front wheel swing also causes the rocking of the front landing gear strut and the front fuselage, and even causes the whole aircraft to flutter from head to tail. At the airport, you can see a S-shaped track of the tire on the runway after the shimmy. The instability degree of shimmy can be from harmful vibration to structural damage, or even landing gear failure. The landing gear shimmy problem has occurred in the development or actual use of domestic and foreign multi-type aircraft, which has caused serious damage to the landing gear structure and even fuselage. When the shimmy diverges sharply, it can directly lead to the landing gear damage and accident.

Shimmy is a major defect in the development of landing gear, which must be eliminated through test verification. The test verification is divided into two stages， ground test validation and flight test validation. Ground test is to validate the shimmy of a single landing gear on a laboratory shimmy platform. The domestic technology development has been relatively mature. In recent years, with the development of civil aircraft flight test technology, shimmy flight test has just started. The first domestic shimmy flight test has been completed, and ARJ21-700 aircraft landing gear support flight test has been completed. This report briefly introduces ARJ21-700 swing flight test technology.

The method of shimmy flight test

[1] AVIC Chinese flight test establishment. TANG Ani: tangani@sohu.com.

The method of shimmy flight test is to apply a lateral and torsional excitation to the landing gear during taxiing, to stimulate the initial vibration of the landing gear, and to evaluate the stability of the landing gear by structural response analysis. Before the test, the acceleration sensor should be installed on the landing gear structure. Tire shimmy needs to excite the initial deflection angle of landing gear (initial swing angle), while structural shimmy needs to excite the vibration modes of landing gear. Generally, the modes of landing gear shimmy include lateral bending and torsion, and they are also the modes that must be analyzed in shimmy test. However, in actual test, the bending mode of the front and back pillars is relatively easy to excite.

Key Technical and Difficulties

The excitation technology is one of the key technologies in shimmy flight test. In order to effectively excite the relevant modes of landing gear shimmy, special excitation measures should be applied to the landing gear. Incentive measures include operating incentives for landing gear, or external incentives through a certain way. External excitation is a way to excite landing gear through special external equipment. The commonly used methods are the unbalanced additional mass method and the excitation plate method. The unbalanced additional mass method is to add a small mass block on one side of the landing gear wheel, so that the landing gear has been subjected to an asymmetric excitation. In the excitation plate method, shimmy board is installed on the runway to make the landing gear impact through the excitation plate at a given speed. Under this excitation landing gear subjected to serious external disturbances is the most effective and dangerous incentive method. The key of the excitation plate method is to develop a suitable excitation plate. The so-called appropriateness refers to the need for sufficient incentive capacity to achieve a significant incentive effect, while taking into account the use of landing gear restrictions, can't damage the landing gear structure. Several key parameters in the development of the excitation plate are the profile shape, height, installation angle and material of the excitation plate.

In order to develop a suitable excitation plate, the landing gear structure was analyzed by force analysis, impact dynamic characteristics analysis and so on, and the multi-body dynamics software was used to simulate the calculation. Finally, it is determined that the material of the excitation plate is made of steel, the section shape is trapezoidal, the thickness is 35mm, the edge is rounded, and the connecting holes are arranged on the plate. As shown in Figure 6-24.

Figure 6-24 The shimmy board of landing gear shimmy test for ARJ21 aircraft

Buffer Stroke Fixation and Its Impact

It is almost impossible to keep the stroke of the landing gear buffer unchanged in the test because the rigidity of the landing gear will change with the change of loading condition and travel. Secondly, the maximum buffer compression stroke and the minimum buffer compression stroke (or fully extended state) are also difficult to control in practice. All these bring great difficulty to flight test and data analysis. In order to solve the above difficulties, some measures have been taken in flight test, such as maintaining a smooth sliding speed before landing gear collision plate, and using pressure rod or pull rod to control the maximum or minimum compression stroke. Classification in data analysis can alleviate the above problems to a certain extent.

The shimmy validation test of the front and main landing gear of ARN21 aircraft was carried out by

installing the excitation plate on the runway. The excitation plate is fixed on the runway at an angle of 45 degrees, and the impact mode is two-wheel impact. Landing gear buffer compress stroke from minimum to maximum, mainly by changing the weight of aircraft taxiing, aircraft taxiing speed selected 25 knots, 40 knots, 80 knots, 100 knots and 120 knots.

The front landing gear is used to verify the tire and structural shimmy respectively when the front wheel turning system is disconnected and connected.

Flight tests show that the excitation method successfully excites the required vibration, but the excitation energy is slightly insufficient.

Data analysis and conclusions

Data analysis is carried out in time domain and frequency domain respectively, and the time history curves of acceleration response, buffer stroke and aircraft taxiing speed after landing gear impacting the excitation plate are given. Figure 6-25 shows the acceleration response curves at both ends of the front landing gear axle in a state. Frequency domain analysis, modal frequency and damping ratio of the front and main landing gear are analyzed by modal analysis method. The results are characterized by the curves of bending, lateral bending, torsion frequency and corresponding modal damping ratio with velocity of the front and rear landing gear under different buffer stroke. For ARU21 aircraft, the damping ratio should be greater than 0.02, and the frequencies of each order are far away from each other. Unfortunately, because this test is the first time in China, it is necessary to test the buffer stroke.

The control is not ideal. Finally, the curves of frequency and damping ratio varying with speed and stroke are given, as shown in Figure 6-26. Even so, it can be shown that the landing gear is shimmy stable.

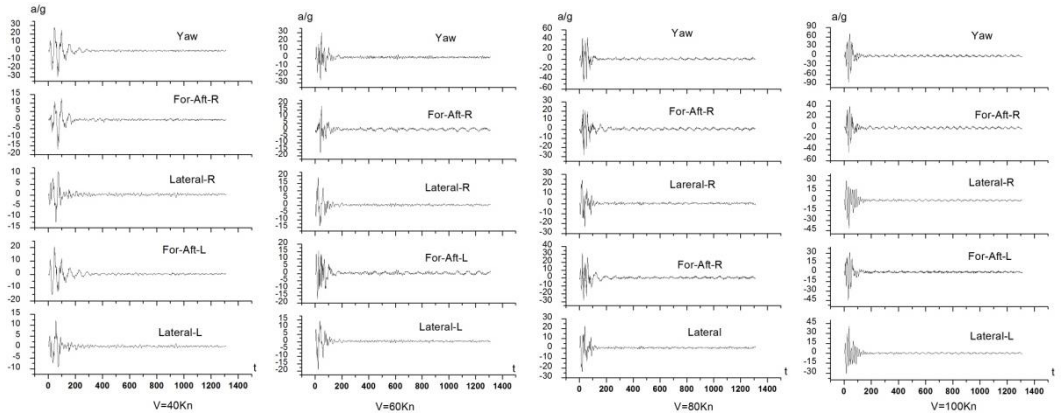

Figure 6-25 Responses of landing gears under different speed (G=30t、NWS ON)

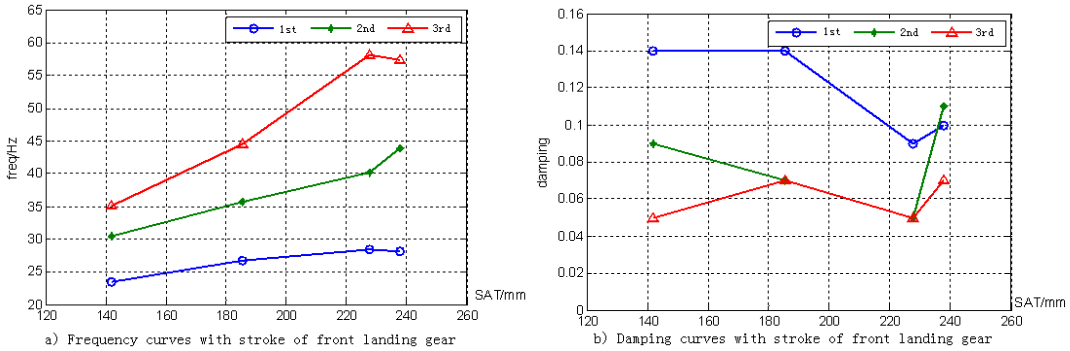

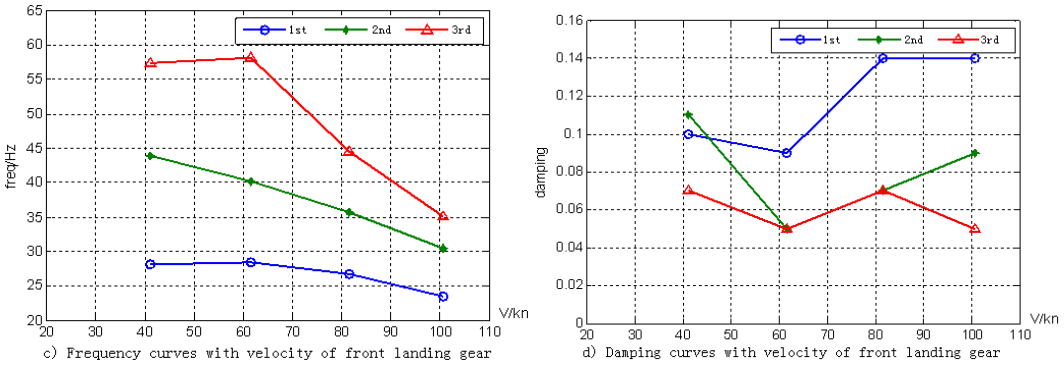

Figure 6-26 Frequency and damping curves with stroke and velocity of front landing gear (NWS on)

6.8 Design and Application of Testing Device for Fuselage Panel Based on 6-DOF System[1]

Figure 6-27 shows the curved-panel testing device, using for static and fatigue test of panel, consisting mainly of general framework, active platform, constraint platform, D-rig, six Hydraulic actuators, Bracket Part and pressurizing device. As the most important component, the nonstandard 6-DOF system in this device is formed by the following process:1) six hydraulic actuators are fixed to the general framework,2) the active end of hydraulic actuator is connected to active platform. During the test, the end of D-rig joint to curved panel is connected with constraint platform, and the other end is connected with active platform, therefore, the nonstandard 6-DOF system controlled by six hydraulic actuators can implement translation and rotation of 3-degree,which can also satisfy the tension and compression，Torsion/Shearing and bending moment of curved panel. In addition, the device is equipped with Pressurizing equipment achieving the internal pressure of curved panel.

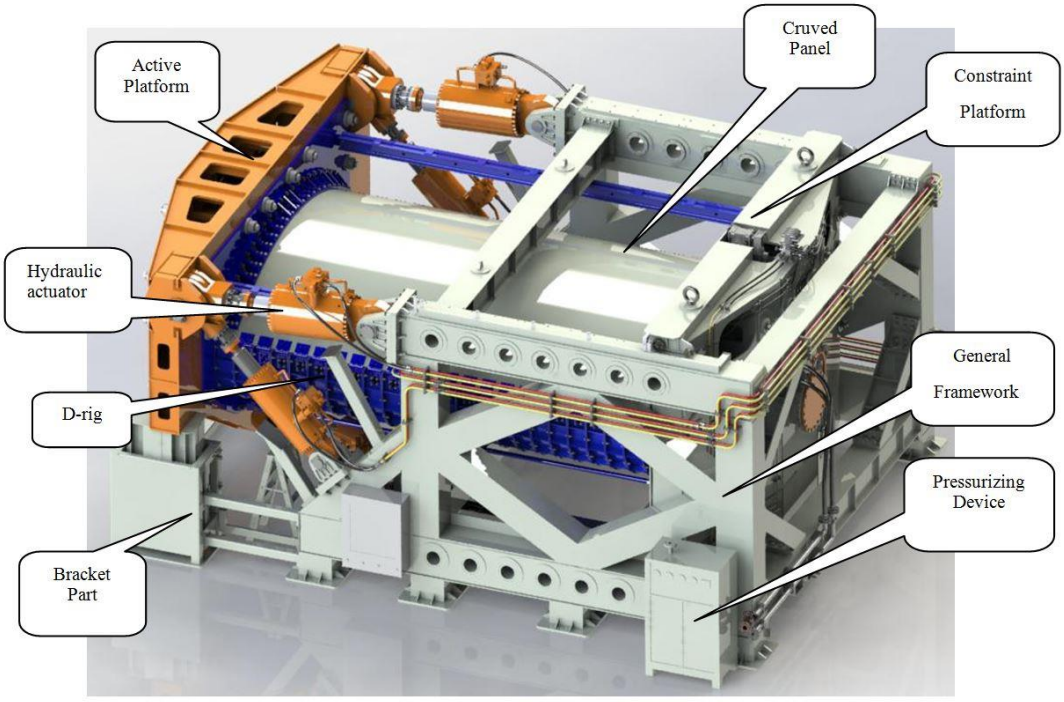

Figure 6-27 The curved-panel testing device

The ultimate load of the testing device are as follows：

- Longitudinal force ： 4000kN, tension and compression

[1] AVIC Aircraft Strength Research Institute. ZHANG Kan: Asri_zk@163.com.

- Torsion/Shearing moment: 3000kN•m
- Bending moment: 3000kN•m, Vertical and Lateral
- Pressurizing load：0.15MPa

The maximum dimensions for a curved panel to be tested are as follows:

- Panel secant: 4500mm
- Panel length: 6000mm

The accuracy of the testing device shall have the following values:

- 1% for single load static test
- 2% for single load fatigue test

6.9 Aircraft Structural Integrity Control Technology Based on Structural Damage Monitoring [1]

Aircraft structural damage monitoring technology can directly monitor structural cracks, corrosion and other damages and damage levels through sensors installed on the aircraft, so that structural damage can be repaired in time to maintain structural integrity.
The structural damage monitoring technology can effectively shorten the detection interval period and timely discover the presence and extension of structural crack damage. An aircraft structural integrity control technology based on structural damage monitoring in this paper is proposed firstly, which includes critical part selection, sensor selection and installation, structural damage monitoring, structural repair, management after structural repair, as shown in Figure 6-28.

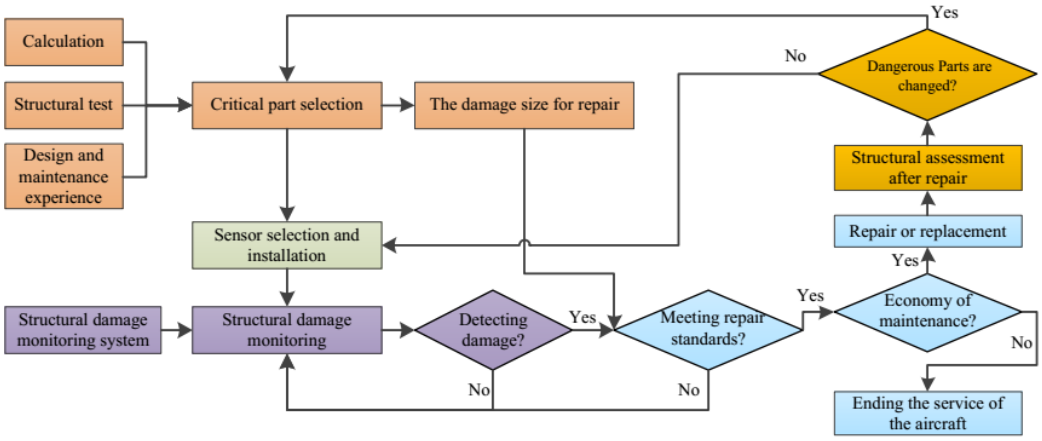

Figure 6-28 Block diagram of aircraft structural integrity control technology based on structural damage monitoring

The main implementation steps are as follows: (a) Selection of dangerous sites. Through calculation and analysis, structural test, design and maintenance experience, the key structure affecting flight safety can be determined, and the critical size of this part can be determined by calculation and analysis; (b) Sensor selection and installation. According to the characteristics of the monitoring site and the critical size, the type of sensor, the monitoring range of the sensor, and the integration of the sensor and structure are selected; (c) Damage monitoring and assessment. In the actual service environment, sensors and structural damage monitoring system are used to monitor the damage status of structures, and continuous monitoring is carried out if there is no damage. If the damage (crack) is found in the monitoring process, the size of the damage (crack length) is given, and whether the structure needs repairing is judged. If the structure does not need repairs, it will continue to monitor the expansion of damage (cracks) and assess whether repairs are needed; if the structure needs repairs, it will carry out economic evaluation of repairs; (d) Repair of the structure. If the repair is economical, make a repair plan, repair or replace it (such as the landing gear); if the repair is not economical, stop repairing, indicating that the structure has reached life; (e) Evaluation and management after structural maintenance. The repaired structure is analyzed to

[1] Air Force Engineering University. HE Yuting: Heyut666@126.com.

determine whether the dangerous parts of the structure have been transferred. If the dangerous parts are transferred, it is necessary to re-determine the important parts and re-select and install sensors for monitoring. If the dangerous part has not been transferred, it is necessary to continue monitoring after installing new sensors in the original monitoring part; this is because the damage may exceed the monitoring scope of the sensor, and may damage the sensor in the structural maintenance, so the sensor needs to be replaced.

Then, principles and methods of selecting the critical components of aircraft structures are established to determine structural damage monitoring sites. The important parts of aircraft structure refer to those parts of aircraft structure which are particularly sensitive to damage and will have a significant impact on flight safety when they fail. The important parts of aircraft structure can generally be divided into fatigue important parts, corrosion important parts and corrosion fatigue important parts. In terms of the important parts of fatigue, the important parts of fatigue are firstly determined in the whole machine range. Secondly, in the selected important parts of fatigue, according to the characteristics of the important weak parts of fatigue, the weak parts of fatigue are screened. For the important parts of corrosion, they are mainly affected by corrosive environment and low stress level, so fatigue damage will not occur in the whole life of the structure, and there is no need for structural fatigue repair. For the important parts of corrosion fatigue, it is necessary to screen out the important parts of corrosion based on the method of determining the important parts of fatigue.

According to the characteristics of typical monitoring components, methods for the selection of sensors are put forward. There are many kinds of sensors that can be used for structural health monitoring. How to select the appropriate monitoring sensors according to the characteristics and damage types of the monitored parts is the key problem to be solved in the practical application of aircraft structural damage monitoring technology. The monitoring methods commonly used in the field of structural damage monitoring are shown in Table 1. From the figure, we can see that all kinds of monitoring methods have their own characteristics and applicable areas, so it is necessary to select monitoring sensors reasonably according to the characteristics of monitoring parts.

Table 6-1 Sensors and their functions commonly used in structural damage monitoring

Sensor Type	Detecting Object	Detectable Damage Type	Detectable part	Detection mode
Fiber	Composite	Fiber or matrix fracture, delamination, debonding	Compoud material local	Online
Comparative vacuum monitoring	Metal	Crack	Surface crack at non-load bearing site	Offline / Online
Acoustic emission	Metal and composite materials	Crack, fiber or matrix fracture, delamination	An integral part of a non-connected part,such as a wallboard	Online
Smart Coating, PVD Thin Film Sensor	Metal	Crack	All Local Metal Structures (including Bolt Holes, etc.)	Off-line/On-line
Ultrasonic guided waves (Lamb waves, SH waves, Rayleigh waves, etc.)	Metals and composites Cracks	Cracks, corrosion, fiber or matrix fracture, delamination, debonding	Walls, piping, non-loading joints	Offline/Online
Eddy current (flexible eddy current array sensor, SHM bolt, etc.)	Metal	Crack, corrosion	Local area of all metal structure surfaces	Offline / Online

Finally, the characteristic advantages of aircraft structural integrity control based on structural damage monitoring are analyzed. In terms of durability, the number of cracks can be given in real time, and the remaining life is predicted, instead of using probabilistic content for durability evaluation. In terms of safety, the crack length can be monitored in real time to predict whether the structure is safe or not; In terms of structural damage monitoring results, accurate maintenance can be performed to improve maintenance support efficiency.

The aircraft structural integrity control technology based on structural damage monitoring proposed in

this paper has the following advantages: (a) Improving inspection efficiency and reducing maintenance costs. After the structural damage monitoring system is installed, the damage state of the structure can be monitored in real time. In the past, inspections that required a lot of crews, equipment, and time to complete can be completed by the monitoring system, which will greatly reduce inspection time and maintenance costs. (b) Expanding the scope of detection, shortening the inspection intervals, and improving the safety of aircraft structure in service. Structural damage monitoring technology can realize real-time monitoring of difficult-to-access locations in daily maintenance, greatly expanding the scope of inspection, greatly shortening the inspection interval. The enlargement of inspection scope and shortening of inspection cycle can greatly improve the safety of aircraft structure. (c) Extending the economic life of the structure. The critical parts that needed to be disassembled to be inspected, in the past, can be monitored in real time through the monitoring system. As long as there is no damage in the critical parts or the damage is within a limited range, the aircraft can always be used. This is equivalent to reducing the dispersion of materials and extending the service life of aircraft structures. (d) Changing the design concept of the aircraft structure. The design and the maintenance procedures of a structure are the result of an optimization of multiple parameters such as loads, material, geometry, weight, manufacturability, maintainability and all associated costs. SHM systems are not expected to have direct impact on each of them individually, but may yield in a better optimization of structures (e.g., weight, cost, etc.). This benefit is expected in longer term when reliability and durability of SHM technologies will be well established.

7. Conclusion

The market forecast has shown: there is strong market requirement for 6200 to 9000 passenger aircraft during 2018~2037 in China. China research institute and Aviation Industry has pay great attention on ICAF research and application to meet the requirement on new aircraft development and old fleet running safely.

But there is a big gap between research and the requirements, all the research institutes in CAE are on the way to manage fill the gap. The 37th Conference & 31th Symposium of the International Committee on Aeronautical Fatigue and Structural Integrity will hold in Xian China in 2021, welcome all friends to join the ICAF activity and to visit the very old and also new city Xian. We wish to work together for further exchange information and cooperation in Xian.